

การวิเคราะห์ความเครียดของหินบริเวณน้ำตกลานสาง จังหวัดตาก ประเทศไทย



นางสาวปิยกมล พลมณี

จุฬาลงกรณ์มหาวิทยาลัย
CHULALONGKORN UNIVERSITY

วิทยานิพนธ์นี้เป็นส่วนหนึ่งของการศึกษาตามหลักสูตรปริญญาวิทยาศาสตรมหาบัณฑิต

สาขาวิชาโลกศาสตร์ ภาควิชาธรณีวิทยา

บทคัดย่อและแฟ้มข้อมูลฉบับเต็มของวิทยานิพนธ์ตั้งแต่ปีการศึกษา 2554 ที่ให้บริการในคลังปัญญาจุฬาฯ (CUIR)

เป็นแฟ้มข้อมูลของนิสิตเจ้าของปีการศึกษา 2556 ที่ส่งผ่านทางบัณฑิตวิทยาลัย

ลิขสิทธิ์ของจุฬาลงกรณ์มหาวิทยาลัย

The abstract and full text of theses from the academic year 2011 in Chulalongkorn University Intellectual Repository (CUIR)

are the thesis authors' files submitted through the University Graduate School.

STRAIN ANALYSIS OF ROCKS IN THE LANSANG WATERFALL, CHANGWAT TAK,
THAILAND

Miss Peekamon Ponmanee



จุฬาลงกรณ์มหาวิทยาลัย
CHULALONGKORN UNIVERSITY

A Thesis Submitted in Partial Fulfillment of the Requirements
for the Degree of Master of Science Program in Earth Sciences

Department of Geology

Faculty of Science

Chulalongkorn University

Academic Year 2013

Copyright of Chulalongkorn University

Thesis Title STRAIN ANALYSIS OF ROCKS IN THE LANSANG
WATERFALL, CHANGWAT TAK, THAILAND
By Miss Peekamon Ponmanee
Field of Study Earth Sciences
Thesis Advisor Assistant Professor Pitsanupong Kanjanapayont,
Dr.rer.nat.

Accepted by the Faculty of Science, Chulalongkorn University in Partial
Fulfillment of the Requirements for the Master's Degree

.....Dean of the Faculty of Science
(Professor Supot Hannongbua, Dr.rer.nat.)

THESIS COMMITTEE

.....Chairman
(Assistant Professor Sombat Yumuang, Ph.D.)

.....Thesis Advisor
(Assistant Professor Pitsanupong Kanjanapayont, Dr.rer.nat.)

.....Examiner
(Vichai Chutakositkanon, Ph.D.)

.....External Examiner
(Krit Won- In, Ph.D.)

ปีย์กมล พลมณี : การวิเคราะห์ความเครียดของหินบริเวณน้ำตกลานสาง จังหวัดตาก ประเทศไทย. (STRAIN ANALYSIS OF ROCKS IN THE LANSANG WATERFALL, CHANGWAT TAK, 85 หน้า.

งานวิจัยนี้มีวัตถุประสงค์ เพื่อวิเคราะห์ความเครียดของหิน และอธิบายการเปลี่ยนแปลงลักษณะที่เกิดขึ้นภายในโครงสร้างของหินในพื้นที่บริเวณน้ำตกลานสาง จังหวัดตาก ประเทศไทย โดยพื้นที่ดังกล่าวตั้งอยู่ในแนวรอยเลื่อนแม่ปิง ซึ่งได้รับอิทธิพลจากการชนกันของแผ่นเปลือกโลกอินเดียกับเอเชีย ทำให้โครงสร้างทางธรณีวิทยาในบริเวณพื้นที่ดังกล่าวเกิดการสะสมความเครียด และตอบสนองต่อความเครียดโดยการเปลี่ยนแปลงลักษณะภายในโครงสร้าง งานวิจัยนี้ได้ศึกษาความเครียดของหินในพื้นที่ดังกล่าวจากแร่ภายในที่มีการเปลี่ยนแปลงลักษณะ และปริมาณความเครียดของหินสามารถอธิบายได้ในรูปของวงรีความเครียดตามวิธีการศึกษาของ Fry (1979)

จากการวิเคราะห์ความเครียดของหิน โดยทำการศึกษาจากแร่ภายในที่มีการเปลี่ยนแปลงลักษณะในบริเวณน้ำตกลานสาง จังหวัดตาก ประเทศไทย ตามวิธีการศึกษาของ Fry (1979) พบว่า จากตัวอย่างหินที่ทำการศึกษาทั้งหมด 13 จุด ค่าเฉลี่ยของอัตราส่วนความเครียดของหิน (R_x) มีค่าระหว่าง 1.35 ถึง 1.69 และมุมที่กระทำระหว่างแกนยาวของวงรีความเครียดกับระนาบของการเปลี่ยนแปลงลักษณะ (α) มีค่าระหว่าง 22° ถึง 41° โดยรูปร่างของวงรีความเครียด และความสัมพันธ์ของทั้งสองค่าที่ได้จากวงรีความเครียดข้างต้น บ่งบอกถึงลักษณะของกลไกที่ทำให้โครงสร้างทางธรณีวิทยาเกิดการสะสมความเครียด และเปลี่ยนแปลงลักษณะไป ซึ่งในพื้นที่ศึกษากลไกดังกล่าวคือแรงเฉือนในแนวระดับที่มีการเคลื่อนตัวไปทางด้านซ้ายในทิศตะวันตกเฉียงเหนือ-ตะวันออกเฉียงใต้ ส่งผลให้โครงสร้างทางธรณีวิทยาในพื้นที่บริเวณน้ำตกลานสาง จังหวัดตาก เกิดการเปลี่ยนแปลงลักษณะขึ้น โดยการเปลี่ยนแปลงลักษณะแบบเฉือนในแนวระดับที่มีการเคลื่อนตัวไปทางด้านซ้ายนี้สอดคล้องกับผลการศึกษาในอดีต ซึ่งน่าจะเกิดขึ้นในยุคอีโอซีน

ภาควิชา ธรณีวิทยา

สาขาวิชา โลกศาสตร์

ปีการศึกษา 2556

ลายมือชื่อนิสิต

ลายมือชื่อ อ.ที่ปรึกษาวิทยานิพนธ์หลัก

5472191823 : MAJOR EARTH SCIENCES

KEYWORDS: STRAIN ANALYSIS / FRY METHOD / LANSANG WATERFALL / THAILAND

PEEKAMON PONMANEE: STRAIN ANALYSIS OF ROCKS IN THE LANSANG WATERFALL, CHANGWAT TAK, THAILAND. ADVISOR: ASST. PROF. PITSANUPONG KANJANAPAYONT, Dr.rer.nat., 85 pp.

The objectives of this research are to quantify the finite strain of rocks and describe the deformation history of rocks in area of Lansang Waterfall, Tak Thailand where located within the Mae Ping shear zone; an affected area of past India- Asia penetration. By this process the structural geology on this area was accumulated strain inside and responded it in form of deformation. This research quantified the finite strain of rocks on this affected area from deformed minerals and a quantity of finite strain can be described by strain ellipsoid of rock followed by Fry's method (Fry, 1979).

From the strain quantitative analysis of rocks from deformed minerals in area of Lansang Waterfall, Tak Thailand followed by Fry's method (Fry, 1979) found that from all 13 rock sample locations, the averaged finite strain ratio of rocks and the angle- value between the longest axes of strain ellipsoid and the deformation boundary ranged between 1.35 to 1.69 and 22 to 41°, respectively. The shape of strain ellipsoid and the relative between that value intense the deformation process that applied and lead structural geology accumulated strain inside and finally deformed which the process of left- lateral simple shear applied on this area on the direction of NW- SE and lead deformation occurred on of Lansang Waterfall, Tak Thailand during the Eocene. Moreover, when compared the result of this research with the further work found that they are corroborated and related to each other.

Department: Geology

Student's Signature

Field of Study: Earth Sciences

Advisor's Signature

Academic Year: 2013

ACKNOWLEDGEMENTS

This thesis is based on the M.Sc. program carried out under the guidance of my advisor Assistant Professor Dr. Pitsanupong Kanjanapayont, Department of Geology, Faculty of Science, Chulalongkorn University and was supported by the 90th years of Chulalongkorn University, TRF and Ratchadaphiseksomphot Endowment Fund, Chulalongkorn University. Dr. Pitsanupong advised and guided me with patience and enthusiasm for approaching my study, providing all knowledge of the field and laboratory techniques. Beside, Dr. Pitsanupong also provided other idea for concluding and completing my thesis. I have a deep gratitude towards Professor Dr. Bernhard Grasmann, Department for Geodynamics and Sedimentology, University of Vienna and Professor Dr. Urs Klötzli, Department of Lithospheric Research, University of Vienna for an opportunity to expand my knowledge. My special thanks due to Assistant Professor Dr. Sombat Yumuang, Dr. Vichai Chutakositkanon, Department of Geology, Faculty of Science, Chulalongkorn University and Dr. Krit Won- In, Department of Earth Sciences, Faculty of Science, Kasetsart University, Thesis Evaluation Committee members who improved my thesis by critical comments.

Moreover, thanks are extended to Miss Somporn Wonglak and Mr. Alongot Fanta who gave me support on the field investigation and laboratory work. Finally, I felt deeply appreciated to my family who always supported me during my thesis study and also my friends in Earth Sciences program and others that I did not mention who cheered me up.

CONTENTS

	Page
THAI ABSTRACT	iv
ENGLISH ABSTRACT	v
ACKNOWLEDGEMENTS	vi
CONTENTS	vii
LIST OF TABLES	ix
LIST OF FIGURES	x
CHAPTER I INTRODUCTION.....	1
1.1 Statement of problem.....	2
1.2 Objectives.....	6
1.3 Scope of the Investigation	6
1.4 Expected Contribution.....	6
CHAPTER II THEORY AND LITERATURE REVIEWS	7
2.1 The geological setting and structural geology of northwestern Thailand	7
2.1.1 Geological setting.....	7
2.1.2 Structural geology.....	11
2.2 The fundamentals of deformation and strain of rocks.....	14
2.2.1 One and two- dimensional strain.....	16
2.2.2 Strain ellipsoid.....	18
2.2.3 The application of kinematic vorticity number (Wk).....	19
2.3 Basic concept about strain quantitative analysis	22
2.3.1 Strain markers and strain in one dimension.....	22
2.3.2 Strain in two dimension.....	23
2.4 Application of Fry method.....	26
CHAPTER III METHODOLOGY AND DATA USED	29
3.1 Methodology.....	29
3.2 Data Collection and Equipment Used.....	31
3.2.1 Field investigation	31

	Page
3.2.2 Preparing rock samples for strain quantitative analysis.....	32
3.3 The processing of strain quantitative analysis.....	34
3.3.1 Selection strain markers of rocks from microscope	34
3.3.2 Calculation of strain ratio (R_s) and the angle (θ) from strain ellipsoid.....	36
3.3.3 Calculation of kinematic vorticity number (W_k).....	38
CHAPTER IV RESULTS	39
4.1 The data collecting from field investigation	39
4.2 Finite strain ratios (R_s) and the angle (θ).....	49
4.3 Kinematic vorticity number, W_k	65
CHAPTER V DISCUSSIONS	68
5.1 Quantifying the deformation.....	69
5.2 The sinistral shear.....	71
5.3 Tectonic implication.....	74
CHAPTER VI CONCLUSION.....	77
REFERENCES	79
APPENDIX.....	80
VITA.....	85

LIST OF TABLES

Table 4. 1 The locations of the rock sample for this research.....	47
Table 4. 2 Strain data of rocks in Lansang Waterfall, Tak, northwestern Thailand.	64



LIST OF FIGURES

Figure 1. 1 Structural sketches drawn from 1: 1,250,000 scale geological maps of Mae Ping shear zone and adjacent area including with Hill shade map from DEM to infer trend of Mae Ping Fault and affected area of past India's penetration; the high strain zone where a proper area for strain quantitative study's area (Modified from Resources, 1999).	4
Figure 1. 2 Simplified geologic map of the Mae Ping shear zone including with locations of strain quantitative analysis; Lansang Waterfall, Tak, northwestern Thailand (Modified from R. Lacassin, Leloup, & Tapponnier, 1993).....	5
Figure 2. 1 Diagram (a) to (c) describes characteristic of rigid body deformation which translation and rotation are both rigid body deformation component. On right down corner of diagram describe the characteristic of homogeneous deformation (Modified from Fossen, 2010).	16
Figure 2. 2 Diagram (a) to (b) describe the characteristic and deformation process of rock when pure shear and simple shear applied on (Modified from Fossen, 2010)....	17
Figure 2. 3 Diagram (a) the strain ellipsoid and designation of the ellipsoid axes defined in terms of vector. Diagram (b) presents characteristic of two circular sections of strain ellipsoid that no strain (Modified from Fossen, 2010).	18
Figure 2. 4 Diagram presents the direction of vorticity vector and by the definition of vorticity, the homogeneous plane strain deformation can be divided into pure shear and simple shear component (Modified from Tikoff & Fossen, 1995).	20
Figure 2. 5 Diagram (a) and (b) describes the methodology of (Fry, 1979) for quantify the finite strain. Diagram (c) presents the product of (Fry, 1979); the vacancy field or strain ellipsoid of rock (Modified from Ramsay & Huber, 1983).	24
Figure 2. 6 Diagram (A) describes the product of (Fry, 1979); the Fry diagram for undeformed situation. Diagram (B) and (C) describes the product of (Fry, 1979) for deformed by pure shear and simple shear, respectively (Modified from Genier & Epard, 2007).	25
Figure 3. 1 Methodological flow chart of this research	30
Figure 3. 2 Diagram (A) Geological map of northwestern Thailand mapped together with the traverse line observation (blue line) along the profile of Lansang Waterfall within the Lansang National Park, Tak and adjacent area. Diagram (B) presents profile of the traverse line along the Lansang Waterfall including with elevation of all sample locations (Modified from Resources, 1999).	32
Figure 3. 3 Flow chart of preparing rock samples into thin section.....	33

Figure 3. 4 Diagram describes the Fry's theory which diagram (A) describe the relative between the center points of rigid particle A to the surrounding particles during the undeformed state while diagram (B) describe the relative between the center points of each particles during the homogeneous deformation state. Diagram (C) presents the rigid particles or deformed minerals that appropriate to use as strain marker for Fry analysis (Modified from Ramsay & Huber, 1983; Genier & Epard, 2007).	35
Figure 3. 5 Methodological flow chart of Fry's method.....	37
Figure 3. 6 Diagram (A) and (B) describe the Fry methodology which the product of Fry represented by the finite strain ellipsoid presenting in diagram (C). Diagram (C) presents strain ellipsoid of rock which consisting of the longest axes, shortest axes and angle (θ), an angle between the longest axes and deformation boundary of the ellipse (Modified from Ramsay & Huber, 1983).....	37
Figure 4. 1 (Left) an outcrop of rock sample location LS-1. (Right) Quartz and feldspar on rock sample LS- 1 have equigranular texture which is the mineralogy of orthogneiss.....	40
Figure 4. 2 (Left) an outcrop of rock sample location number LS-4. (Right) rock sample number LS- 4 presents dominant feature of porphyroblastic texture of quartz and feldspar in biotite.	40
Figure 4. 3 (Left) an outcrop of rock sample location number LS-5. (Right) rock sample number LS- 5 presents dominant feature of augen texture or porphyroblastic texture of quartz and feldspar.....	41
Figure 4. 4 (Left) an outcrop of rock sample location number LS-10. (Right) rock sample number LS- 10 mainly consist equigranular texture of quartz and feldspar which represent the common characteristic of orthogneiss.....	42
Figure 4. 5 (Left) an outcrop of rock sample location number LS-11. (Right) rock sample number LS- 11 mainly consists fine grained of quartz and feldspar which clearly intense the mineralogy of orthogneiss.....	42
Figure 4. 6 (Left) an outcrop of rock sample location number LS-12. (Right) rock sample mainly consists of white fine grained of quartz and feldspar which clearly intense the mineralogy of orthogneiss within this outcrop.....	43
Figure 4. 7 (Left) an outcrop of rock sample location number LS-13. (Right) rock sample number LS- 13 presents dominant feature of paragneiss within this outcrop.	44
Figure 4. 8 (Left) an outcrop of rock sample location number LS-14. (Right) rock sample number LS- 14 mostly consist the characteristic of paragneiss within this outcrop.	44

Figure 4. 9 (Left) present the outcrop of rock sample location number LS-15. (Right) most of rock samples within this outcrop present the dominant feature of paragneiss.	45
Figure 4. 10 (Left) presents the outcrop of rock sample location number LS-16 which mostly is paragneiss. (Right) presents the characteristic of rock samples within rock sample location number LS- 17 which rock samples have dominant feature of paragneiss.....	46
Figure 4. 11 (Left) presents the rock sample of location number LS-18 which mainly consists fine grained of quartz and feldspar, the common mineral of orthogneiss. (Right) the rock sample of location number LS- 23 which mainly consists coarse grained of quartz and feldspar.	47
Figure 4. 12 Geological map of Lansang Waterfall and adjacent area, including with the rock sample locations along the profile of Lansang Waterfall within Lansang National Park, Tak, northwestern Thailand (Modified from Resources, 1999).	48
Figure 4. 13 Diagram (A) XY thin sections of rock sample LS- 1 in Lansang Waterfall while diagram (B) presents strain marker; recrystallized quartz grains (red dot) for Fry analysis. Diagram (C) XY plane of the finite strain ellipsoid of rock sample LS- 1 followed by Fry's method, including with strain ratio value.	50
Figure 4. 14 Diagram (A) XY thin sections of rock sample LS- 4 in Lansang Waterfall while diagram (B) presents strain marker; recrystallized quartz grains (red dot) for Fry analysis. Diagram (C) XY plane of the finite strain ellipsoid of rock sample LS- 4 followed by Fry's method, including with strain ratio value.	51
Figure 4. 15 Diagram (A) XY thin sections of rock sample LS- 5 in Lansang Waterfall while diagram (B) presents strain marker; recrystallized quartz grains (red dot) for Fry analysis. Diagram (C) XY plane of the finite strain ellipsoid of rock sample LS- 5 followed by Fry's method, including with strain ratio value.	52
Figure 4. 16 Diagram (A) XY thin sections of rock sample LS- 10 in Lansang Waterfall while diagram (B) presents strain marker; recrystallized quartz grains (red dot) for Fry analysis. Diagram (C) XY plane of the finite strain ellipsoid of rock sample LS- 10 followed by Fry's method, including with strain ratio value.	53
Figure 4. 17 Diagram (A) XY thin sections of rock sample LS- 11 in Lansang Waterfall while diagram (B) presents strain marker; recrystallized quartz grains (red dot) for Fry analysis. Diagram (C) XY plane of the finite strain ellipsoid of rock sample LS- 11 followed by Fry's method, including with strain ratio value.	54
Figure 4. 18 Diagram (A) XY thin sections of rock sample LS- 12 in Lansang Waterfall while diagram (B) presents strain marker; recrystallized quartz grains (red dot) for Fry	

analysis. Diagram (C) XY plane of the finite strain ellipsoid of rock sample LS- 12 followed by Fry's method, including with strain ratio value.	55
Figure 4. 19 Diagram (A) XY thin sections of rock sample LS- 13 in Lansang Waterfall while diagram (B) presents strain marker; recrystallized quartz grains (red dot) for Fry analysis. Diagram (C) XY plane of the finite strain ellipsoid of rock sample LS- 13 followed by Fry's method, including with strain ratio value.	56
Figure 4. 20 Diagram (A) XY thin sections of rock sample LS- 14 in Lansang Waterfall while diagram (B) presents strain marker; recrystallized quartz grains (red dot) for Fry analysis. Diagram (C) XY plane of the finite strain ellipsoid of rock sample LS- 14 followed by Fry's method, including with strain ratio value.	57
Figure 4. 21 Diagram (A) XY thin sections of rock sample LS- 15 in Lansang Waterfall while diagram (B) presents strain marker; recrystallized quartz grains (red dot) for Fry analysis. Diagram (C) XY plane of the finite strain ellipsoid of rock sample LS- 15 followed by Fry's method, including with strain ratio value.	58
Figure 4. 22 Diagram (A) XY thin sections of rock sample LS- 16 in Lansang Waterfall while diagram (B) presents strain marker; recrystallized quartz grains (red dot) for Fry analysis. Diagram (C) XY plane of the finite strain ellipsoid of rock sample LS- 16 followed by Fry's method, including with strain ratio value.	59
Figure 4. 23 Diagram (A) XY thin sections of rock sample LS- 17 in Lansang Waterfall while diagram (B) presents strain marker; recrystallized quartz grains (red dot) for Fry analysis. Diagram (C) XY plane of the finite strain ellipsoid of rock sample LS- 17 followed by Fry's method, including with strain ratio value.	60
Figure 4. 24 Diagram (A) XY thin sections of rock sample LS- 18 in Lansang Waterfall while diagram (B) presents strain marker; recrystallized quartz grains (red dot) for Fry analysis. Diagram (C) XY plane of the finite strain ellipsoid of rock sample LS- 18 followed by Fry's method, including with strain ratio value.	61
Figure 4. 25 Diagram (A) XY thin sections of rock sample LS- 23 in Lansang Waterfall while diagram (B) presents strain marker; recrystallized quartz grains (red dot) for Fry analysis. Diagram (C) XY plane of the finite strain ellipsoid of rock sample LS- 23 followed by Fry's method, including with strain ratio value.	62
Figure 4. 26 An error bar graph presents the correlative between the average finite strain ratio of all rock samples ($R_{s, avg.}$) and their locations along the profile of Lansang Waterfall within Lansang National Park, Tak, northwestern Thailand.	65
Figure 4. 27 Diagram plots of the averaged kinematic vorticity number ($W_{k, avg.}$) and the angle between the longest axes of strain ellipse and the deformation boundary (θ) showing the strain ratios of the finite strain ellipsoid (R_s).	66

Figure 4. 28 Geological map of Lansang Waterfall, Tak, northwestern Thailand and adjacent area, including with rock sample locations and XY plane of finite strain ellipsoid of all 13 locations along the profile of Lansang Waterfall.....	67
Figure 5. 1 Diagram presents W_k ranged of this research; ranged between 0.79 to 1.00 which corroborated with theory and clearly described the characteristic of simple shear- dominated in area of Lansang Waterfall, Tak, northwestern Thailand.....	71
Figure 5. 2 Diagram presents the macro and micro scale of strain quantitative study, including with rock sampling (upper left), selection strain marker (upper right) and the Fry's product (lower left and right) which represented by strain ellipsoid of rocks....	73
Figure 5. 3 Diagram presents the strain ellipsoid of rocks in area of Lansang Waterfall followed by Fry's method which clearly intense the characteristic of sinistral shear and corroborated with sense of movement of kinematic indicator; σ - clast of (R. Lacassin, Maluski, H., Leloup, P. H., Tapponnier, P., Hinthong, C., Siribhakdi, K., Chauaviroj, S. and Charoenravat, A, 1997).....	74
Figure 5. 4 Diagram describes the model of tectonic evolution of (R. Lacassin, Maluski, H., Leloup, P. H., Tapponnier, P., Hinthong, C., Siribhakdi, K., Chauaviroj, S. and Charoenravat, A, 1997) by the plotted of age of the motion of the major strike- slip faults of eastern and southeastern Asia. An open squares and bold gray line define motion of India relative with Asia at 5.8 cm/yr. Arrowed lines show approximate distances between India and fault traces of left- lateral motion (dotted) and end of the motion (long dashes) while the short dashes show the right- lateral motion (Modified from R. LACASSIN, MALUSKI, H., LELOUP, P. H., TAPPONNIER, P., HINTHONG, C., SIRIBHAKDI, K., CHAUAVIROJ, S. AND CHAROENRAVAT, A, 1997).....	76

CHAPTER I

INTRODUCTION

Despite there were widely spread studied on Plate- scale kinematic reconstruction of past India into Asia collision by using dating technique, geomorphological offsets or Global Positioning System (GPS) measurement, but the better understand and clearly conclusion about the structural evolution still difficult. Besides, the movement and timing of the extrusion of Indochina block that affected the strike- slip faults, and also the age of major deformation phases on both affected area; Ailao- Shan- Red River and Mae Ping shear zone also be questioned.

Nevertheless, to better understand in the deformation history of this past continental deformation require not only the recognition and dating on the large shear zone, but also in senses of quantitative analysis for determine the direction and sense of movement in this shear zones. The strain quantitative analysis refers and relates to the useful of mathematical description which quantify the finite strain from the geometry of shear criteria; strain markers of rocks which reveal how much rock obtained strain inside after the collision occurred. Then, (R. Lacassin, Leloup, & Tapponnier, 1993) applied one dimension strain quantitative analysis; boudinaged restoration estimated the minimum finite strain of rock from offset geological markers, the boudinage structure on Ailao- Shan- Red River and Mae Ping shear zones for indicate the movement of shear zone.

Thus it motivate this research to describe the movement and deformation history of this past collision shear zone by applied two dimension strain quantitative analysis; technique of (Fry, 1979) quantify the finite strain of rocks from deformed minerals in area of Lansang waterfall, Tak, northwestern Thailand.

1.1 Statement of problem

The large strain area in Tibet and adjacent regions has induced by the indentation of India into Asia (R. Lacassin, Maluski, H., Leloup, P. H., Tapponnier, P., Hinthong, C., Siribhakdi, K., Chauaviroj, S. and Charoenravat, A, 1997). The N- S crustal shortening was imprinted by geological and geophysical evidences that occurred in the region that facing with the Indian's indenter. On the sides of the collision zone this past penetration has produced a large area of deformation and later successively pushing Indochina and Tibet/ South China toward the ESE along the sinistral strike-slip faults which removed the volume of Asia lithosphere after the collision. Besides, by the strike-slip motion, such shortening was mentioned that transformed into crustal extension, seafloor spreading and also subduction nearby the strike-slip faults (P. Tapponnier, Peltzer, G., Le Dain, A. Y. and Armijo, R, 1982; P. Tapponnier, Peltzer, G. and Armijo, R, 1986).

The prominent evidences of the past indentation present on rocks of the Ailao- Shan- Red River and Mae Ping shear zones which motivated most of the studies aim toward in modeling tectonic evolution of this extrusion on both shear zone (Fig. 1.1). One of the models of the Tertiary extrusion of Indochina and concurrent opening of the South China Sea used evidence on rocks of the Ailao- Shan- Red River shear zone and the field investigation and later modeled and proposed that the sinistral motion occurred between 35Ma to 15Ma by ductile shear. Moreover, the southern part of the Indochina claimed to be the major deformation phases which reported to be Paleozoic or Lower Mesozoic age (R. Lacassin, Maluski, H., Leloup, P. H., Tapponnier, P., Hinthong, C., Siribhakdi, K., Chauaviroj, S. and Charoenravat, A, 1997).

However, the previous studied aim in line of recognition or dating on rocks on this large shear zone, thus to propose the truly model and understanding about the timing of major deformation phases, an extrusion of the Indochina block and also the movement of this strike-slip faults and shear zones still be questioned (P. Tapponnier, Peltzer, G. and Armijo, R, 1986; R. Lacassin, Maluski, H., Leloup, P. H., Tapponnier, P., Hinthong, C., Siribhakdi, K., Chauaviroj, S. and Charoenravat, A, 1997).

For quantitative analysis, (R. Lacassin, Leloup, & Tapponnier, 1993) focused only in one dimension strain quantitative analysis on boudinage structure from Ailao- Shan-Red River and on the entrance of Lansang National Park where located within Mae Ping shear zone (Fig. 1.2). This study applies the Fry's method (Fry, 1979) for two dimension strain quantitative analysis to gain an accuracy finite strain data of deformed rocks that occurred under homogeneous deformation through the geometric of strain markers. Fry's theory focused on the reaction of all strain markers center in deformed rock after sheared under the microscope (Ramsay & Huber, 1983). Thus it could clearly define how the direction and orientation of marker has changed from the boundary and represented it in forms of strain ellipsoid. Besides, the relative between finite strain ratios (R_s) and the kinematic vorticity number (W_k) also the material that used for describe the mechanism of this shear zone, the Mae Ping shear zone in term of deformation types and the flow patterns.

Therefore, it lead this study has strong motivation to use (Fry, 1979) as a material in quantify the finite strain of deformed rocks on Lansang waterfall, Tak, northwestern Thailand which claimed to be a part of complex area, the Mae Ping shear zone.

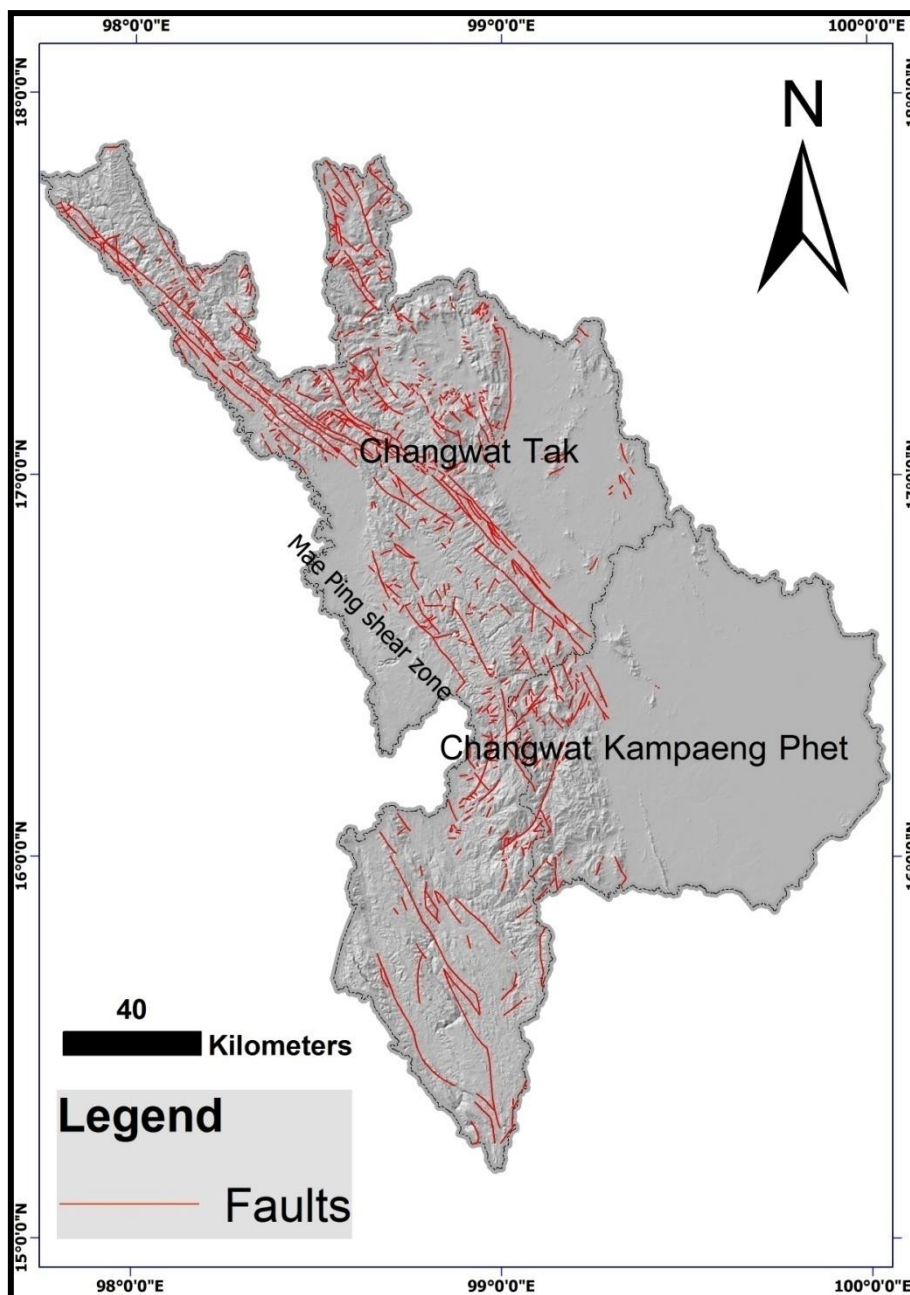


Figure 1. 1 Structural sketches drawn from 1: 1,250,000 scale geological maps of Mae Ping shear zone and adjacent area including with Hill shade map from DEM to infer trend of Mae Ping Fault and affected area of past India's penetration; the high strain zone where a proper area for strain quantitative study's area (Modified from Resources, 1999).

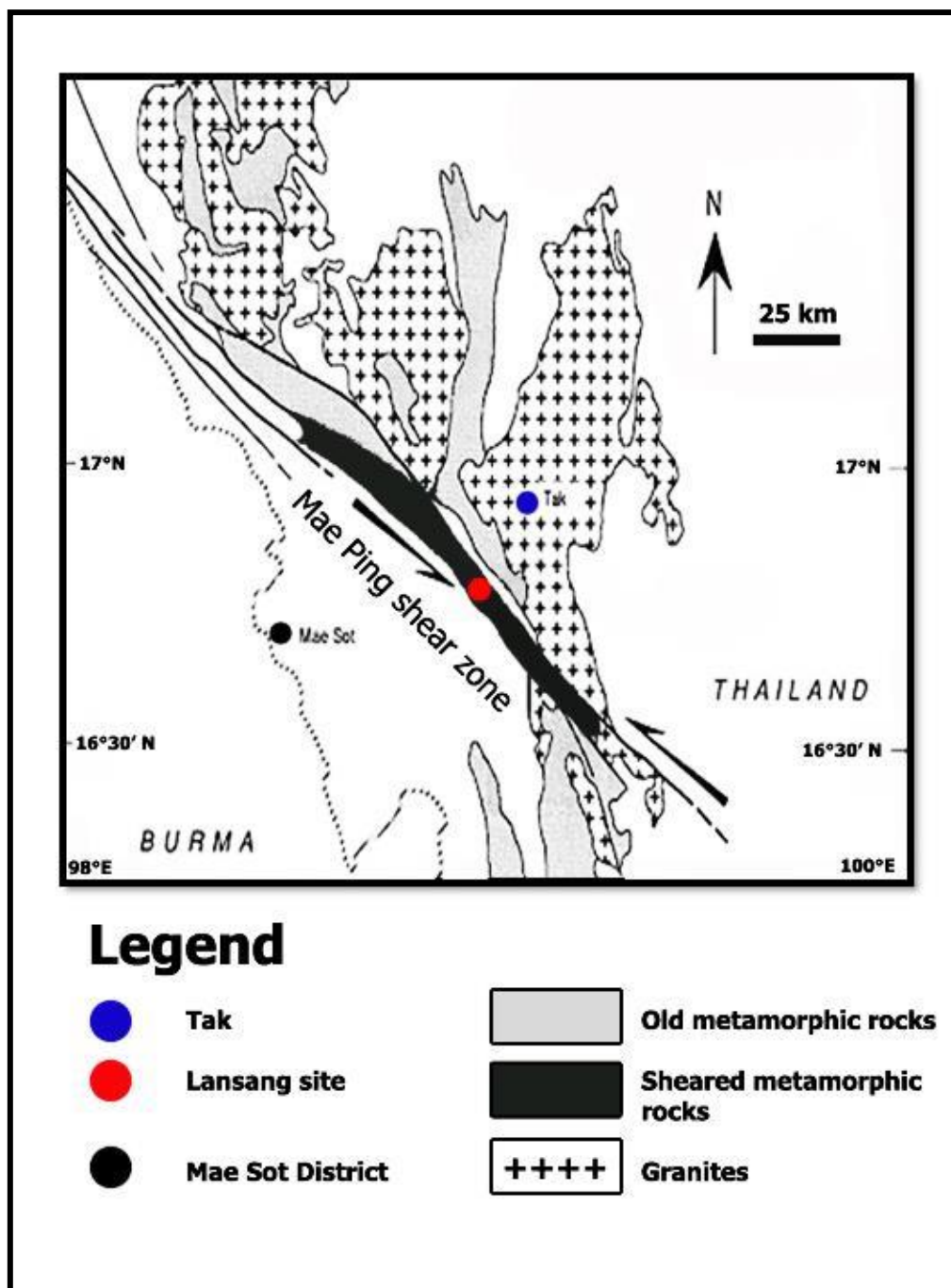


Figure 1. 2 Simplified geologic map of the Mae Ping shear zone including with locations of strain quantitative analysis; Lansang Waterfall, Tak, northwestern Thailand (Modified from R. Lacassin, Leloup, & Tapponnier, 1993).

1.2 Objectives

The objectives of this study are quantify the finite strain of rocks from strain markers; deformed minerals in area of Lansang waterfall, Tak, northwestern Thailand by using Fry's method (Fry, 1979). Moreover, describe the deformation history of rock that occurred in area of Lansang waterfall, Tak, northwestern Thailand by using these finite strain data.

1.3 Scope of the Investigation

This research applies (Fry, 1979) for quantify the finite strain of especially deformed rocks from strain marker; recrystallized quartz grains along Lansang waterfall where located on Lansang National Park; a part of Mae Ping shear zone, Tak, northwestern Thailand.

1.4 Expected Contribution

The expected contribution of this research are to obtain the better finite strain of rock data on Lansang waterfall, Tak, northwestern Thailand by using (Fry, 1979) and more understanding in deformation history of rocks, including deformation type and sense of movement that occurred in this area by these data.

CHAPTER II

THEORY AND LITERATURE REVIEWS

Theory and literature reviews that are related in this research are discussed in this chapter. On section 2.1 review the geological setting and structural geology of northwestern Thailand where Lansang Waterfall located within. For section 2.2 the fundamentals of deformation and strain of rocks, including with some of useful mathematical description are mentioned. Then on section 2.3 presents the basic concept of strain quantitative analysis. Finally, literature reviews which related to this research are discussed in last section.

2.1 The geological setting and structural geology of northwestern Thailand

2.1.1 Geological setting

The tectonic model proposed to describe the structural evolution of Tibet and adjacent area which were affected by the India's penetration. The hypothesizes is large continental crust; Sundaland, Tibet and South China have been extruded toward the east and southeast away from the Indian indenter direction by the strike-slip faults motion (P. Tapponnier, Peltzer, G. and Armijo, R, 1986). Later, the model for describe the activity of strike- slip faults mentioned that related to rift systems during the Tertiary from past evidence and the Tertiary evolution of SE Asia model can be divided into two main types: a pure escape tectonics model with no proto-South China and subduction of proto- South China Sea crust beneath Borneo (C. K. Morley, 2002).

An area of Mae Ping fault zone and adjacent dominantly left- lateral strike-slip motion which branching off the right- lateral Sagaing fault in Myanmar. The fault supported the extrusion of Sundaland which occurred in period of Late Eocene- Early Oligocene with the geological offset of 120 to 150 km estimated by displace of high-grade gneisses and granites of the Chiang Mai- Lincang belt, CM- L belt (Palin et al., 2013).

The most imprint structural feature of the NW Thailand that located in the triangle- shaped northern corner of Indochina is the CM- L belt. The CM- L belt is a north- south metamorphic and magmatic rock widely about 70 km and offset the plenty of strike- slip faults which the most dominant ones is the left- lateral Mae Ping and Three Pagodas fault zones. Within this are the metamorphic rocks that mostly high- grade paragneisses, orthogneisses and micaschists (R. Lacassin, Maluski, H., Leloup, P. H., Tapponnier, P., Hinthong, C., Siribhakdi, K., Chauaviroj, S. and Charoenravat, A, 1997).

By the overlain of less metamorphic Paleozoic rocks lead this metamorphic rock: gneisses and micaschist defined to Precambrian age. Later they pass and deformed into migmatites and are intruded by mainly Permo- Triassic age of granitic plutons. The syntectonic migmatization and granite intrusion involved with two important stages: during a Permo- Triassic age instead of Precambrian for the high- grade metamorphism and during Cretaceous or Tertiary granite for an event of younger magmatic and metamorphic in the CM- L belt. Besides, the characteristic of left- laterally which occurred by the Three Pagodas fault zone presence in Cretaceous to Paleogene granite plutons located on the west of the belt along the Tenasserim mountain of southern Burma and Shan scarp region. On Eastern part of CM- L belt, the low- grade Paleozoic rocks of the Sukhothai fold belt have intruded by the other large Triassic granite plutons. Apart from the Siluro- Devonian rocks on east of Chiang Mai, the Sukhothai belt is made of a series of upper Paleozoic to Mesozoic of sedimentary, volcanic and volcanoclastic rocks. Most of the Sukhothai belt located along the Simao basin where it is clear to the ENE- WSW compression during the Tertiary.

Moreover, across the NW Thailand, the N-S trending fold axes are curved into an S shape toward the strike- slip faults, north of Chiang Rai and later upright through eastward- southeastward presence along the border of the Sukhothai belt. During the Late Cenozoic, the grabens are located along synclines of this fold belt which has bound by the nearly N- S normal faults and claims it to be activated. Besides, the N- S grabens also located beneath Quaternary sediments and including with the Gulf of Thailand.

The suture zone, an area between the eastern of active margin Shan- Thai block and the passive margin of the Kontum- Khorat block was marked by the Sukhothai belt which is bound to the east by the right- lateral Dien Bien Phu fault zone and presence reversed sense or left- lateral sense in plenty of segments. Eastern part of suture zone localized the Loei fold belt which affected by strong folding during the Triassic and later presence pre- Upper Devonian deformation and metamorphism. Beside, on the SE of this suture present the clearly post- Early Triassic folds and thrusts on the Khorat plateau. In addition the geological maps of western mountain of Thailand and western part of Kanchanaburi were mapped the exposure of metamorphic rocks as Precambrian or Lower Paleozoic (Dheeradilok & Lumjuan, 1983). The metamorphic facie series was proposed in two main facies; the low pressure of Amphibolite facie series (high T/ low P) of the Precambrian to Carboniferous rocks which orientated along the axial part of the metamorphic belt and the low pressure Greenschist (high T/ low P) facie series of Lower Paleozoic age which occurred along both sides of the NS trending metamorphic belt (Dheeradilok & Lumjuan, 1983).

These metamorphic rocks generally steep foliation and horizontal stretching lineation with oriented NW- SE trending parallel to the Three Pagodas Fault zone. Within the Lansang National Park where an area apart of the Mae Ping Fault zone, deformed rocks are exposed in forms of 5- 8 km wide belt mylonitic gneisses or Lansang gneisses. On northwestward of Lansang National Park present an offset of triangular facets and suggest that the recent uplift of the gneisses core occurred by NE dipping fault which push the gneisses to NE.

The yield of metamorphic rocks on the NW Thailand has been studied since late 1970s by various dating techniques depends on limitation of data set. For the study the yield of metamorphic rocks on the NW Thailand that using Rb- Sr dating technique, the yield was recorded in a series. For instance Tak granodioritic to syenogranitic batholiths gave ages between 208 ± 4 and 219 ± 12 Ma, as same as for the Lampang granite and the granitoids in both CM- L and Sukhothai belts fell in the same range 212 ± 12 Ma and 240 Ma to 200 Ma, respectively. Unless, the Lincang

batholiths and the Thabsila gneisses gave age older 270 ± 59 Ma and 391 to 560 Ma, respectively.

For the K- Ar dating studied, K- Ar dating on biotites and illites from Lansang gneisses yielded in range between 31.9 Ma to 29.6 Ma which claimed to be the result from Tertiary cooling as same as for biotites and muscovites from the eastern border of the CM- L belt, Bhumibol dam and nearby Hot and Chiang Mai gave ages 18 Ma to 22 Ma. Beside, on the south of the Gulf of Thailand, U- Pb dating on the main batholith gave the ages ranging between 220Ma to 198 Ma which imply the age of the N- S magmatic belt in Triassic. On the west of Chiang Mai, orthogneisses from the Doi Inthanon was yielded by U- Pb zircon dating gave ages between 211 and 203 Ma that interpreted to the age of the granitic intrusion. For monazites gave U- Pb zircon dating nearly concordant of 84 ± 2 and 72 ± 1 Ma and claimed as the age of the high- grade metamorphism. Moreover, the K- Ar dating of biotites from the Thabsila gneisses gave the Tertiary ages of 36 ± 1 and 33 ± 2 Ma. All of these results concluded that the CM- L belt has on period of Upper Cretaceous, Tertiary deformation and metamorphic events (R. Lacassin, Maluski, H., Leloup, P. H., Tapponnier, P., Hinthong, C., Siribhakdi, K., Chauaviroj, S. and Charoenravat, A, 1997).

Moreover, (R. Lacassin, Maluski, H., Leloup, P. H., Tapponnier, P., Hinthong, C., Siribhakdi, K., Chauaviroj, S. and Charoenravat, A, 1997) used $^{40}\text{Ar}/^{39}\text{Ar}$ dating the age of Lansang gneisses along Mae Ping shear zone which suppose that the deformation phrase occurred together with Ailao- Shan- Red River shear zone. The results concluded that the deformation started around 30.5 Ma and the lower Mesozoic metamorphic and magmatic belt of northern Thailand had rapid cooling in the period of Tertiary or about 23 Ma. Based on the results, the extrusion of a part of Indochina occurred during the upper Eocene- lower Oligocene, thus the age of Lansang gneisses suggested to be an evidence of ductile left- lateral shear zone.

(C. K. Morley, Smith, M., Carter, A., Charusiri, P. and Chantraprasert, S, 2007) divided dating data from the past published into two groups for describe the history of cooling- age data in western part of Thailand and the better discussion about the deformation of Mae Ping fault. Two group of data are the cooling- age data along

Mae Ping fault zone and high- temperature cooling age data (apatite- zircon fission track dating data), and plotted in regional map of NW Thailand. After that (Palin et al., 2013) studied on geochronological analysis of monazite from sheared biotite- K-feldspar orthogneiss and the result implied two events of recrystallization. For the core regions, Th- Pb ages between c. 123 to c. 114 and for the rim regions ages younger between c. 45 to c. 37 Ma. Based on these result, the ductile shearing along the Mae Ping fault occurred during or after the metamorphic events which the last event of metamorphism occurred during the Eocene. Besides, the monazite analyzed from undeformed garnet- two- mica granite dyke, which intruding the metamorphic rock at Bhumibol Lake, a Th- Pb ages between 66.2 ± 1.6 Ma. From this age implied that the Mae Ping fault cut earlier formed magmatic and high- grade metamorphic rocks.

2.1.2 Structural geology

The structural geology of the Mae Ping – Lansang shear zone mostly presents the widespread mylonitic fabrics with the foliations, stretching lineation that are criteria to refer the left- lateral shear under the microscope (R. Lacassin, Maluski, H., Leloup, P. H., Tapponnier, P., Hinthong, C., Siribhakdi, K., Chauaviroj, S. and Charoenravat, A, 1997). These shear criteria imply that sinistral shear occurred on Lansang gneisses belt which claim to be the major left- lateral ductile shear zone. However, there is no clear evidence that intense this shear zone occurred under the high- temperature conditions as same as the Ailao Shan- Red River shear zone. The characteristic of left- lateral shear clearly occurred under the decreasing P/ T conditions and lead the shear planes present various obliquities to the foliation planes. The oblique shear plane strike more easterly compared to the trend of Lansang gneisses represented the C' planes. Beside, a part of this brittle- ductile left- lateral shear planes contained chlorite, calcsilicates and also marbles which deformed under low- temperature condition, thus it implied that cataclastic shear could be occurred in fine grained ribbons surrounding rounded porphyroclasts. All of these evidences suggested that the progressive left- lateral shear occurred along the

P/ T path (R. Lacassin, Maluski, H., Leloup, P. H., Tapponnier, P., Hinthong, C., Siribhakdi, K., Chauaviroj, S. and Charoenravat, A, 1997).

Based on (R. Lacassin, Leloup, & Tapponnier, 1993), an area of Mae Ping shear zone are marked by cores of metamorphic rocks which made of mylonitic paragneisses and orthogneisses with the steep foliation and clear left- lateral shear criteria. Beside, by the petrography and general structure studied on Lansang mylonitic gneisses by (R. Lacassin, Maluski, H., Leloup, P. H., Tapponnier, P., Hinthong, C., Siribhakdi, K., Chauaviroj, S. and Charoenravat, A, 1997), it can be concluded that the Lansang gneiss core is made up by strongly deformed metasediments (quartz-feldspar- biotite (Q- F- Bi) paragneisses, micaschists, calcsilicate rocks and marbles), orthogneisses, veins of pegmatite, quartz and microgranite which they dip steeply toward to the northeast and for the SW of the gneisses the foliation and banding are steep to nearly vertical.

The quartz- feldspar- biotite gneisses are the most frequent rocks as well as the calcsilicate rocks and marbles occurred as bands of laminated mylonites which parallel to the foliation or as the layering around gneisses and also are the interbanded with paragneisses, micaschists, deformed pegmatite veins and orthogneisses. The calcsilicate rocks compound with alternating green and brown bands of quartz, plagioclase, pyroxene, hornblende, calcite, muscovite and garnet (Campbell, 1976). In these rocks, from the microprobe analysis or amphibole/ plagioclase thermobarometry yielded an estimate of temperature for the high- grade metamorphism into $800 \pm 50^{\circ} \text{C}$ (R. Lacassin, Maluski, H., Leloup, P. H., Tapponnier, P., Hinthong, C., Siribhakdi, K., Chauaviroj, S. and Charoenravat, A, 1997).

Beside, marbles are made up by laminated dark rocks with mostly compound calcite. Both of them contain up the wide boudin of calcsilicate rocks and leucocratic granite. According to (Campbell, 1976) and (Ahrendt, 1993), the timing of high- grade metamorphism, migmatization and emplacement of leucocratic intrusion was occurred during the Precambrian followed by the intrusion of granodioritic rocks and from the U- Pb dating result showed that the high- grade metamorphism was occurred around 200 Ma, respectively.

Moreover, the characteristic of ductile deformation affect in all rock types of the Lansang gneisses as shown by strongly in steep foliation and nearly horizontal lineation on both calcsilicate and marble band which formed on the central part of the gneiss stripe. Along the Huai Lansang present clear macroscopic evidence of nearly horizontal stretching and shear, including with asymmetric boudinaged and pulled- apart elements. Also under the microscope the white and dark bands of calcsilicate rocks show the strongly fine grained. The white bands made up by quartz and stretching feldspar porphyroclasts and the dark bands are made of fine grained, calcitic matrix surrounding with small rounded porphyroclasts of K- feldspar, plagioclase, hornblende, pyroxene epidote, garnet and quartz. Because of all these structure it could imply that the grain boundary sliding has been the dominant deformation mechanism on this calcitic band which the mylonitization has not been involved by this calcite recrystallization (R. Lacassin, Maluski, H., Leloup, P. H., Tapponnier, P., Hinthong, C., Siribhakdi, K., Chauaviroj, S. and Charoenravat, A, 1997).

The characteristic of ductile deformation of the past penetration dominant feature in all rock types of Lansang gneiss as shown by paragneisses, micaschists and orthogneisses from Huai Lansang which present the left- lateral shear bands. Thus, both geochronological and strain quantitative analysis motivated studied on Lansang gneiss for model the tectonic evolution of this past penetration. The deformation is strong in the most deformable calcsilicate and marble band in central part of the gneiss stripe (R. Lacassin, Maluski, H., Leloup, P. H., Tapponnier, P., Hinthong, C., Siribhakdi, K., Chauaviroj, S. and Charoenravat, A, 1997). The granitic and pegmatitic veins are also deformed as same as gneisses. Under microscope study of (R. Lacassin, Maluski, H., Leloup, P. H., Tapponnier, P., Hinthong, C., Siribhakdi, K., Chauaviroj, S. and Charoenravat, A, 1997) found that the gneisses generally compound with biotite and elongated ribbons of quartz and feldspar that outline the stretching lineation together. Muscovite appears as sheared asymmetric crystals that sometimes also form trails of pull a part fragments. As well as quartz rich in gneisses and micaschists form ribbons of elongated quartz crystal with a shape fabric oblique to the foliation and banding of rock.

In addition boudinaged structure also clearly intense the left- lateral shears sense (R. Lacassin, Maluski, H., Leloup, P. H., Tapponnier, P., Hinthong, C., Siribhakdi, K., Chauaviroj, S. and Charoenravat, A, 1997) and a quantity of strain can be quantified by one- dimension strain equations. According to (R. Lacassin, Leloup, & Tapponnier, 1993), the amount of strain at Ailao- Shan- Red River shear zone and Mae Ping shear zone are 7 ± 3 and 7 ± 4 , respectively. Thus the direction of deformed structure was controlled by the direction of shearing and made these two zones have characteristic of left- lateral shear zone which have been interpreted to the result of India- Asia collision.

Moreover, (R. Lacassin, Maluski, H., Leloup, P. H., Tapponnier, P., Hinthong, C., Siribhakdi, K., Chauaviroj, S. and Charoenravat, A, 1997) studied in sense of microstructure of samples along Huai Lansang and found that the left- lateral shear sense clearly presented by rolling structure, boudinage structure, C or C' planes, deformed mica fishes and also the oblique shape fabrics of quartz. In marbles, the stretching leucogranite or quartz veins developed the rolling structure that connected into elongated tails which later gave the left- lateral shear sense. Moreover, the foliation structure refolded already into foliated marbles with boudins of mylonite, pegmatite, quartz and offset of the long occurrence of mylonitic fabrics can be intense the shear sense of this area.

2.2 The fundamentals of deformation and strain of rocks

Based on previous worked (e.g. R. Lacassin, Leloup, & Tapponnier, 1993) the amount of the direction and sense of movement that occurred in the shear zone can be analyzed by quantitative method that involved with mathematical equation for quantify the finite strain ellipse of deformed rocks from the geometry of the strain markers. Thus to earn the well understanding in strain quantitative analysis, the fundamentals of deformation and strain which including the definitions and explanation of deformation process choose be focused.

When geological materials for instance rock obtained force either from inside or outside their body, it started to accumulate strain inside and then responded it as known as deformation of rock. Thus, it could be said that deformation is the difference between deformed and undeformed state of rock and strain markers represent the evidence of it and be able to use later as a key or material in strain quantitative analysis. When deformation applied to the rocks in sense of volume, it could be classified in many ways for instance in sense of types of deformation which divided into rigid body deformation and non- rigid body deformation.

The rigid body deformation are shape and size of the object always constant after deformation occurred, thus the deformation style for instances rotation and translation are classified as rigid body deformation whereas distortion (or defined in term of strain) and dilation (volume change) are non- rigid body deformation (Fossen, 2010) (Fig. 2.1). The deformation styles are classified into homogeneous and heterogeneous deformation. For homogeneous deformation or homogeneous strain, all particles in rock that have originally straight or parallel lines will be the same proportion after deformation (Fig. 2.1). In addition, the strain ratio, volume change and area change will be constant too, vice versa, its heterogeneous deformation (Fossen, 2010).

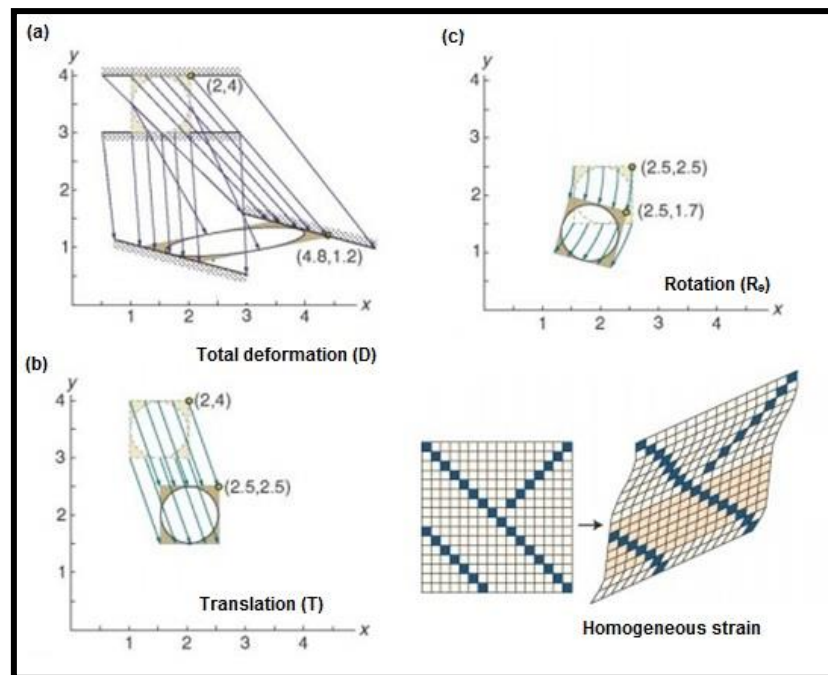


Figure 2. 1 Diagram (a) to (c) describes characteristic of rigid body deformation which translation and rotation are both rigid body deformation component. On right down corner of diagram describe the characteristic of homogeneous deformation (Modified from Fossen, 2010).

2.2.1 One and two- dimensional strain

Strain in one dimension concern about stretching and shortening of linear or straight objects which does not change in shape but change in length and including with change in shape of circle object into ellipse also described by the change in length of line of different orientation (Fossen, 2010). Besides, there are some specific mathematical terms that involved in strain quantitative analysis for instance elongation, extension, stretching and quadratic elongation.

Moreover, in two dimensions is an observation of strain in plane which rotation also the factor that involved in deformation process and the strain quantity described by angular shear (φ), shear strain (γ), area change and the strain ellipse. The strain ellipse describes a quantity of elongation in all direction in a plane of

homogeneous deformation which defined by a long x- axis and short y- axis and the ratio of the axes described the ellipticity of the ellipse (R) or strain ratio (R_s):

$$R = X/Y \quad (2- 1)$$

In case that $R= 1$ imply that no strain occurred and in case that there is shear applied on, the three deformation types are defined as; pure shear, simple shear and general or subsimple shear (Wallis, 1992) (Fig. 2.2).

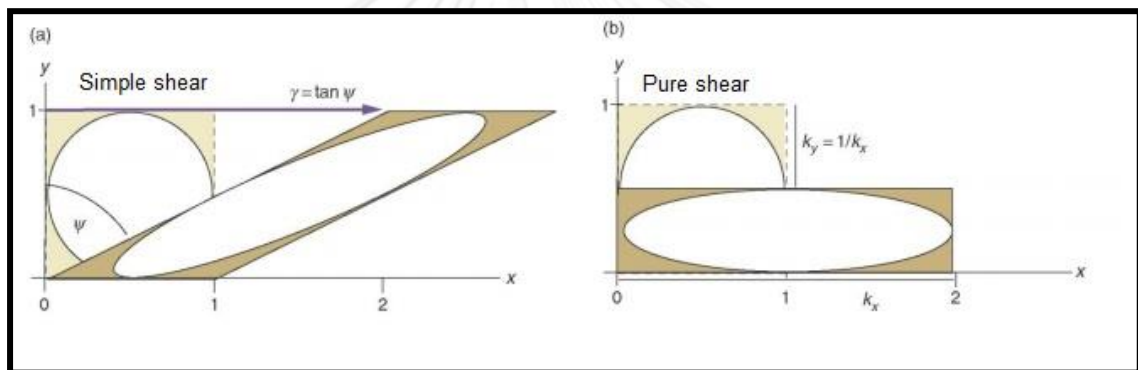


Figure 2. 2 Diagram (a) to (b) describe the characteristic and deformation process of rock when pure shear and simple shear applied on (Modified from Fossen, 2010).

Thus, strain marker in this case is the objects that have initial linear shape with variety of orientations or circular shape, for instance breccias and conglomerates rock. By the useful proposed of (Ramsay & Huber, 1983) nowadays there are many useful methods for quantified finite strain from this kind of strain markers and one of them are the (Fry, 1979) that will be described later in section 2.3.2.

2.2.2 Strain ellipsoid

The strain ellipsoid defined as the deformed shape of an imaginary sphere that has been deformed along with the rock in homogeneous deformation (Fossen, 2010). The shape of the strain ellipsoid refers how the deformation occurred for instance the oblate strain implies that flattening strain relates to the gravity- driven collapse. Besides, the orientation of the strain ellipsoid indicates which deformation types were occurred on rock. Therefore, when able to define the strain ellipsoid, the strain quantity can be quantified.

The strain ellipsoid has three orthogonal symmetry planes, called the principal planes of strain which intersected along three axes referred to the principal strain axes. Their values of length are called the principal stretches (ϵ) which defined by three vectors e_1, e_2, e_3 of the longest (X), intermediate (Y) and shortest (Z) axis of the ellipse respectively. When the ellipsoid is fixed, then the vectors will define length and orientation of the ellipsoid (Fig. 2.3). The strain ellipsoid use for identical the states of strain, called strain invariants where shear strain, volumetric strain and kinematic vorticity number (W_k) are the example of it and were focused on in many researchers.

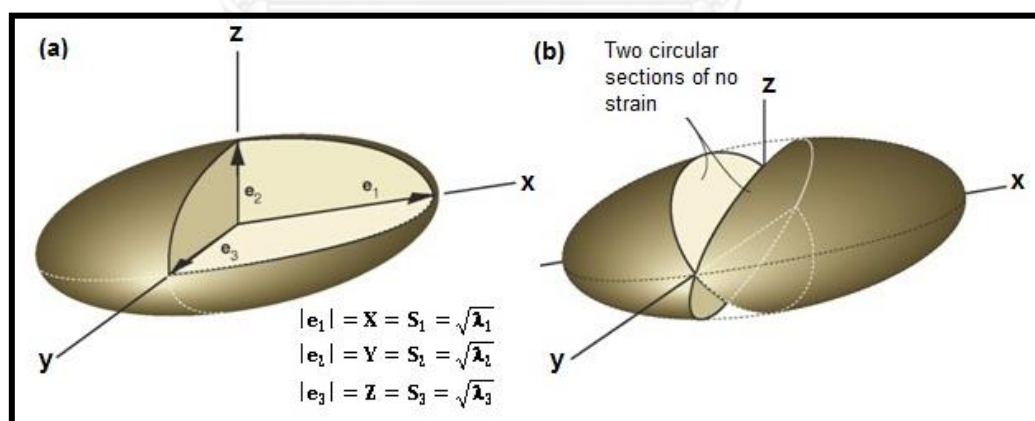


Figure 2. 3 Diagram (a) the strain ellipsoid and designation of the ellipsoid axes defined in terms of vector. Diagram (b) presents characteristic of two circular sections of strain ellipsoid that no strain (Modified from Fossen, 2010).

2.2.3 The application of kinematic vorticity number (W_k)

The deformation types; simple shear, pure shear and subsimple shear relate to both undeformed and deformed states of rocks where the place between them is the deformation history. To define the deformation history, the focus on the study of flow always involved. The flow parameter; vorticity is a parameter that occurred instantaneously during the deformation history, thus it could be implied the deformation type and history of rocks that had occurred on high strain zone (Fossen, 2010).

The function of vorticity defines how fast particles rotate during the deformation (Tikoff & Fossen, 1995). The term of vorticity comes from the field of fluid dynamics which is defined as a quantity of internal rotation during the deformation state as shown by the paddle wheel moving along with the flow (Fig. 2.4). In case that the wheel does not turn meant that the axis of the wheel parallel to the vorticity vector, then there is no rotating or vorticity and it implies the characteristic of coaxial deformation. However, if it does turn around, there is a vorticity (Fossen, 2010; Tikoff & Fossen, 1995).

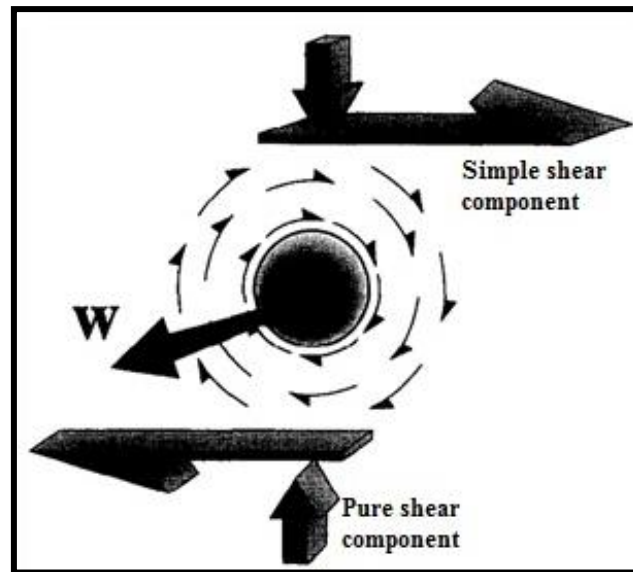


Figure 2. 4 Diagram presents the direction of vorticity vector and by the definition of vorticity, the homogeneous plane strain deformation can be divided into pure shear and simple shear component (Modified from Tikoff & Fossen, 1995).

Thus, it could be implied that the vorticity vector indicate both of the direction and rate of rotation of the fluid (Fossen, 2010; Tikoff & Fossen, 1995). The concept of vorticity as mentioned earlier implies the relationship between the finite strain and internal rotation as: the more strain, the more rotation and this relation is the function of kinematic vorticity number, W_k (Bailey & Eyster, 2003; Fossen, 2010).

A quantity of W_k can be quantified by the mathematical function between strain ratio (R_s) and the angle θ , angle between the longest axes of the strain ellipsoid and the deformation boundary (Sarkarinejad, 2007).

$$W_k = \sin \left\{ \tan^{-1} \left[\frac{\sin(2\theta)}{(R_s+1)/(R_s-1) - \cos(2\theta)} \right] \right\} \times \frac{(R_s+1)}{(R_s-1)} \quad (2- 2)$$

Based on this function the powerful function, W_k has been mentioned in previous studies (e.g. W. D. Means, Hobbs, Lister, & Williams, 1980; W. D Means, 1994; Wallis, 1992; Tikoff & Fossen, 1995; Bailey & Eyster, 2003; Sarkarinejad, 2007) that is a material for define the deformation type on high strain zone. The deformation type can be classified by value of W_k into three cases: $W_k = 0$ for pure shearing, $W_k = 1$ for simple shearing and $0 < W_k \leq 1$ for subsimple shearing (Wallis, 1992; Fossen & Tikoff, 1993; Bailey & Eyster, 2003; Sarkarinejad, 2007; Fossen, 2010).

Therefore, the progressive simple shear or simple shearing, the progressive pure shear (pure shearing) and the progressive subsimple shear (subsimpl shearing) are defined by the definition of W_k function. For simple shearing there is no stretching and shortening of planar structures or lines parallel to the shear plane. The lines will rotate toward the shear direction as same as the plane will rotate toward the shear plane, and then lead the longest axis of strain ellipse rotate toward the shear direction during the shearing history. For pure shearing, it is a two dimensional coaxial deformation which the stretching and shortening are symmetrically to the axes of strain ellipse and a strain marker will be parallel to one of the axes of the strain ellipse. Besides, for subsimpl shearing can be defined as the combination of simple shearing and pure shearing because it has internal rotation involved on the deformation state but lower than in case of simple shear (Fossen, 2010).

However, in nature the plane strain deformation always occurred in the combination of a vertical simple shearing and pure shearing which can be described in terms of transpressional- transtensional deformation. According to (Fossen & Tikoff, 1993), the transpressional deformation can be divided into pure shear- dominated and simple shear- dominated components which depend on the angle of convergence and value of W_k . For pure shear- dominated transpression, kinematic vorticity number ranging between $0 < W_k \leq 0.81$, whereas in simple shear- dominated transpression case, W_k ranging between $0.81 \leq W_k < 1$ (K. Sarkarinejad, Samani, Faghih, Grasmann, & Moradipoor, 2010).

2.3 Basic concept about strain quantitative analysis

During the last twenty years the motivation on finding more understanding on the deformation history, including with the conditions and mechanism that occurred significantly on high- strain zone, the number of techniques for quantify finite strain in deformed rocks are increased (Bailey & Eyster, 2003; Erslev, 1988). The strain quantitative analysis of rocks corroborated with the function of kinematic vorticity number offer an opportunity to define the state of strain in rocks, the deformation types and also the deformation history by using the mathematical equation quantify the finite strain on high strain zone from the different geometry of shear criteria; strain marker.

2.3.1 Strain markers and strain in one dimension

The geometric description of strain marker which concerns about the movement of rock particles during the deformation state and the knowledge about the change in shape before deformation occurs until the end of it are important parameters in strain analysis. Strain markers on deformed rocks represent how much rocks have been strained and information about the nature of the deformation that they were obtained. Based on this data the model and a series of studies which focus on the deformation history on the shear zone will more understanding and can be defined a state of strain (Fossen, 2010).

In one dimension, strain markers are stretching lines or linear objects, for instance boudinaged dikes or layers, linear fossils and also linear minerals which do not change in shape but changes in length. Therefore, the strain analysis in this case focuses on reconstruction the original length of markers which then can quantify the value of stretching or shortening. Meanwhile in two- dimensional strain analysis, the strain markers are an object that able to define initial shape or linear markers with a various orientation for instance conglomerates, breccias or oolites. Besides, two- dimension strain can also quantify from one- dimension data which have different directions in same plane (Fossen, 2010).

As mentioned earlier, the concept of one- dimensional strain analysis is about reconstruction the initial length of the objects. The specific terms that involve with this reconstruction are elongation, extension, stretching and quadratic elongation. Elongation (e or \mathcal{E}) of a line is use to define the relationship between the length of the line before deformation (l_0) and after deformation (l) as below (Fossen, 2010):

$$e = (l - l_0)/l_0 \quad (2-3)$$

Extension of a line is identical to elongation when the elongation of a horizontal refers the extension. Moreover, stretching (S) of a line is defining as a ratio of length after deformation (l) and length before deformation (l_0):

$$S = l/l_0 \quad (2-4)$$

Quadratic elongation (λ) is defining as the square of the stretching:

$$\lambda = S^2 \quad (2-5)$$

2.3.2 Strain in two dimension

There are shearing and rotation involved in deformation state as mentioned earlier (Fossen, 2010). When shear applied on object, the decreasing occurred on object's volume and increasing in the object's pressure that lead the change in angle between two originally perpendicular lines which could be quantities expressed by function of angular shear (φ) and then a shear strain (γ) can be calculated. In addition, the strain ellipse is the way to define that rock obtained or non- obtained

strain inside and by the proposed of (Ramsay & Huber, 1983) there are many useful methods for create strain ellipse and quantified finite strain from strain markers.

The Fry method (Fry, 1979) is one of all useful and simply modern structural techniques for quantified the finite strain in deformed rocks as mentioned by (Ramsay & Huber, 1983) which was applied from the nearest- neighbor centre- to- centre technique (Sarkarinejad, 2007) and proposed by Norman Fry in 1979. This powerful and useful method was applied for quantified finite strain of rocks from rigid particles for instance quartz grains, tillites or pebbles in conglomerates (Genier & Epard, 2007). This method works on a plot of the position of each particle center with respect to a particle put at the origin, then the origin repeated placed on others particle center and plot the relative position of every other particle center (Fig. 2.5). This product called a Fry diagram which presents an elliptical vacancy field around the origin and for homogeneous deformation these vacancy field is representative of finite strain ellipse (Erslev, 1988; Genier & Epard, 2007) (Fig. 2.6).

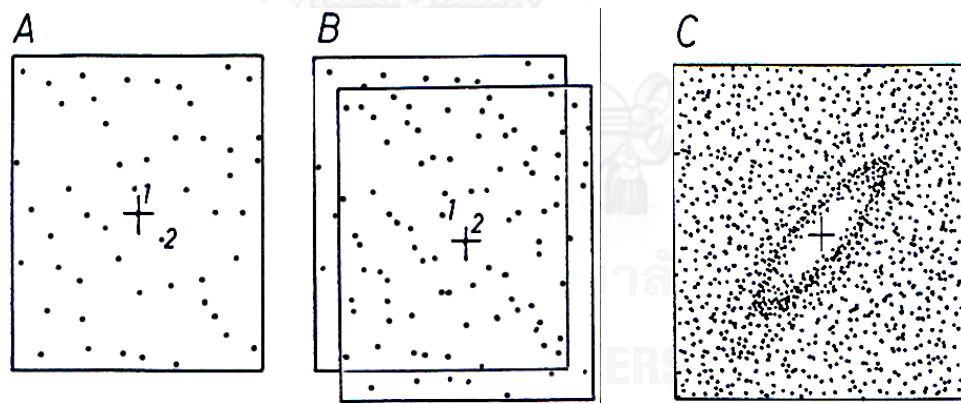


Figure 2. 5 Diagram (a) and (b) describes the methodology of (Fry, 1979) for quantify the finite strain. Diagram (c) presents the product of (Fry, 1979); the vacancy field or strain ellipsoid of rock (Modified from Ramsay & Huber, 1983).

The successful and clearly result of an elliptical vacancy field of Fry diagram mentioned earlier that depends on size, number and pattern of natural particles center distribution. For homogeneous deformation, the distribution type and number of particles center mentioned as anticlustered and isotropic which refer that the deposition of particle occurred on random pattern (Fry, 1979; Erslev, 1988; Genier & Epard, 2007) and about hundreds of particles would give a strongly anticlustered distribution and clearly vacancy field of Fry diagram respectively (R. Lacassin & Van Den Driessche, 1983). Moreover, for the size distribution, in generally the large grains distribution tends to be more anticlustered (Crespi, 1986). However, in cases of sorting, packed or well sorted particles do not mention that always produce a successful result of Fry diagram (Genier & Epard, 2007).

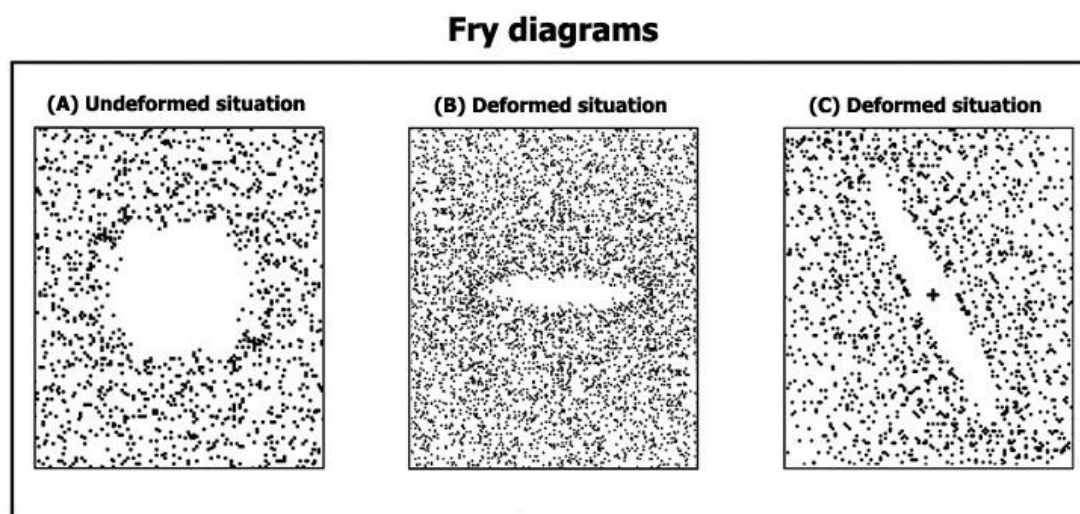


Figure 2. 6 Diagram (A) describes the product of (Fry, 1979); the Fry diagram for undeformed situation. Diagram (B) and (C) describes the product of (Fry, 1979) for deformed by pure shear and simple shear, respectively (Modified from Genier & Epard, 2007).

The product of (Fry, 1979) or strain ellipsoid of rock consisting of finite strain ratio (R_s) and the angle (θ) component. The finite strain ratios estimated from the ratios of strain ellipsoid axes in Fry's plot and the value of vector in all strain ellipsoid axes is: $X>Y>Z$ which the ratios of this minimum and maximum distance are called X/Y and Y/Z strain ratios. Besides, θ also measure from strain ellipsoid axes which described as a degree between the longest axes of strain ellipsoid and the plane boundary. Therefore, when the finite strain ratio and the angle θ were quantified, then the function of kinematic vorticity number able to define followed by the mathematical function as mentioned earlier which will give more understand and the better model of ductile deformation history (Bailey & Eyster, 2003).

2.4 Application of Fry method

In late 1970s, one of the strain quantitative analyses of rocks was proposed by Norman Fry for quantify the finite strain of rocks from the strain marker of rock; deformed rigid object or mineral. The deformed mineral or tectonites individual crystal reveals the effected from shear that rocks in the area of shear zone were obtained. The characteristic of mineral or object that suitable for analyzed by (Fry, 1979) are random, anticlustering distribution and also have homogeneous deformation. Fry's method mentioned to be the simple and accurate quantitative method, thus later there are many studies used, applied and developed the Fry's method on the high- strain zone.

According to (Hanna & Fry, 1979) applied and compared the variety of methods in two- dimensional strain analysis of deformed oolitic limestone from Southwest Dyfed and adjacent areas which shown that (Fry, 1979) and (Dunnet & Siddans, 1971) are the best method to use in quantified finite strain of rocks on that area. Nevertheless, when compared between these two methods, (Fry, 1979) is better and suitable than (Dunnet & Siddans, 1971) because it can apply in many types of rock and the methodology doesn't complicate. (Crespi, 1986) and (Erslev, 1988) studied on the patterns of natural point distributions in order to how degrees

of anticlustering of point distributions affect the character or shape of Fry diagrams. The result is the deposition, spacing, size variations, shape and sorting of mineral also involved with the natural point distributions of rock, especially by size variations and imperfect sorting will decrease the anticlustering of natural aggregates.

Later, (Ailleres & Champenois, 1994) used image processing method to normalize Fry diagrams resolution into best fitted characteristics ellipse. Then, (Ghaleb & Fry, 1995) presented a useful program for the better understand in Fry's plot: CSTRAIN program which written in FORTRAN 77 for used to calculate two-dimension isotropic distributions with different degrees of anticlustering, including with or without rotation and shown it from random to strongly anticlustered distributions.

Moreover, (R. Lacassin & Van Den Driessche, 1983) used (Fry, 1979) determine deformed gneissic rocks from different porphyroid gneiss samples on the southern Massif Central, France. The result shown that the density of mineral in ranged of 100 to 400 gave the best fitted strain ellipse and the ellipsoids are close to both plane strain and constriction field which are characterized by k parameter. After that, (Genier & Epard, 2007) used Morishita diagram test homogeneity characteristic on K-feldspars phenocrysts of both deformed porphyritic granites from Elba and orthogneiss from Alps, Switzerland and found that it satisfy to use as a strain marker to quantify strain with (Fry, 1979). The result of this study is shown in form of strain ellipse which has value between 2.8 to 5.3.

Moreover, there are many study reviewed and proposed the relative between the finite strain ratio (R_s) and the angles between the long axis of the strain ellipse and boundary which shown in form of kinematic vorticity number (W_k). According to (W. D. Means, Hobbs, Lister, & Williams, 1980) described the deformation history of rocks by using this relative into cases of coaxial history, $W_k = 0$, $W_k > 0$ for non-coaxial and $W_k = 1$ for simple shearing. Later, (W. D Means, 1994) estimated the kinematic vorticity number of naturally deformed rocks in different locality and characterized the deformation type by kinematic vorticity number which W_k ranging from 0.35 to 0.9, indicate character between pure shear and simple shear.

The usefulness of kinematic vorticity number in describing the deformation type of rock was used widely in many studies. According to (Wallis, 1992) measured the finite strain in deformed metachert from Sanbagawa Belt, Southwest Japan and quantified the kinematic vorticity number from the estimates of degree of non-coaxiality during deformation and the finite strain. The consistent result shows that the deformation was between simple shear and pure shear.

(Bailey & Eyster, 2003) quantified the finite strain of granitic mylonites from Pinaleno Mountains metamorphic core complex in southeastern Arizona and used the kinematic vorticity number to describe the deformation type that had occurred on this area. The results show that for protomylonites and mylonites, the kinematic vorticity number (W_k) ranged from 0.6 to 0.9 and for ultramylonites, W_k ranged from 0.1 to 0.3, thus the deformation type on this area recorded general shear deformation (W_k range between 0- 1.0). In addition, (Sarkarinejad, 2007) applied Fry method to quantify finite strain from microfossils of the Chah Sabz anticline, northeast of the Ghouri area and used kinematic vorticity number to describe the deformation type along the Zagros orogenic belt, the Ghouri area in southwest Iran. The result shows that the value of angle θ , an angle between the maximum horizontal axes of the instantaneous strain ellipsoid and the transpressional zone boundary is 32° guarantee the pure shear dominated transpression with a high proportion of simple shear components.

Nevertheless, (Tikoff & Fossen, 1995) presented that in case of steady-state deformation the kinematic vorticity number, (W_k) can be estimated from finite strain in both two and three-dimensional geological deformations, but the knowledge of deformation types in case of three-dimensional deformation also required. Therefore, this work discussed on the use and limitations of the kinematic vorticity number in three-dimensions. Besides, (Tikoff & Fossen, 1999) proposed the twelve idealized end member of three-dimensional deformations followed by the concepts of kinematic axes and strain facies and also involved with the combination of orthogonal simple shear component and coaxial component: constriction, flattening and pure shear.

CHAPTER III

METHODOLOGY AND DATA USED

The methodology as well as the data used is described in section 3.1. Moreover, in Section 3.2 described about the data collection of all rock samples and equipment that involved in this research. Finally, the processing of strain quantitative analysis of deformed rocks in Lansang Waterfall is discussed in section 3.3.

3.1 Methodology

The methodology of this study divides into three main parts. The first part is field investigation on area of Lansang waterfall; Lansang National Park, Tak, northwestern Thailand for collecting rock sample followed by traverse line method and recording the orientation and other physical data of both rock samples and outcrop which are macro scale study. Besides, preparing all rock samples into thin section for microscope laboratory involved in this part. Then is micro scale study under microscope followed by Fry's method (Fry, 1979) for selection strain markers which later is a source for quantifies the finite strain of rocks in this study area. In this part each thin section will be sampling at least 3 times for quantify in sense of statistical analysis.

Finally, strain markers from all samples will be used for quantify the finite strain of rock followed the Fry's method and later the Fry's product will be represented by the strain ellipsoid of rock. Two values from strain ellipsoid; the strain ratio (R_s) and the angle (θ) are quantified by the ratio between the strain ellipse axes and the angle between the longest axes of the strain ellipse and the deformation boundary. Therefore, the deformation history that occurred on this area will be discussed and concluded by the function of kinematic vorticity number (W_k) which quantified by the mathematical function of two relative factors; the strain ratio and angle θ of the strain ellipse. All of those steps can be concluded and described by figure 3.1, a flow chart of this research methodology.

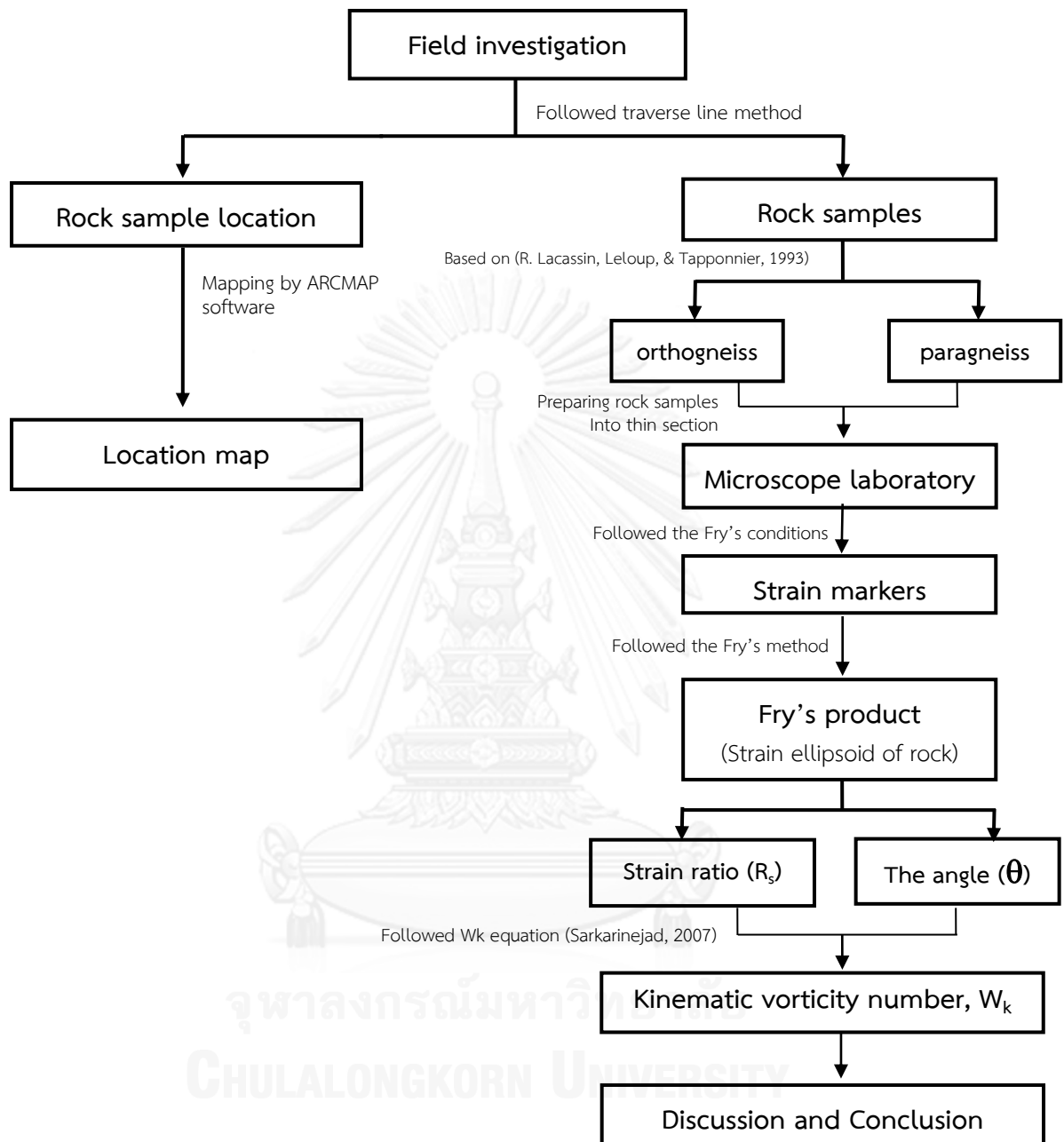


Figure 3. 1 Methodological flow chart of this research

3.2 Data Collection and Equipment Used

3.2.1 Field investigation

In part of field investigation involve with collecting rock samples followed by traverse line method, including with orientation and Global Positioning System (GPS) location of rock samples. Followed by the traverse line method the structural geology and deformed rocks of Lansang Waterfall will be investigated and collected as shown by Figure 3.2. The rock sample locations of this research will be recorded by Global Positioning System (GPS) measurement and later will map with the geological map of northwestern Thailand by ARCGIS software for describe the geological characteristic of Lansang Waterfall and sample locations map.

In addition, all rock samples will be orientated, classified rock type and recorded physical characteristic from hand specimens. The classification based on (R. Lacassin, Leloup, & Tapponnier, 1993) and texture identification which equigranular texture of quartz, feldspar and biotite indicate the mineralogy of orthogneiss. While the alternating of felsic and mafic bands of minerals indicate the mineralogy of paragneiss. Thus, rock sample of this research can be divided into orthogneiss and paragneiss which later will be prepared into thin section for selection strain marker under microscope.

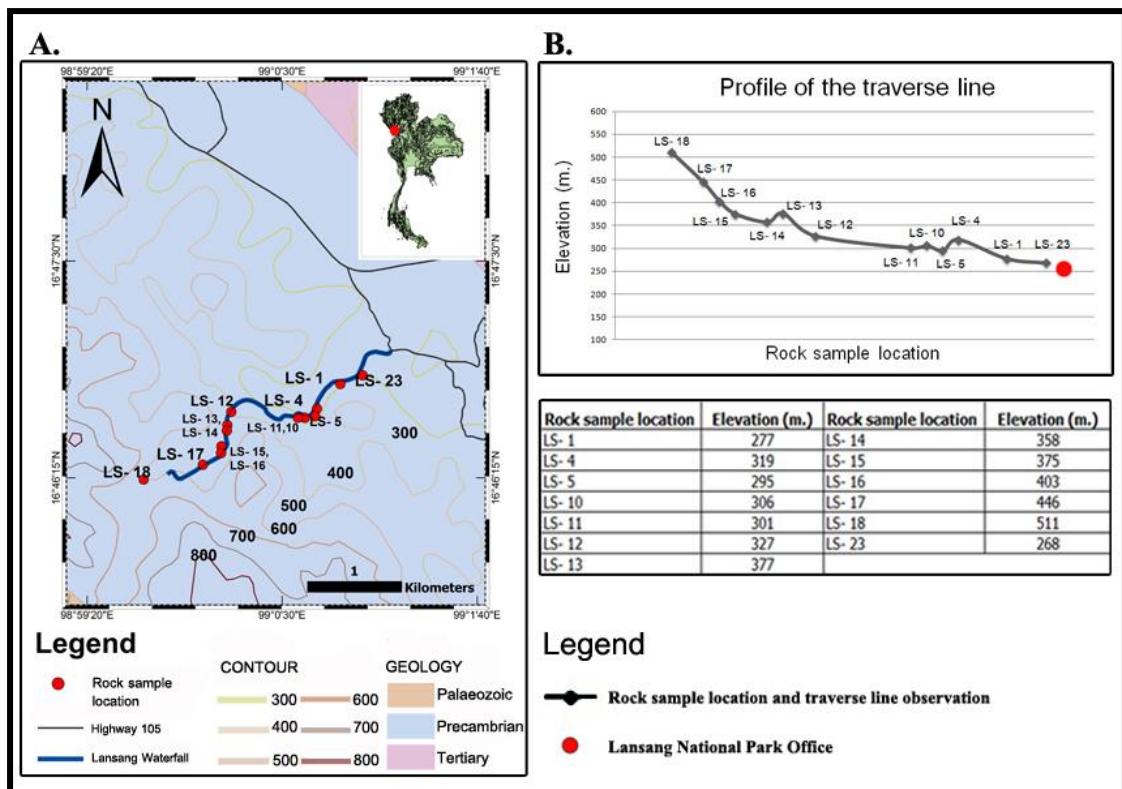


Figure 3. 2 Diagram (A) Geological map of northwestern Thailand mapped together with the traverse line observation (blue line) along the profile of Lansang Waterfall within the Lansang National Park, Tak and adjacent area. Diagram (B) presents profile of the traverse line along the Lansang Waterfall including with elevation of all sample locations (Modified from Resources, 1999).

3.2.2 Preparing rock samples for strain quantitative analysis

The methodology of (Fry, 1979) works under microscope for select rigid particles which appropriate to Fry's conditions to be a strain marker, thus all rock samples must be prepared into thin section as followed by this step. After clean up the machine, then using the Buehler slab saw cut all oriented rock samples into slab which cut perpendicular to foliation and parallel to the trending of lineation and will give the best plane to view shear sense movement and direction that occurred on rocks. Then use rock-cutting blade resize the slabs into chips which have the size

correct to a glass slide. Before glue the chip to the slide, the chips are grinded for remove marks from the saw blade using 240 grit grinding wheel, then use the epoxy glue glues slide and chip together and let it cures for 2 days. Thus, it led a rock chip epoxied to a glass slide, then grin chip that remains on slide away as much as possible. Finally, the slide is scrubbed by Silicon Carbide powder number 600 and number 1000 (Appendix 1). Figure3.3 present flow chart of preparing rock samples into thin section.

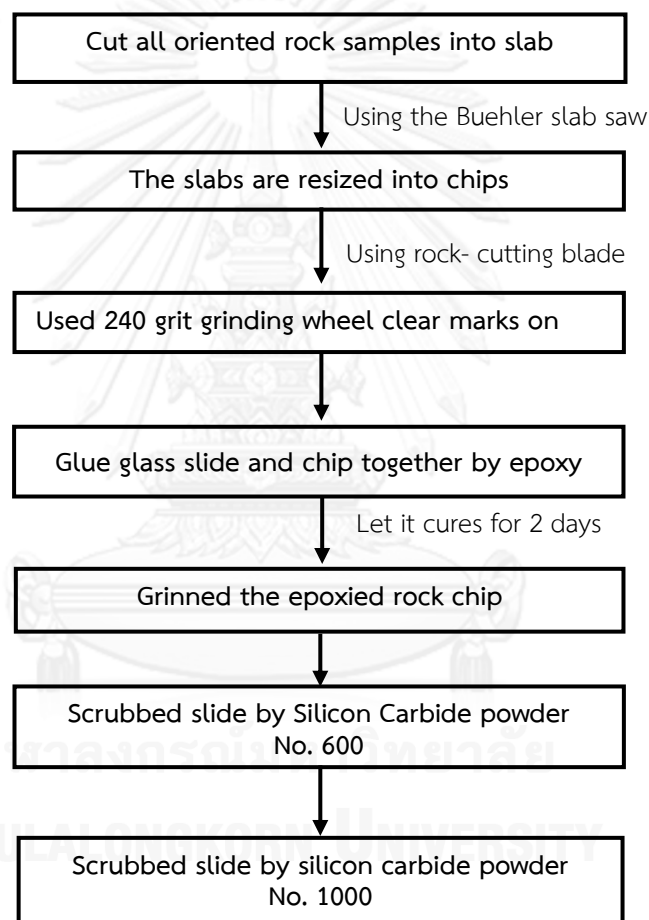


Figure 3. 3 Flow chart of preparing rock samples into thin section.

3.3 The processing of strain quantitative analysis

3.3.1 Selection strain markers of rocks from microscope

Since the proposed of (Ramsay & Huber, 1983), the number of method for quantify the finite strain of rock in sense of one, two or three- dimension are increasing. The Fry's method (Fry, 1979) is one of them which mainly focus in sense of two- dimension and were mentioned widely by previous studied that are sample and accurate method. Besides, the previous strain quantitative studied in area of Mae Ping shear zone focus only in one- dimension and never applied Fry's method before, thus it motivated this research to use Fry's method for the first time quantify the finite strain of rock in area of Lansang Waterfall, Tak, northwestern Thailand.

The Fry's method was derived from the technique of nearest- neighbor centre- to- centre which can be presented the relative in distance between the center point of each rigid particles or minerals which also same size and packing in same conditions, thus when the homogeneous deformation applied on will be lead the change in this relative occurred and review how much strained inside (Ramsay & Huber, 1983). According to Figure 3.4 the rigid particles or minerals have been constructed to two- dimension close packing circles with equal in radius. When mark a line from the center point of A particle to surrounding particles or neighbor particle will show their relative in distance. In case that homogeneous deformation applied on these particles, the distance between particle centers are changed by strain that particles accumulated and followed by Fry's method a quantity of strain will be quantified and represented by strain ellipsoid.

Therefore, to select the strain markers for strain quantitative analysis using Fry's method, the Fry's condition requires the homogeneously deformed of strain marker and the distribution of marker center that satisfy with isotropic and anticlustered (Genier & Epard, 2007; Ramsay & Huber, 1983). Based on previous studied that applied Fry's method, the characteristic of recrystallized mineral for instance quartz was mentioned that satisfies with Fry's condition for used as strain marker in Fry analysis. Beside, deformed rocks for instance gneiss are rich in quartz grains which will give a clearly Fry's plot and the mineralogy of quartz that no

cleavage and strongly to the deformation temperature of Mae Ping shear zone advantage to observe the minimum distance between different grains of strain markers. Therefore, recrystallized quartz grains were mentioned that appropriate to Fry's condition and can be used as strain marker of rock (Genier & Epard, 2007; R. Lacassin & Van Den Driessche, 1983). However, (R. Lacassin & Van Den Driessche, 1983) mentioned that the broken quartz grains which are coarse grain were eliminated to use as strain marker.

Under the microscope laboratory, crossed polarized light and plane-polarized light are material which participated in selection rigid particles or deformed minerals to use as strain markers of rock. The crossed polarized light and plane-polarized light under microscope use for determine the mineral grains relief and separate each grain boundary. When the strain markers which have characteristic as shown in Figure 3.4 were selected, then are the steps to establish the strain ellipsoid of this deformed rocks as mentioned earlier in chapter II. Finally, from the strain ellipsoid followed by Fry's method, a quantity of strain can be defined.

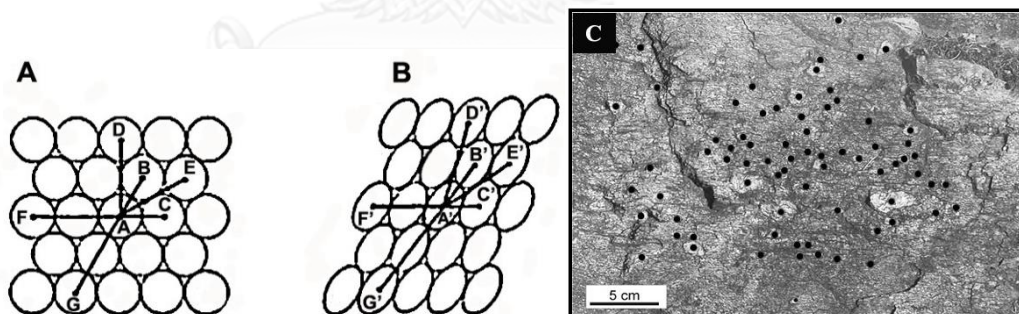


Figure 3. 4 Diagram describes the Fry's theory which diagram (A) describe the relative between the center points of rigid particle A to the surrounding particles during the undeformed state while diagram (B) describe the relative between the center points of each particles during the homogeneous deformation state. Diagram (C) presents the rigid particles or deformed minerals that appropriate to use as strain marker for Fry analysis (Modified from Ramsay & Huber, 1983; Genier & Epard, 2007).

3.3.2 Calculation of strain ratio (R_s) and the angle (θ) from strain ellipsoid

After selected the recrystallized quartz grains to be the strain marker of rocks in this area, then is the strain quantitative analysis using Fry's method. Two important factors; the strain ratio (R_s) and the angle (θ) of strain ellipsoid are quantified follow the Fry's methodology. The Fry's methodology works based on a plot of each strain marker center with respect to the first selected marker which put at the origin, then when the origin repeat place on others center, the relative in distance between all marker centers will be plotted.

Followed this idea, all recrystallized quartz grain centers are marked on the first tracing paper, and later the paper is covered by second tracing paper which marked the center of paper already. Move it on first selected recrystallized quartz grain center and then mark all the rest of selected grain center. After that move the center of second tracing paper without rotation to the other selected recrystallized quartz grain center and do it repeatedly. Figure 3.5 Methodological flow chart of strain quantitative analysis followed by Fry's method (Appendix 2).

By the relative in distance between different grains of strain markers produces a Fry's plot or Fry diagram which presents an elliptical vacancy field around the origin and for homogeneous deformation this vacancy field represent the finite strain ellipse. The axes ratios (X/Y) or strain ratios, a ratio between the longest and shortest axes of strain ellipse and the angles between the longest axes of the strain ellipse and deformation boundary will quantify as shown by Figure 3.6.

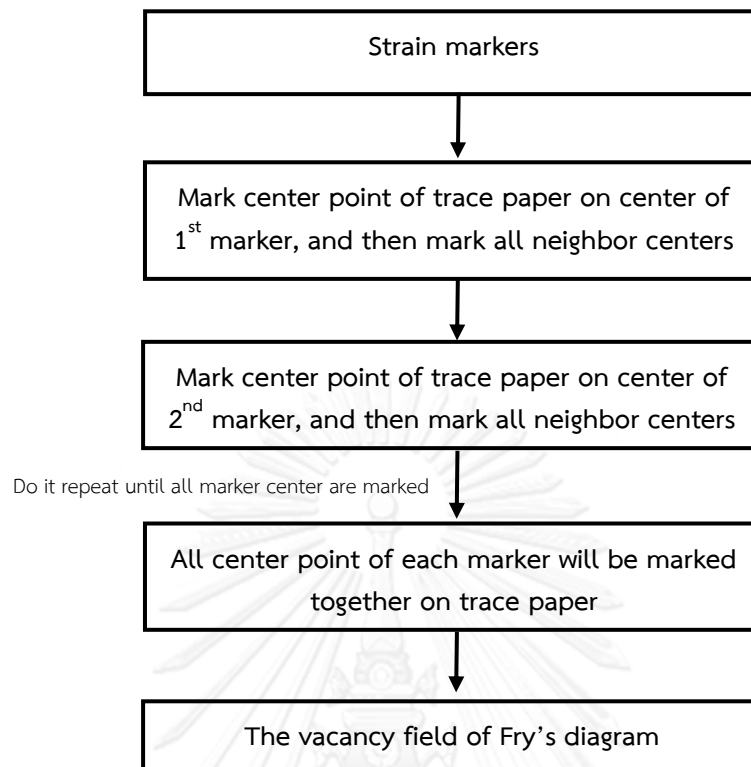


Figure 3. 5 Methodological flow chart of Fry's method.

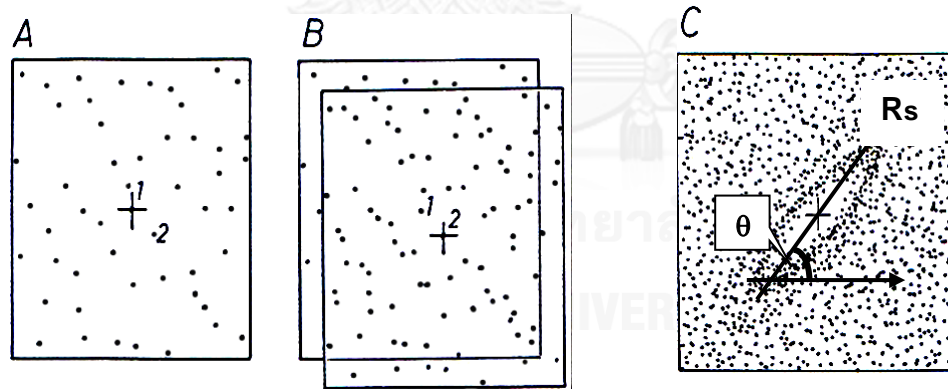


Figure 3. 6 Diagram (A) and (B) describe the Fry methodology which the product of Fry represented by the finite strain ellipsoid presenting in diagram (C). Diagram (C) presents strain ellipsoid of rock which consisting of the longest axes, shortest axes and angle (θ), an angle between the longest axes and deformation boundary of the ellipse (Modified from Ramsay & Huber, 1983).

3.3.3 Calculation of kinematic vorticity number (W_k)

The relationship between the value of strain ratio and the angle (θ) of strain ellipsoid can be described by the function of kinematic vorticity number (W_k) which use as a material for describe the deformation history; the deformation type and sense of shear that occurred on this area. The quantity of W_k is in ranged between $0 < W_k \leq 1$ which the deformation type can be classified into three cases; $W_k = 0$ for pure shearing, $W_k = 1$ for simple shearing and $0 < W_k \leq 1$ for subsimple shearing.

To calculate a quantity of kinematic vorticity number, this mathematical equation has been used for all samples (Sarkarinejad, 2007):

$$W_k = \sin \left\{ \tan^{-1} \left[\frac{\sin(2\theta)}{(R_s+1)/(R_s-1) - \cos(2\theta)} \right] \right\} \times \frac{(R_s+1)}{(R_s-1)} \quad (3- 1)$$

CHAPTER IV

RESULTS

After the field investigation, the strain quantitative analysis by using the Fry's methodology, and quantified the kinematic vorticity number by mathematical function as described earlier in chapter II and III, the results of this research present in this chapter. This chapter composed of three sections: (1) the data collecting from field investigation, (2) finite strain ratio, R_s and the angle θ , (3) kinematic vorticity number, W_k .

4.1 The data collecting from field investigation

After the field investigation for collecting rock samples followed by traverse line method, the structural geology and deformed rocks of Lansang Waterfall were investigated and collected as shown by Figure 4.1- 4.11. Based on the field investigation and texture identification as mentioned in chapter 3, the rocks in area of Lansang Waterfall can be divided into two groups: orthogneiss and paragneiss as shown by Table 4.1. Besides, the rock sample locations of this research were recorded by Global Positioning System (GPS) measurement (Table 4.1) and later mapped together with the geological map of northwestern Thailand by ARCMAP software for imply the geological characteristic of Lansang Waterfall and rock sample locations map (Figure 4.12).

Rock sample LS- 1 located on $16^{\circ} 46' 47''$ N, $99^{\circ} 00' 50''$ E and high 277 m. from the mean sea level with the foliation about $335/ 65^{\circ}$ SW. Based on field observation, the minerals; quartz, feldspar and biotite of rocks on this outcrop intense an equigranular texture. Besides, the kinematic indicator as σ - clast applied in rock and indicated the sinistral strike- slip deformation.

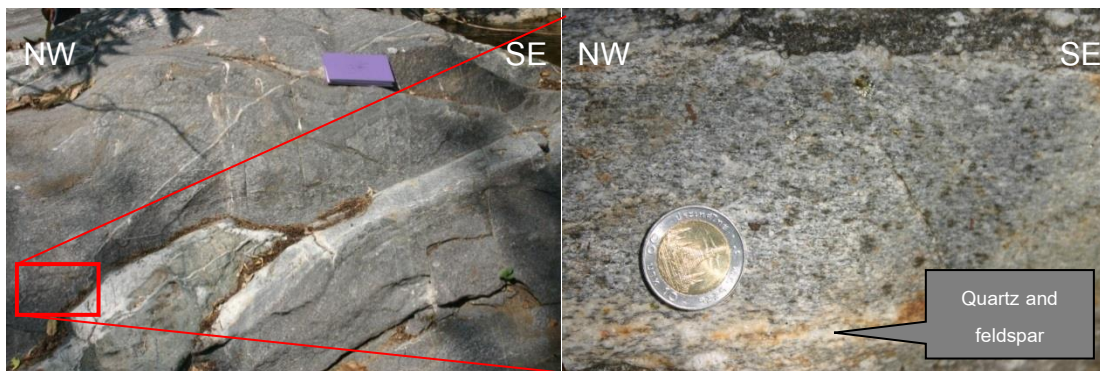


Figure 4. 1 (Left) an outcrop of rock sample location LS-1. (Right) Quartz and feldspar on rock sample LS- 1 have equigranular texture which is the mineralogy of orthogneiss.

Rock sample LS- 4 located not too far from LS- 1 but higher than (Elev. = 319 m.) on $16^{\circ} 46' 38''$ N, $99^{\circ} 00' 42''$ E with the foliation is about $323/ 65^{\circ}$ SW. The mineralogy of rock on this outcrop presented the dominant porphyroblastic texture of quartz and feldspar or augen texture and the kinematic indicator as σ - clast also applied in rock and indicated that sinistral strike- slip deformation was applied on.



Figure 4. 2 (Left) an outcrop of rock sample location number LS-4. (Right) rock sample number LS- 4 presents dominant feature of porphyroblastic texture of quartz and feldspar in biotite.

Rock sample LS- 5 located nearly LS- 4 but lower than (Elev. = 295 m.) on $16^{\circ} 46' 36''$ N, $99^{\circ} 00' 41''$ E. The foliation of the outcrop is about $338/ 71^{\circ}$ SW and the mineralogy of rock presented the dominant porphyroblastic texture of quartz and feldspar as same as mineralogy of LS- 4. Besides, the kinematic indicator not only σ -clast but also s-c fabric applied on rock and indicated sinistral strike- slip deformation.

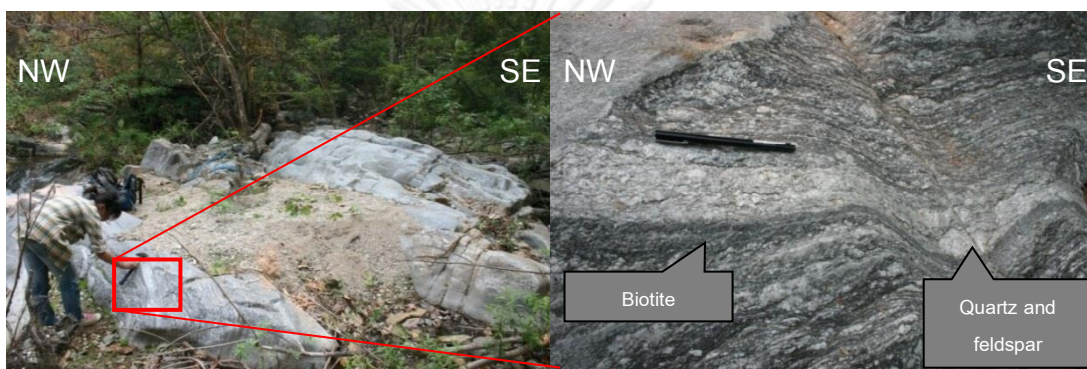


Figure 4. 3 (Left) an outcrop of rock sample location number LS-5. (Right) rock sample number LS- 5 presents dominant feature of augen texture or porphyroblastic texture of quartz and feldspar.

Nearby the previous outcrop, rock sample LS- 10 located on $16^{\circ} 46' 35''$ N, $99^{\circ} 00' 38''$ E and high from the mean sea level 306 m. Based on field observation, the foliation is about $338/ 69^{\circ}$ SW and the minerals such as quartz, feldspar and biotite of rocks on this outcrop intense an equigranular texture and quartz usually deformed into the σ -clast which indicated the sinistral strike- slip deformation.



Figure 4. 4 (Left) an outcrop of rock sample location number LS-10. (Right) rock sample number LS- 10 mainly consist equigranular texture of quartz and feldspar which represent the common characteristic of orthogneiss.

Next to LS- 10 is rock sample LS- 11 which located nearby on $16^{\circ} 46' 35''$ N, $99^{\circ} 00' 35''$ E and high from the mean sea level 301 m. The foliation of the outcrop is about $343/ 53^{\circ}$ and the minerals such as quartz, feldspar and biotite of rocks on this outcrop intense an equigranular texture and quartz usually deformed into the σ - clast and s-c fabric which indicated and assured the sinistral strike- slip deformation.

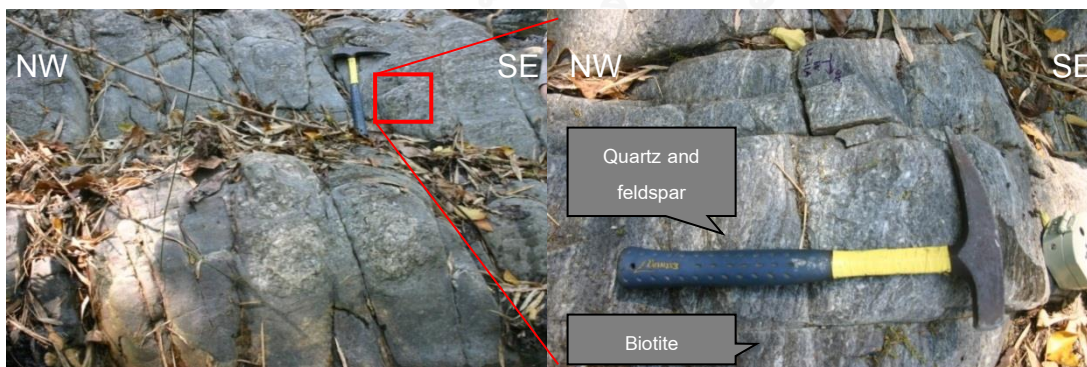


Figure 4. 5 (Left) an outcrop of rock sample location number LS-11. (Right) rock sample number LS- 11 mainly consists fine grained of quartz and feldspar which clearly intense the mineralogy of orthogneiss.

Rock sample LS- 12 called Lansang Waterfall where located higher and farther than LS- 11 on $16^{\circ} 46' 37''$ N, $99^{\circ} 00' 11''$ E, thus classified as the first location of second group of rock sample location. The foliation of outcrop is about $325/ 58^{\circ}$ SW and the mineralogy intense equigranular texture of quartz and feldspar and the s-c fabric which is the kinematic indicator applied on felsic band and indicated the sinistral strike- slip deformation.

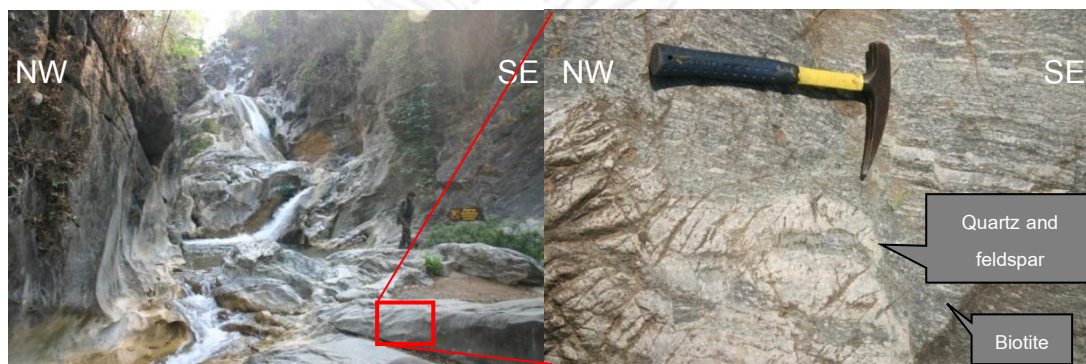


Figure 4. 6 (Left) an outcrop of rock sample location number LS-12. (Right) rock sample mainly consists of white fine grained of quartz and feldspar which clearly intense the mineralogy of orthogneiss within this outcrop.

Rock sample LS- 13 located higher (Elev. = 377 m.) on $16^{\circ} 46' 33''$ N, $99^{\circ} 00' 10''$ E. The foliation of outcrop is about $327/ 86^{\circ}$ and the mineralogy of rock on this area is different from previous locations that could not defined grain relief but has the alternating band of felsic band and mafic band, thus rock type on this area was classified as paragneiss. Besides, the asymmetric fold applied on this area and indicated sinistral strike- slip deformation.

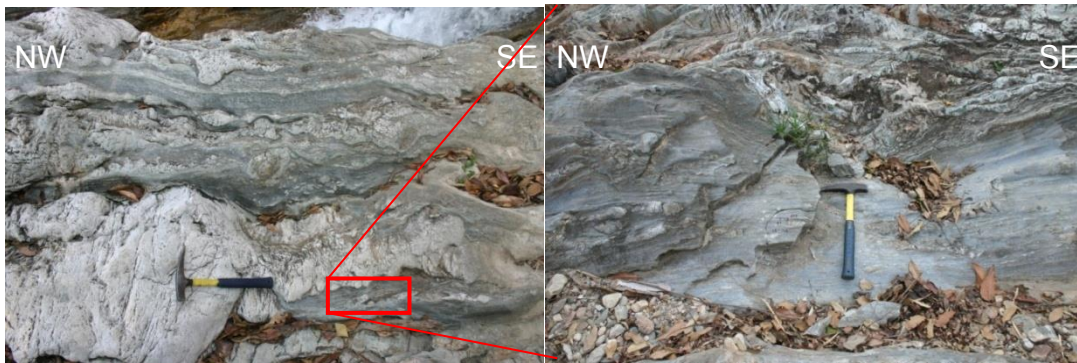


Figure 4. 7 (Left) an outcrop of rock sample location number LS-13. (Right) rock sample number LS- 13 presents dominant feature of paragneiss within this outcrop.

Rock sample LS- 14 located on $16^{\circ} 46' 31''$ N, $99^{\circ} 00' 10''$ E with the elevation 358 m. nearby LS- 13 and has the same mineralogy and some structural with LS- 13. The foliation of the outcrop is about $333/50^{\circ}$ SW and the asymmetric fold applied in large scale on paragneiss and a part of them indicated that the sinistral strike- slip deformation was applied along the Lansang Waterfall.



Figure 4. 8 (Left) an outcrop of rock sample location number LS-14. (Right) rock sample number LS- 14 mostly consist the characteristic of paragneiss within this outcrop.

Rock sample LS- 15 located on $16^{\circ} 46' 25''$ N, $99^{\circ} 00' 08''$ E with an elevation 375 m. from the mean sea level. On this location the foliation is about $313/55^{\circ}$ SW and the alternating band of felsic and mafic band of mineral clearly intense on large scale of paragneiss as shown in figure 4.9 (right). Besides, the s-c fabric and rolling structure on paragneiss indicated the sinistral strike- slip deformation.



Figure 4. 9 (Left) present the outcrop of rock sample location number LS-15. (Right) most of rock samples within this outcrop present the dominant feature of paragneiss.

Next to is rock sample LS- 16 which located nearby LS- 15 on $16^{\circ} 46' 23''$ N, $99^{\circ} 00' 07''$ E with the foliation $316/78^{\circ}$ SW and has the same mineralogy and structure for indicate the kinematic of deformation as same as on previous location. Beside, on figure 4.10 (right) present the rock sample location LS- 17 located on $16^{\circ} 46' 19''$ N, $99^{\circ} 00' 01''$ which mostly intense the alternating of felsic and mafic bands on paragneiss. The foliation of the outcrop is about $318/63^{\circ}$ SW and the sinistral strike- slip deformation was defined by s-c fabric on the felsic band.



Figure 4. 10 (Left) presents the outcrop of rock sample location number LS-16 which mostly is paragneiss. (Right) presents the characteristic of rock samples within rock sample location number LS- 17 which rock samples have dominant feature of paragneiss.

On the highest point of Lansang Waterfall (Elev. = 511 m.) where the location of LS- 18 on $16^{\circ} 46' 14''$ N, $98^{\circ} 59' 40''$ E which the foliation is about $315/61^{\circ}$ SW and the mineralogy show the equigranular texture of quartz and feldspar and assured that it is the characteristic of orthogneiss. Finally, last location of this research observation is LS- 23 located on the lowest part of Lansang Waterfall nearly with the office of Lansang National Park ($16^{\circ} 46' 50''$ N, $99^{\circ} 00' 58''$ E). On this location the foliation is about $331/61^{\circ}$ SW and the mineralogy of rock on this area present the porphyroblastic texture or augen texture of quartz and feldspar and the σ - clast applied on quartz and indicated sinistral strike- slip deformation.



Figure 4. 11 (Left) presents the rock sample of location number LS-18 which mainly consists fine grained of quartz and feldspar, the common mineral of orthogneiss. (Right) the rock sample of location number LS- 23 which mainly consists coarse grained of quartz and feldspar.

Table 4. 1 The locations of the rock sample for this research

Rock Sample	Rock type	Locations	
		Latitude	Longitude
LS- 1	Orthogneiss	16° 46' 47"	99° 00' 50"
LS- 4	Orthogneiss	16° 46' 38"	99° 00' 42"
LS- 5	Orthogneiss	16° 46' 36"	99° 00' 41"
LS- 10	Orthogneiss	16° 46' 35"	99° 00' 38"
LS- 11	Orthogneiss	16° 46' 35"	99° 00' 35"
LS- 12	Orthogneiss	16° 46' 37"	99° 00' 11"
LS- 13	Paragneiss	16° 46' 33"	99° 00' 10"
LS- 14	Paragneiss	16° 46' 31"	99° 00' 10"
LS- 15	Paragneiss	16° 46' 25"	99° 00' 08"
LS- 16	Paragneiss	16° 46' 23"	99° 00' 07"
LS- 17	Paragneiss	16° 46' 19"	99° 00' 01"
LS- 18	Orthogneiss	16° 46' 14"	98° 59' 40"
LS- 23	Orthogneiss	16° 46' 50"	99° 00' 58"

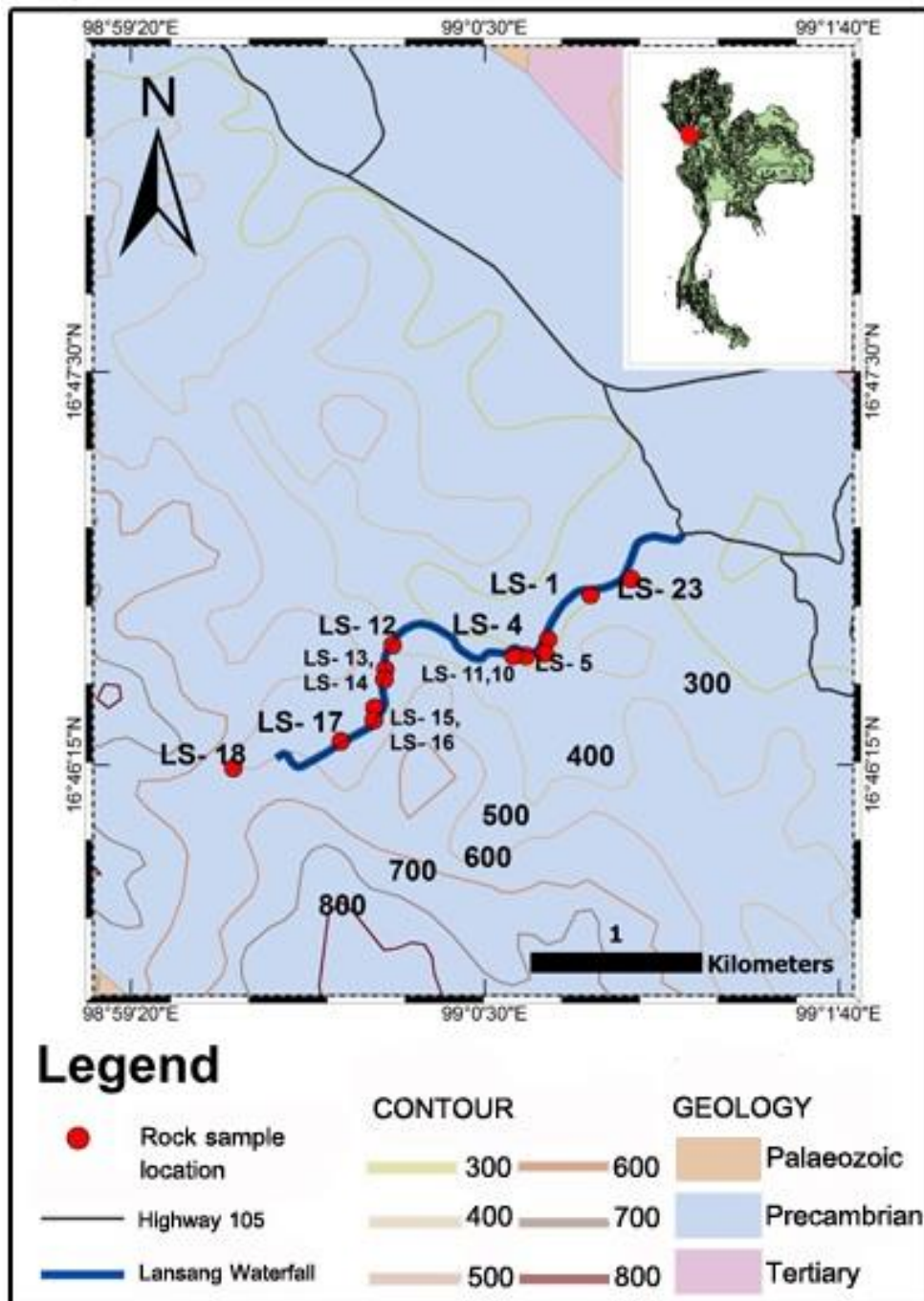


Figure 4. 12 Geological map of Lansang Waterfall and adjacent area, including with the rock sample locations along the profile of Lansang Waterfall within Lansang National Park, Tak, northwestern Thailand (Modified from Resources, 1999).

4.2 Finite strain ratios (R_s) and the angle (θ)

Based on the research methodology that mentioned in chapter III, the progress after field investigation is the section of microscope laboratory. The result of microscope laboratory for select strain markers are the recrystallized quartz grains which appropriate to Fry's condition and clearly intense shear sense. By the theory and methodology of (Fry, 1979) as described in chapter II and III respectively, the results of strain quantitative analysis of rocks from recrystallized quartz grains in Lansang Waterfall within Lansang National Park, Tak, northwestern Thailand are presenting in this section. The vacancy field of Fry's plot or finite strain ellipsoid which were derived from XY thin section of all rock samples are presenting in Figure 4.13- 4.25.

Thin section of rock sample LS- 1 was derived from XY plane of orthogneiss and later was sampling the strain marker under 10x of microscope. The recrystallized quartz grains were selected as strain marker of this sample and when analyzed by Fry's method, the XY plane of finite strain ellipsoid was produced. The strain ratio (R_s) and the angle (θ) were measured and later calculated together followed the W_k equation as mentioned in chapter 3.

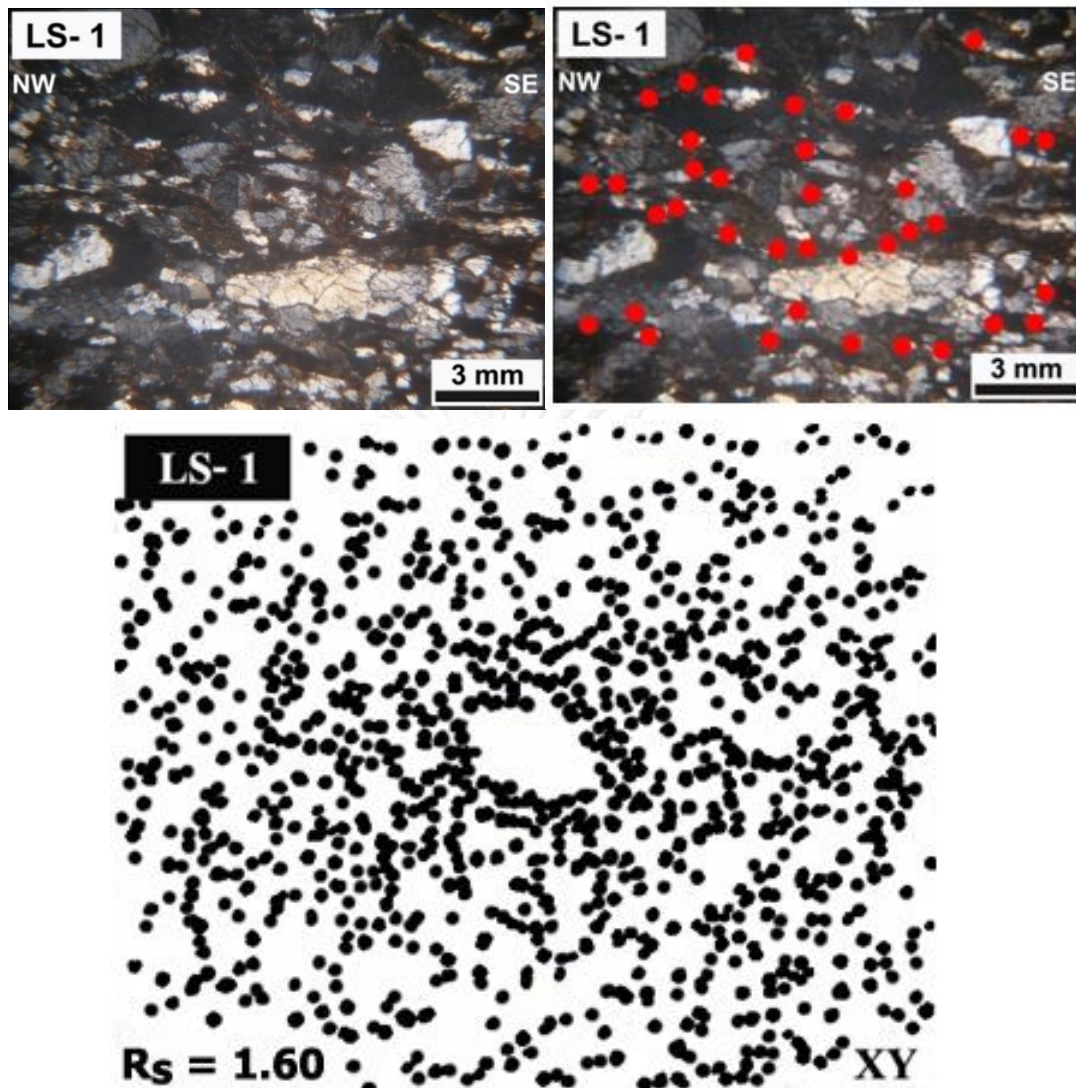


Figure 4. 13 Diagram (A) XY thin sections of rock sample LS- 1 in Lansang Waterfall while diagram (B) presents strain marker; recrystallized quartz grains (red dot) for Fry analysis. Diagram (C) XY plane of the finite strain ellipsoid of rock sample LS- 1 followed by Fry's method, including with strain ratio value.

Thin section of rock sample LS- 4 was derived from XY plane of orthogneiss and later was sampling the strain marker under 10x of microscope. The recrystallized quartz grains were selected as strain marker of this sample and when analyzed by Fry's method, the XY plane of finite strain ellipsoid was produced as shown in figure below.

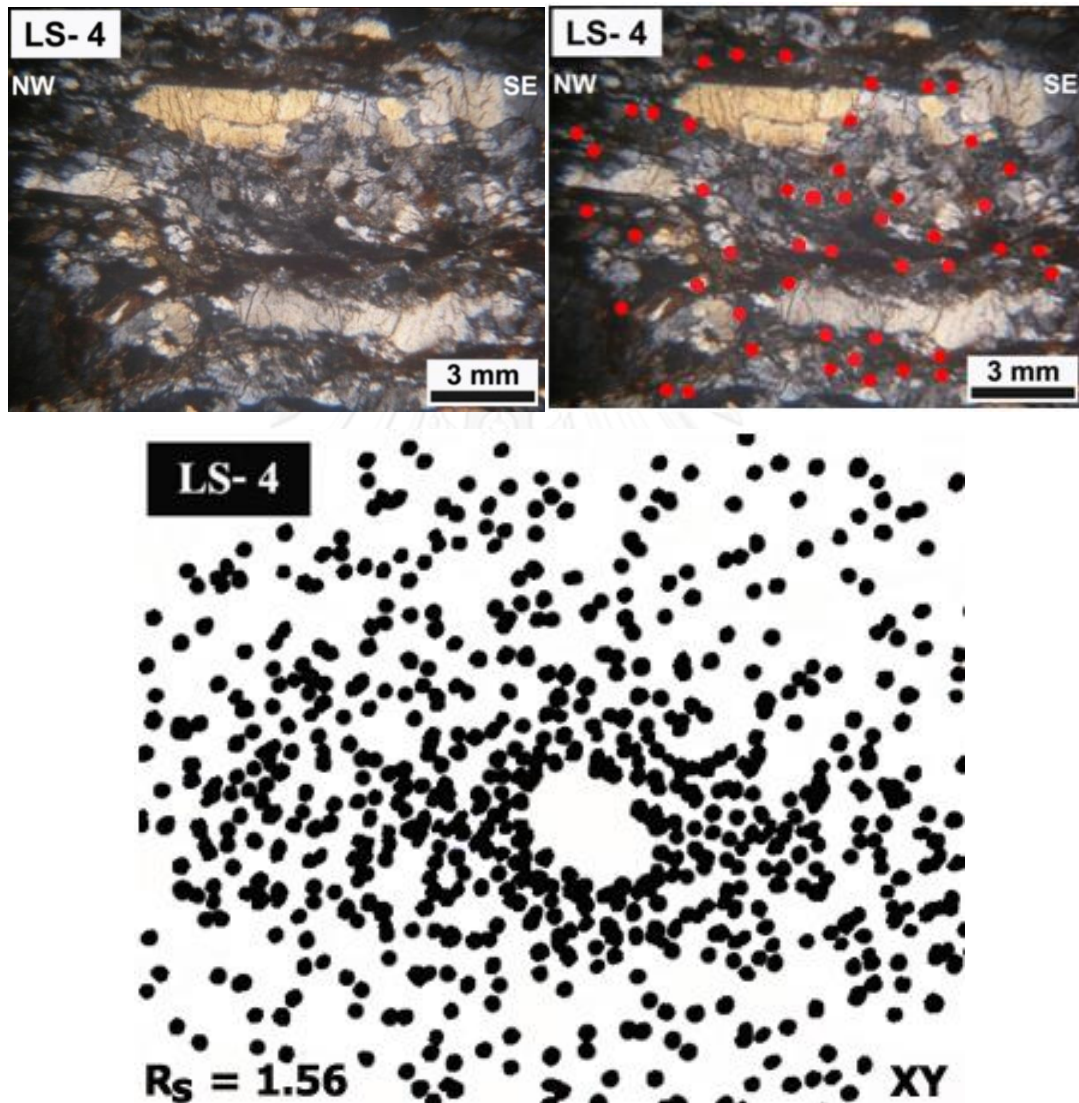


Figure 4. 14 Diagram (A) XY thin sections of rock sample LS- 4 in Lansang Waterfall while diagram (B) presents strain marker; recrystallized quartz grains (red dot) for Fry analysis. Diagram (C) XY plane of the finite strain ellipsoid of rock sample LS- 4 followed by Fry's method, including with strain ratio value.

Thin section of rock sample LS- 5 was derived from XY plane of orthogneiss and later was sampling the strain marker under 10x of microscope. The recrystallized quartz grains were selected as strain marker of this sample and when analyzed by Fry's method, the XY plane of finite strain ellipsoid was produced as shown in figure below.

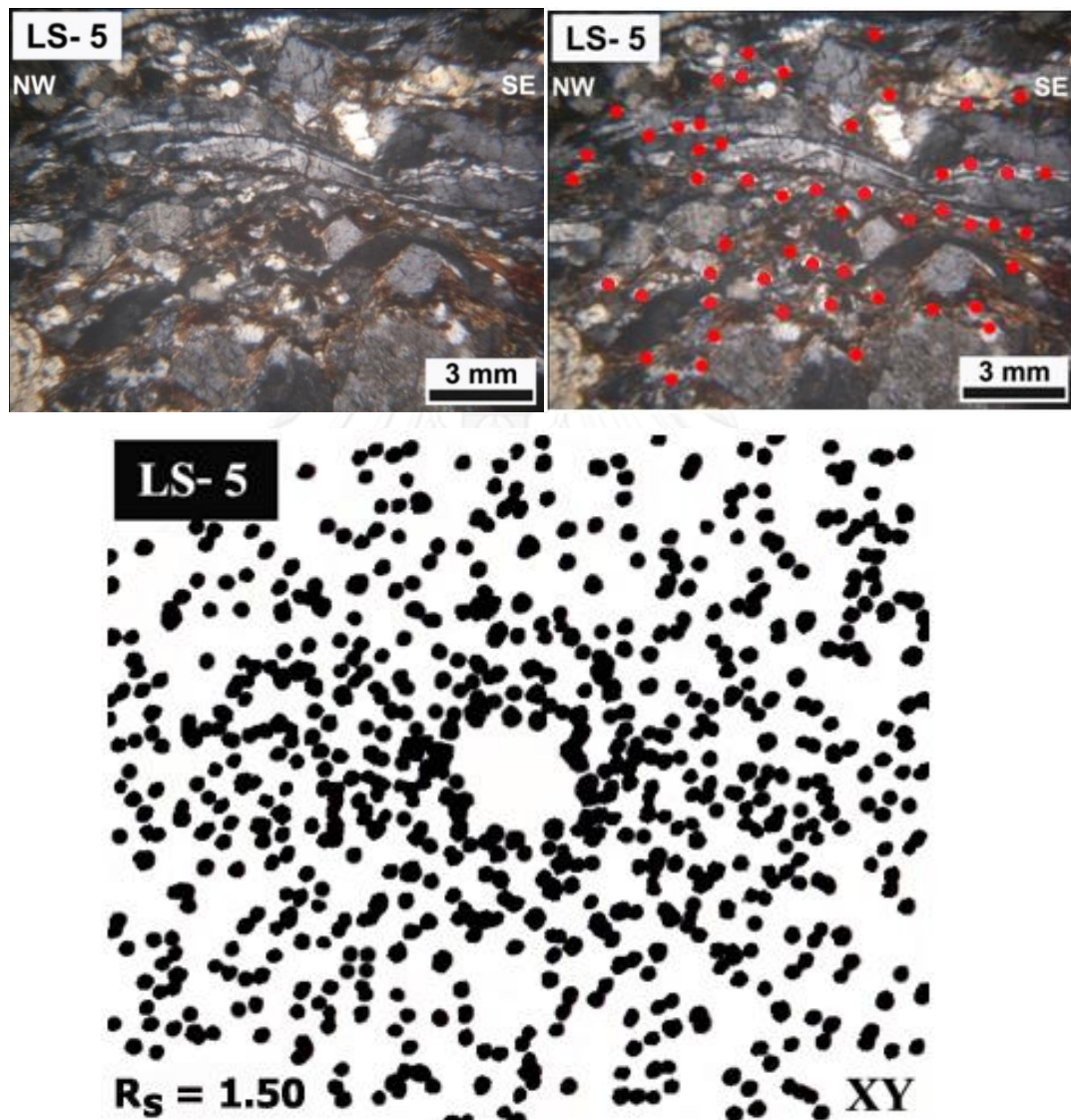


Figure 4. 15 Diagram (A) XY thin sections of rock sample LS- 5 in Lansang Waterfall while diagram (B) presents strain marker; recrystallized quartz grains (red dot) for Fry analysis. Diagram (C) XY plane of the finite strain ellipsoid of rock sample LS- 5 followed by Fry's method, including with strain ratio value.

Thin section of rock sample LS- 10 was derived from XY plane of orthogneiss and later was sampling the strain marker under 10x of microscope. The recrystallized quartz grains were selected as strain marker of this sample and when analyzed by Fry's method, the XY plane of finite strain ellipsoid was produced as shown in figure below.

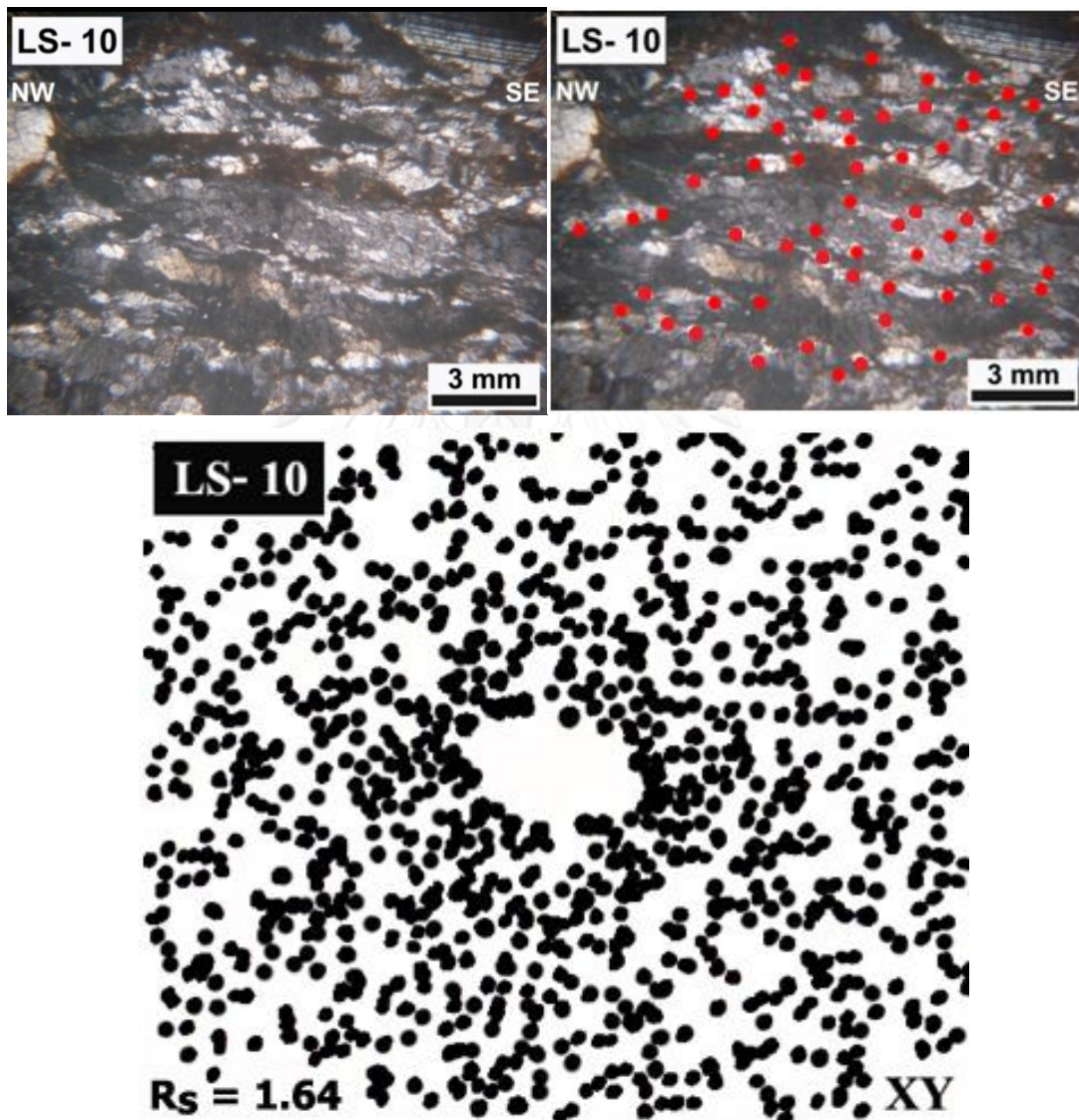


Figure 4. 16 Diagram (A) XY thin sections of rock sample LS- 10 in Lansang Waterfall while diagram (B) presents strain marker; recrystallized quartz grains (red dot) for Fry analysis. Diagram (C) XY plane of the finite strain ellipsoid of rock sample LS- 10 followed by Fry's method, including with strain ratio value.

Thin section of rock sample LS- 11 was derived from XY plane of orthogneiss and later was sampling the strain marker under 10x of microscope. The recrystallized quartz grains were selected as strain marker of this sample and when analyzed by Fry's method, the XY plane of finite strain ellipsoid was produced as shown in figure below.

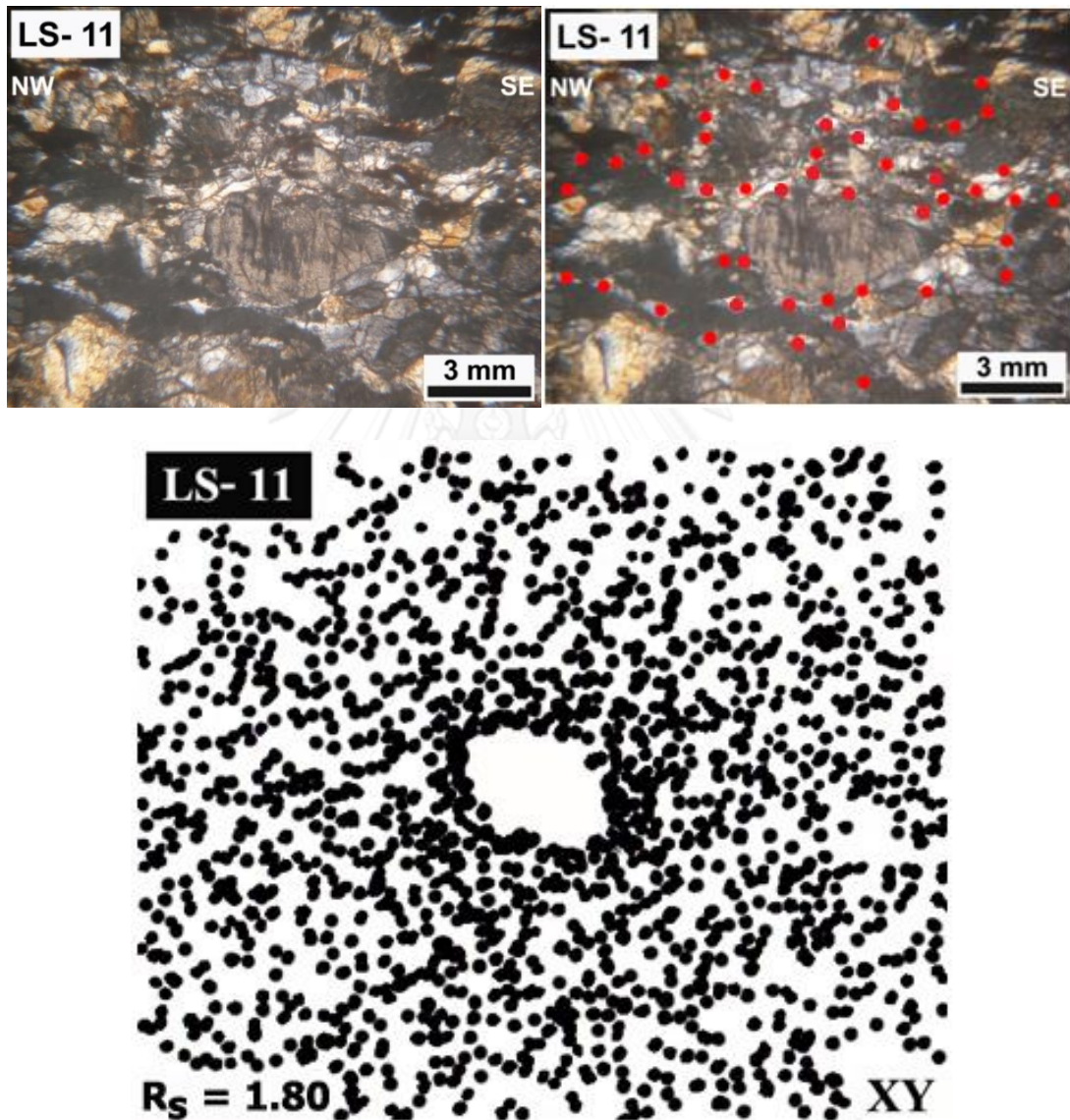


Figure 4. 17 Diagram (A) XY thin sections of rock sample LS- 11 in Lansang Waterfall while diagram (B) presents strain marker; recrystallized quartz grains (red dot) for Fry analysis. Diagram (C) XY plane of the finite strain ellipsoid of rock sample LS- 11 followed by Fry's method, including with strain ratio value.

Thin section of rock sample LS- 12 was derived from XY plane of orthogneiss and later was sampling the strain marker under 5x of microscope. The recrystallized quartz grains were selected as strain marker of this sample and when analyzed by Fry's method, the XY plane of finite strain ellipsoid was produced as shown in figure below.

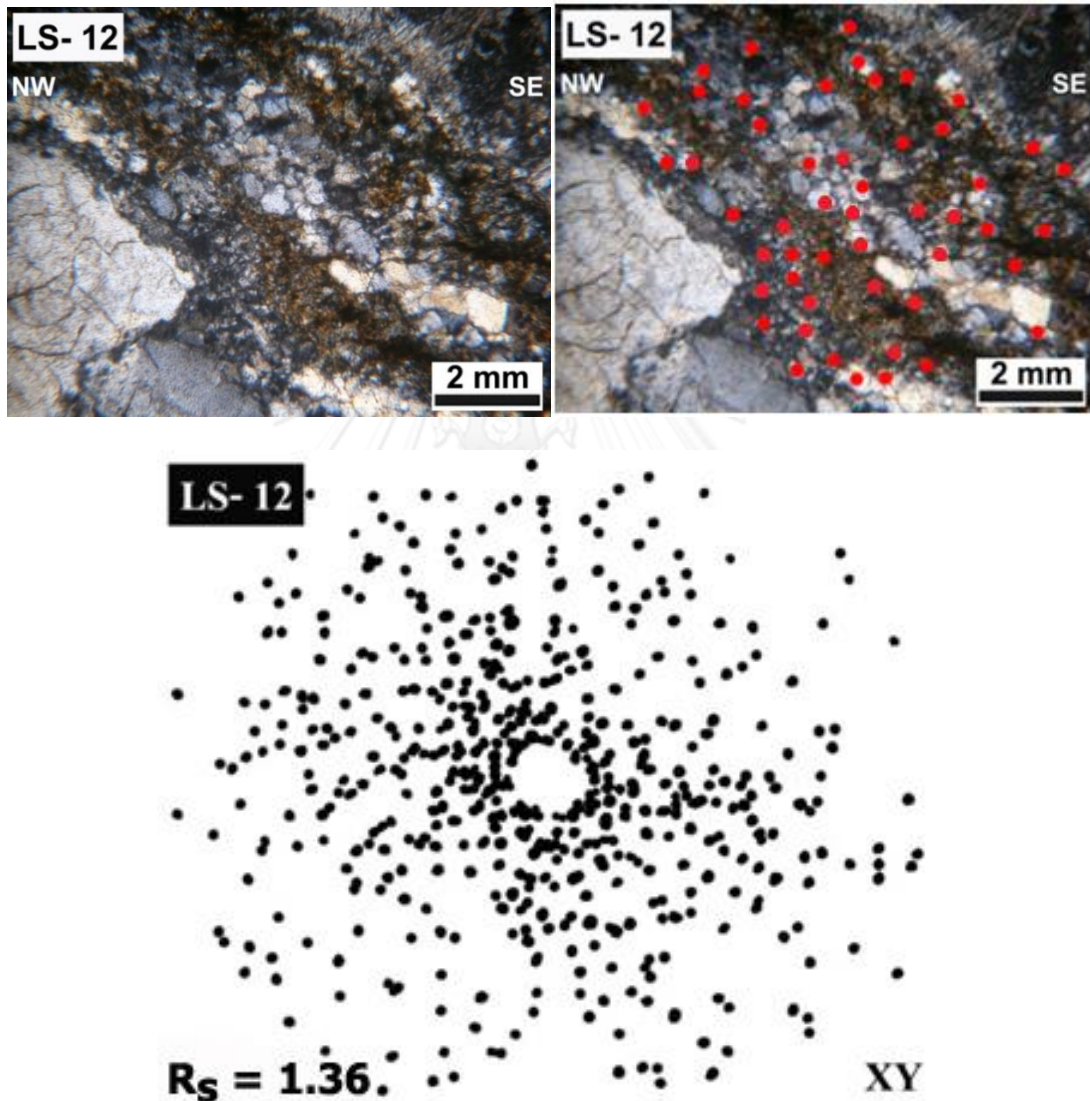


Figure 4. 18 Diagram (A) XY thin sections of rock sample LS- 12 in Lansang Waterfall while diagram (B) presents strain marker; recrystallized quartz grains (red dot) for Fry analysis. Diagram (C) XY plane of the finite strain ellipsoid of rock sample LS- 12 followed by Fry's method, including with strain ratio value.

Thin section of rock sample LS- 13 was derived from XY plane of paragneiss and later was sampling the strain marker under 5x of microscope. The recrystallized quartz grains were selected as strain marker of this sample and when analyzed by Fry's method, the XY plane of finite strain ellipsoid was produced as shown in figure below.

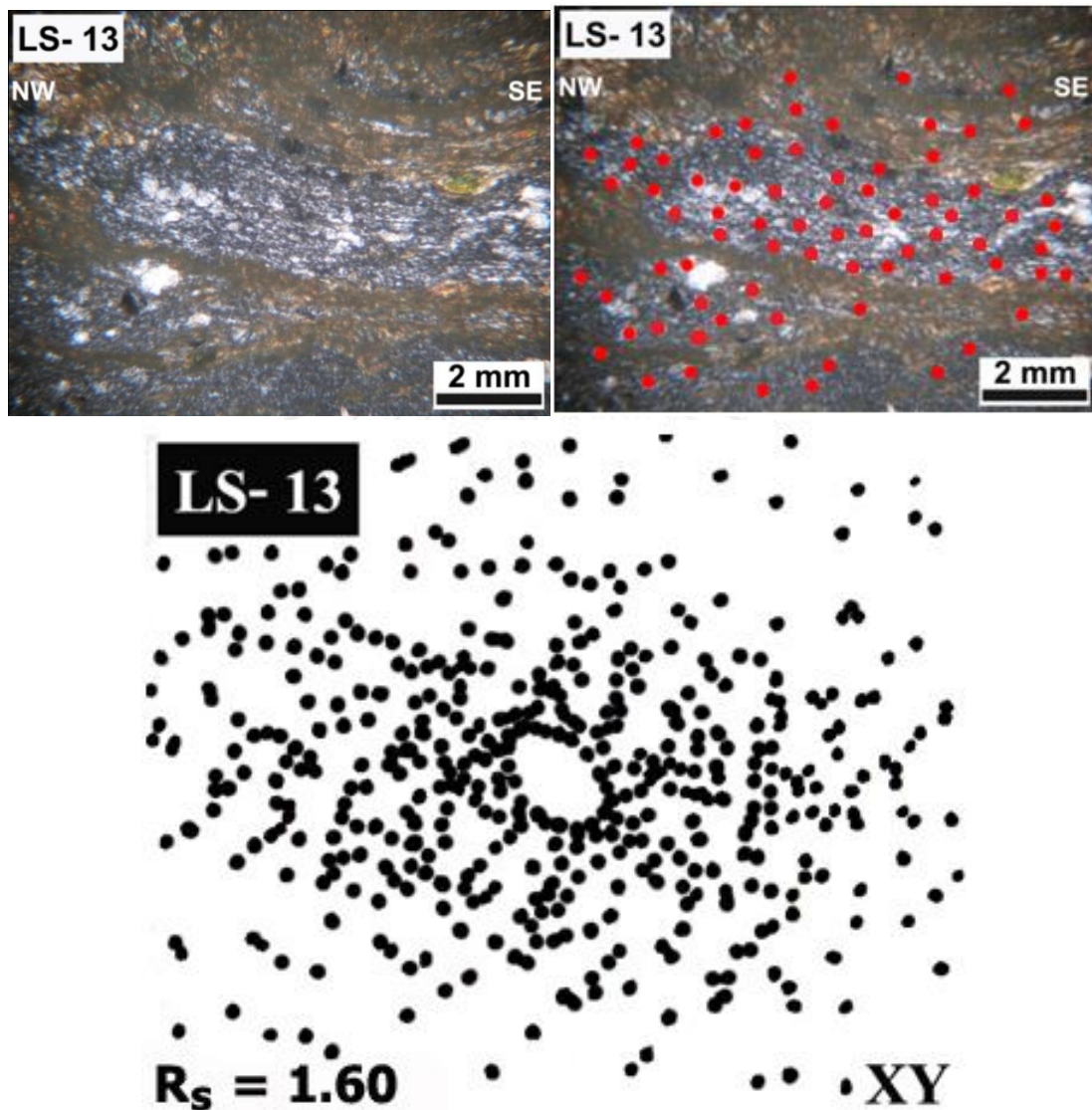


Figure 4. 19 Diagram (A) XY thin sections of rock sample LS- 13 in Lansang Waterfall while diagram (B) presents strain marker; recrystallized quartz grains (red dot) for Fry analysis. Diagram (C) XY plane of the finite strain ellipsoid of rock sample LS- 13 followed by Fry's method, including with strain ratio value.

Thin section of rock sample LS- 14 was derived from XY plane of paragneiss and later was sampling the strain marker under 10x of microscope. The recrystallized quartz grains were selected as strain marker of this sample and when analyzed by Fry's method, the XY plane of finite strain ellipsoid was produced as shown in figure below.

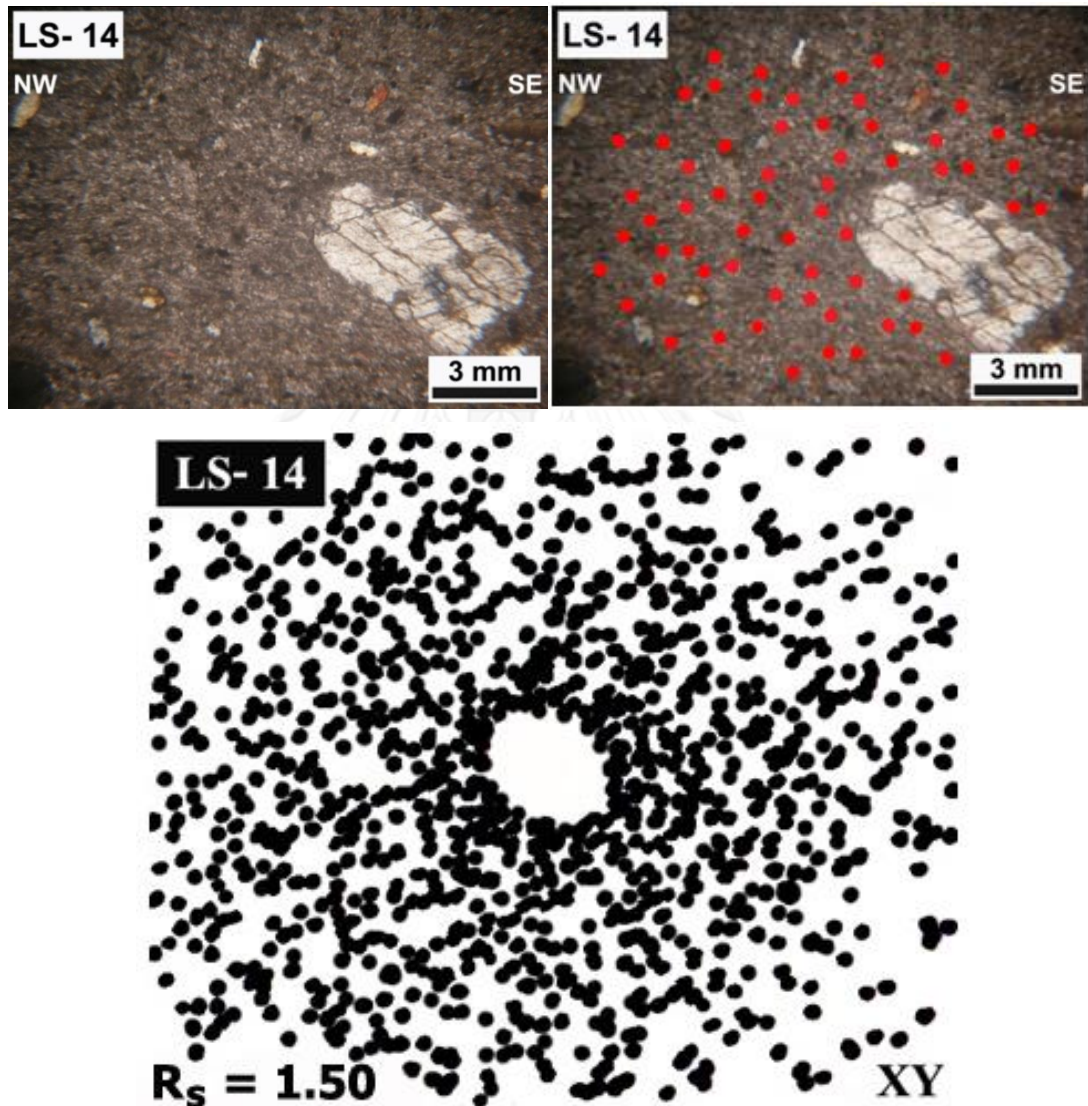


Figure 4. 20 Diagram (A) XY thin sections of rock sample LS- 14 in Lansang Waterfall while diagram (B) presents strain marker; recrystallized quartz grains (red dot) for Fry analysis. Diagram (C) XY plane of the finite strain ellipsoid of rock sample LS- 14 followed by Fry's method, including with strain ratio value.

Thin section of rock sample LS- 15 was derived from XY plane of paragneiss and later was sampling the strain marker under 5x of microscope. The recrystallized quartz grains were selected as strain marker of this sample and when analyzed by Fry's method, the XY plane of finite strain ellipsoid was produced as shown in figure below.

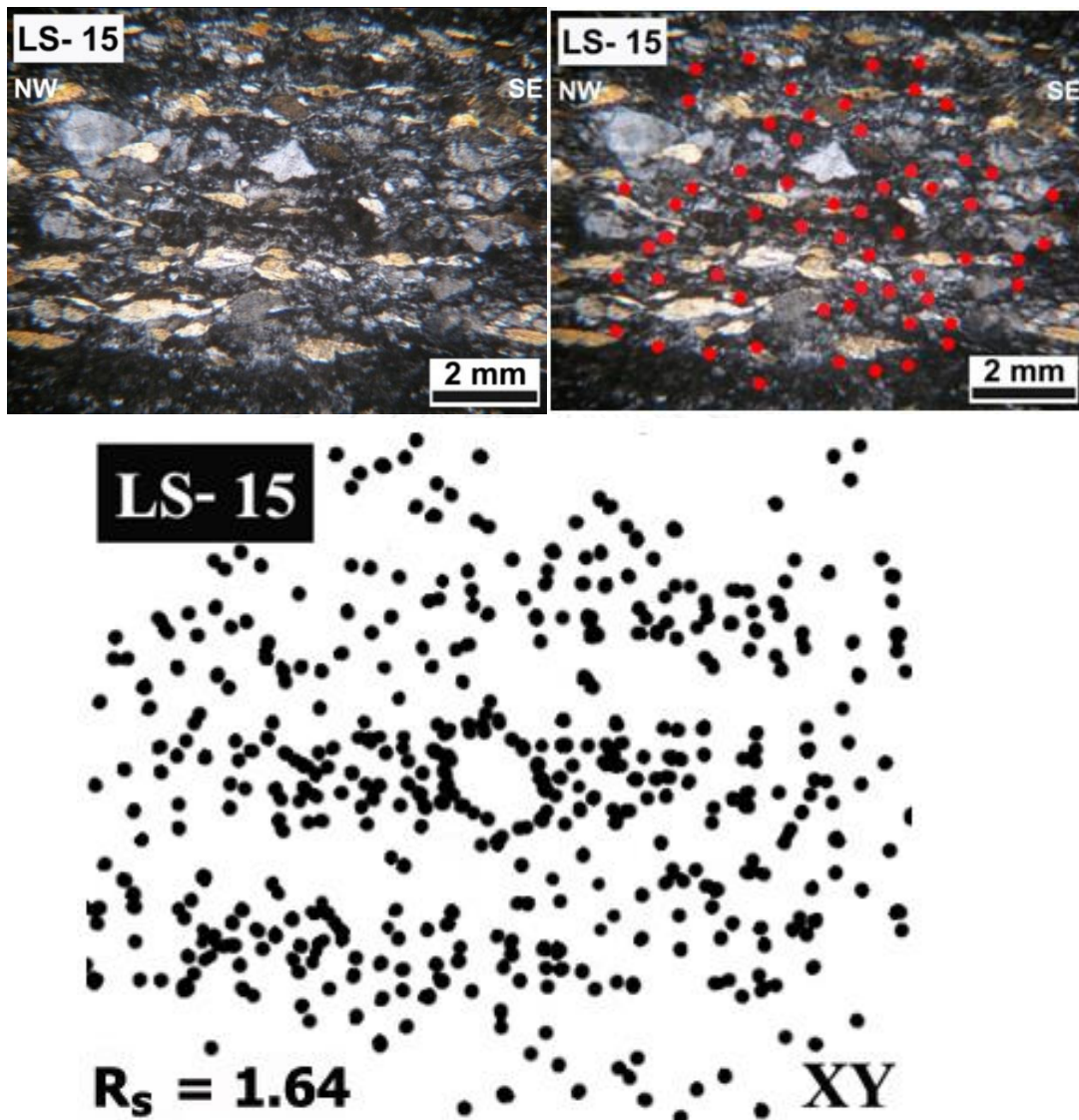


Figure 4. 21 Diagram (A) XY thin sections of rock sample LS- 15 in Lansang Waterfall while diagram (B) presents strain marker; recrystallized quartz grains (red dot) for Fry analysis. Diagram (C) XY plane of the finite strain ellipsoid of rock sample LS- 15 followed by Fry's method, including with strain ratio value.

Thin section of rock sample LS- 16 was derived from XY plane of paragneiss and later was sampling the strain marker under 10x of microscope. The recrystallized quartz grains were selected as strain marker of this sample and when analyzed by Fry's method, the XY plane of finite strain ellipsoid was produced as shown in figure below.

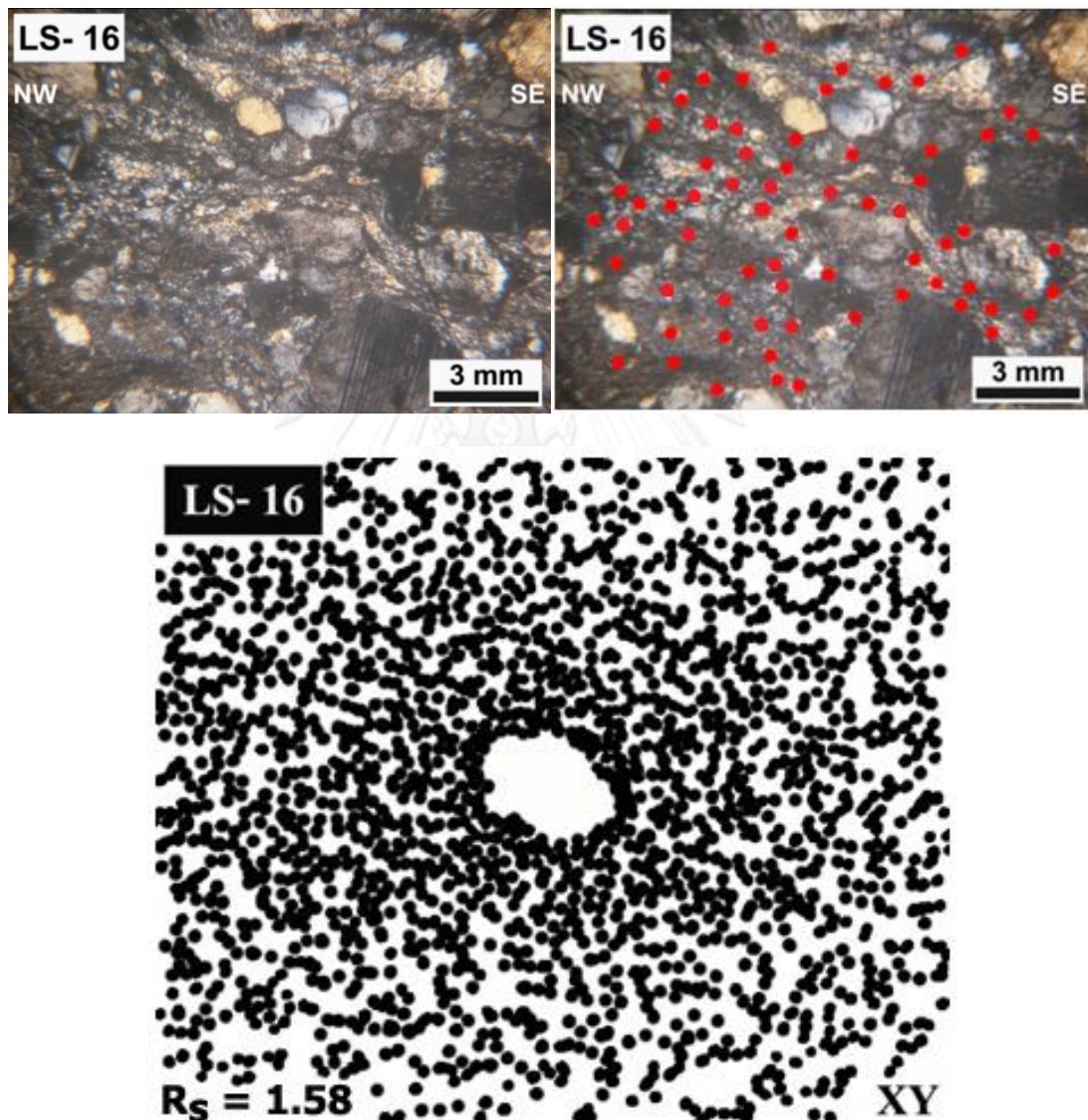


Figure 4. 22 Diagram (A) XY thin sections of rock sample LS- 16 in Lansang Waterfall while diagram (B) presents strain marker; recrystallized quartz grains (red dot) for Fry analysis. Diagram (C) XY plane of the finite strain ellipsoid of rock sample LS- 16 followed by Fry's method, including with strain ratio value.

Thin section of rock sample LS- 17 was derived from XY plane of paragneiss and later was sampling the strain marker under 5x of microscope. The recrystallized quartz grains were selected as strain marker of this sample and when analyzed by Fry's method, the XY plane of finite strain ellipsoid was produced as shown in figure below.

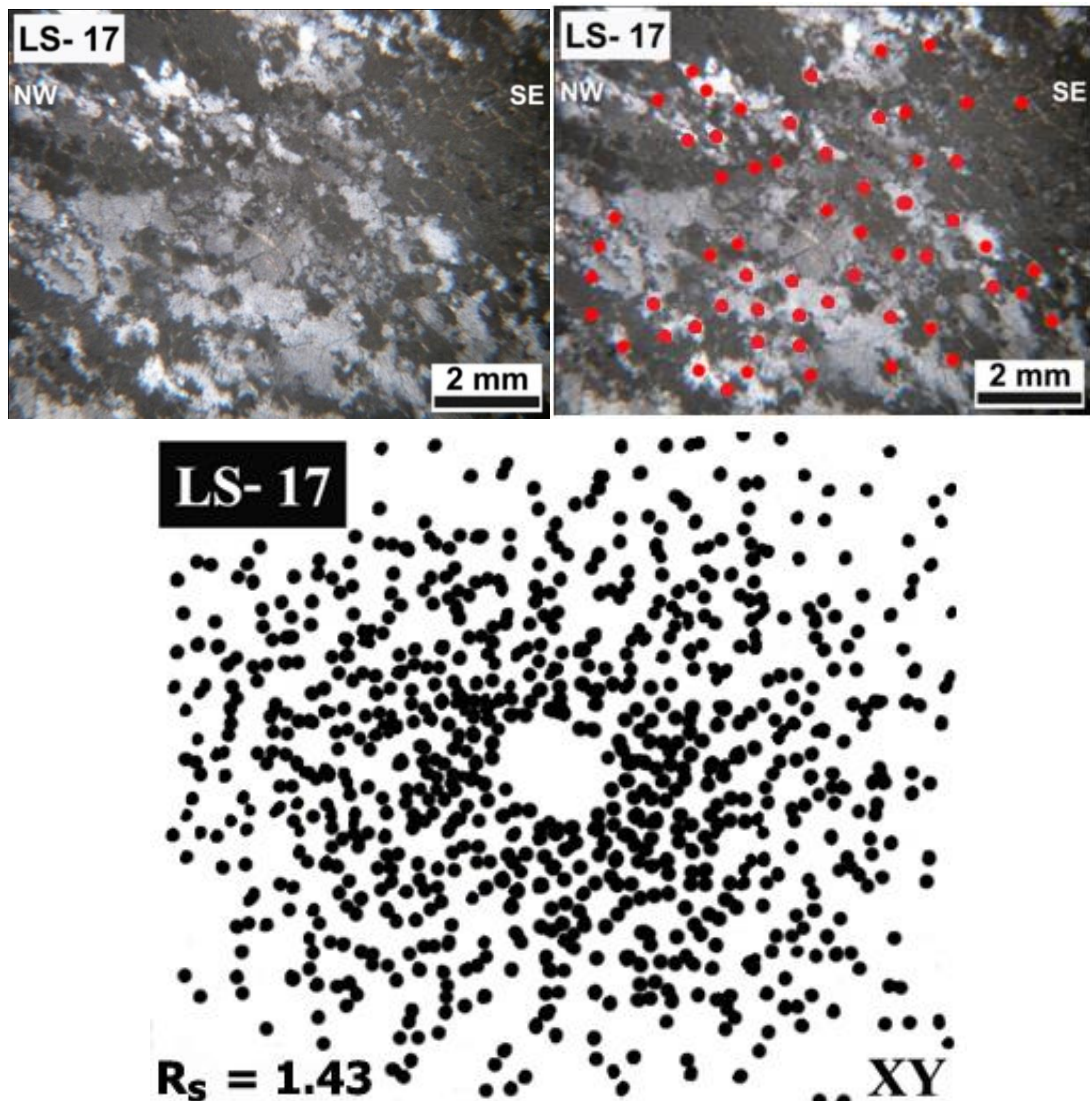


Figure 4. 23 Diagram (A) XY thin sections of rock sample LS- 17 in Lansang Waterfall while diagram (B) presents strain marker; recrystallized quartz grains (red dot) for Fry analysis. Diagram (C) XY plane of the finite strain ellipsoid of rock sample LS- 17 followed by Fry's method, including with strain ratio value.

Thin section of rock sample LS- 18 was derived from XY plane of orthogneiss and later was sampling the strain marker under 10x of microscope. The recrystallized quartz grains were selected as strain marker of this sample and when analyzed by Fry's method, the XY plane of finite strain ellipsoid was produced as shown in figure below.

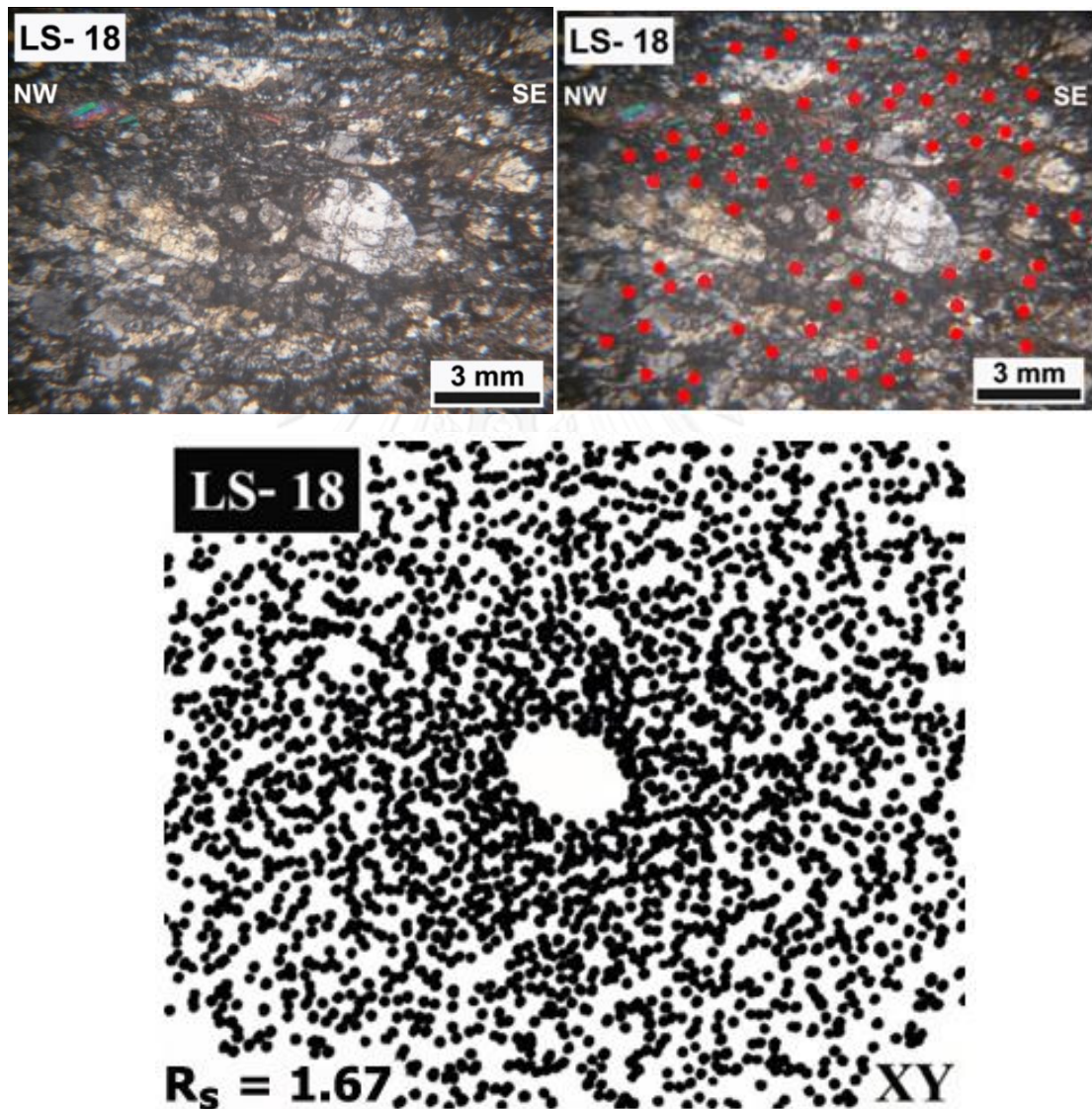


Figure 4. 24 Diagram (A) XY thin sections of rock sample LS- 18 in Lansang Waterfall while diagram (B) presents strain marker; recrystallized quartz grains (red dot) for Fry analysis. Diagram (C) XY plane of the finite strain ellipsoid of rock sample LS- 18 followed by Fry's method, including with strain ratio value.

Thin section of rock sample LS- 23 was derived from XY plane of orthogneiss and later was sampling the strain marker under 10x of microscope. The recrystallized quartz grains were selected as strain marker of this sample and when analyzed by Fry's method, the XY plane of finite strain ellipsoid was produced as shown in figure below.

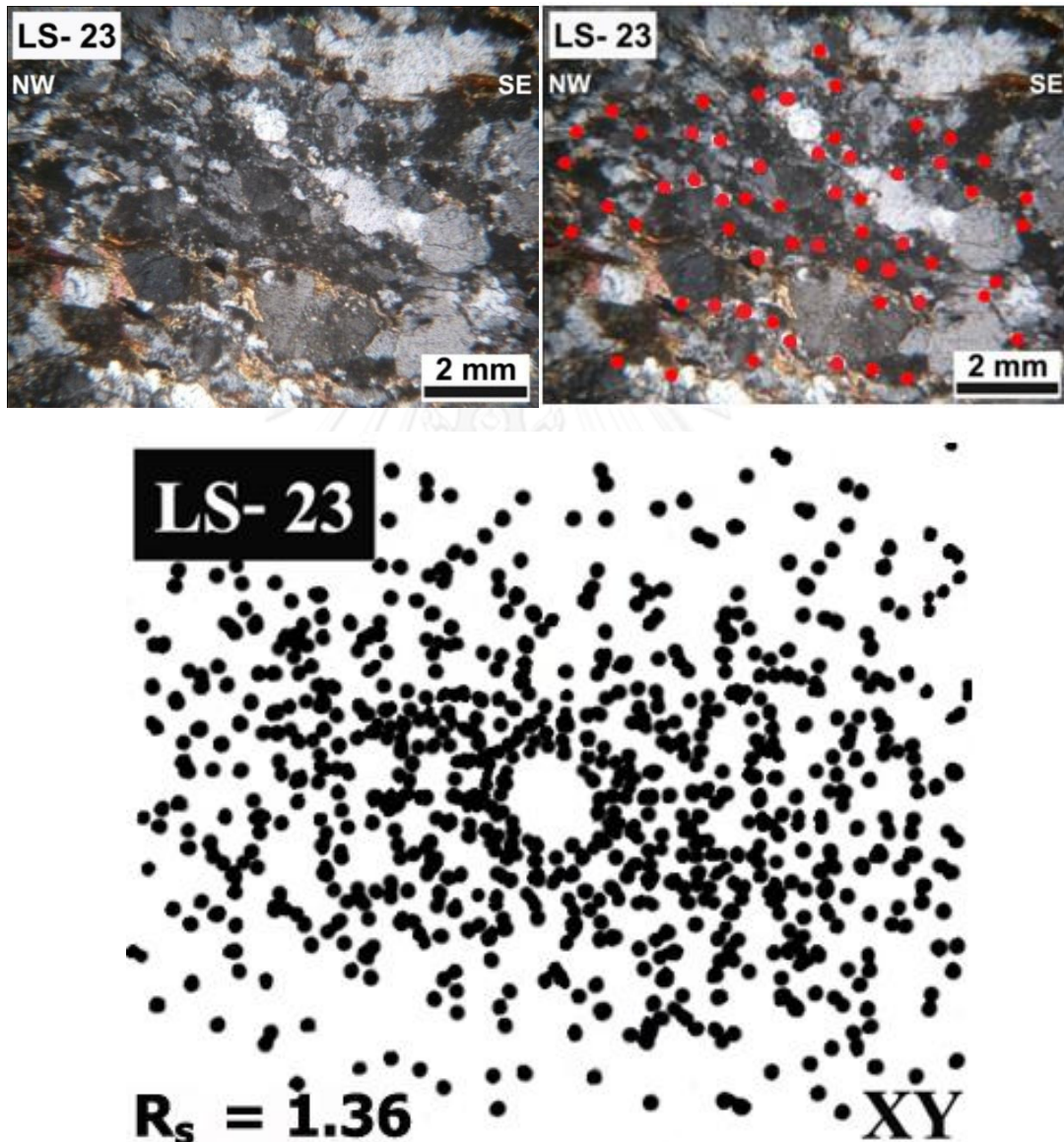


Figure 4. 25 Diagram (A) XY thin sections of rock sample LS- 23 in Lansang Waterfall while diagram (B) presents strain marker; recrystallized quartz grains (red dot) for Fry analysis. Diagram (C) XY plane of the finite strain ellipsoid of rock sample LS- 23 followed by Fry's method, including with strain ratio value.

The finite strain ratios (R_s) and the angle (θ) of all 13 rock samples along Lansang Waterfall were quantified from the strain ellipsoid and the result present in table 4.2. The averaged strain ratio value ($R_{s, avg.}$) of all samples fall in ranged between 1.35 to 1.69. The $R_{s, avg.}$ of rock sample location number LS-5 and LS- 13 fall in same value, $R_{s, avg.} = 1.49$. LS- 15 and LS- 18 also fall in same value, $R_{s, avg.} = 1.53$ while LS- 1 fall nearby, $R_{s, avg.} = 1.54$. The lowest and highest value of averaged strain ratio are gave by LS- 23 and LS- 16, respectively while the $R_{s, avg.}$ -value of LS- 12 and LS- 11 fall nearby the lowest and highest value of all samples respectively. The others are ranged between 1.56 to 1.59. In addition, the average finite strain ratio of all rock samples ($R_{s, avg.}$) are considered together in sense of correlation and the result clearly present correlative between each other as shown by Figure 4.26. Moreover, the value of angle θ of all samples in Lansang Waterfall fall in ranged between 22° to 41° which related to the value of kinematic vorticity number (W_k) as described earlier and are presenting in Figure 4.27.

Table 4. 2 Strain data of rocks in Lansang Waterfall, Tak, northwestern Thailand.

Rock sample	Strain ratio			Angles (min- max.)			Kinematic vorticity number		
	(Rs) min- max.	(Rs) avg.	SD.	θ (°)	(2 θ)	(Radian)	(WK) min- max.	(WK) avg.	SD.
LS- 1	1.45- 1.60	1.54	0.06	30- 40	60- 80	1.05- 1.40	0.94- 1.00	0.96	0.03
LS- 4	1.38- 1.80	1.59	0.15	33- 40	66- 80	1.15- 1.40	0.97- 1.00	0.99	0.01
LS- 5	1.45- 1.56	1.49	0.04	32- 33	64- 66	1.12- 1.15	0.96- 0.98	0.97	0.00
LS- 10	1.38- 1.64	1.56	0.10	22- 40	44- 80	0.77- 1.40	0.82- 1.00	0.92	0.08
LS- 11	1.45- 1.80	1.68	0.16	30- 40	60- 80	1.05- 1.40	0.97- 1.00	0.99	0.01
LS- 12	1.33- 1.40	1.37	0.03	30- 40	60- 80	1.05- 1.40	0.93- 1.00	0.98	0.03
LS- 13	1.38- 1.60	1.49	0.09	29- 40	58- 80	1.01- 1.40	0.92- 1.00	0.97	0.04
LS- 14	1.50- 1.70	1.57	0.09	36- 39	72- 78	1.26- 1.36	0.99- 1.00	1.00	0.00
LS- 15	1.46- 1.64	1.53	0.08	22- 35	44- 70	0.77- 1.22	0.79- 0.99	0.88	0.08
LS- 16	1.50- 2.00	1.69	0.22	27- 40	54- 80	0.94- 1.40	0.93- 1.00	0.96	0.03
LS- 17	1.31- 1.91	1.58	0.16	23- 40	46- 80	0.80- 1.40	0.85- 1.00	0.97	0.04
LS- 18	1.42- 1.67	1.53	0.12	26- 35	52- 70	0.91- 1.22	0.91- 0.98	0.96	0.03
LS- 23	1.29- 1.45	1.35	0.07	25- 41	50- 82	0.87- 1.43	0.84- 1.00	0.94	0.06

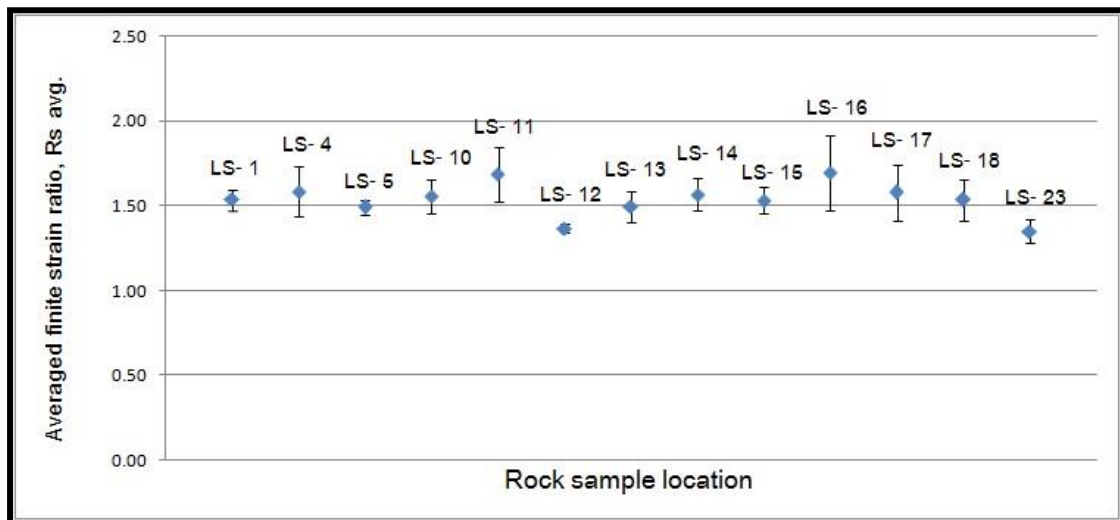


Figure 4. 26 An error bar graph presents the correlative between the average finite strain ratio of all rock samples ($R_{s, avg.}$) and their locations along the profile of Lansang Waterfall within Lansang National Park, Tak, northwestern Thailand.

4.3 Kinematic vorticity number, W_k

Based on the theory and mathematical equation of kinematic vorticity function which were mentioned earlier in chapter II, the relative between finite strain ratios (R_s) and the angle (θ) of the strain ellipse could be described. Later the value of W_k - function of all samples were used for determine the deformation type and describe the deformation history of rocks on this area, Lansang Waterfall. The results are presenting in this section as shown in table 4.2 that W_k - value of all samples fall in ranged between 0.79to 1.00.

According to Figure 4.27, some of W_k and angle θ values of each rock sample location are chose and plotted together and give the diagram which intense the correlative between two function, W_k and angle θ . Beside, by this diagram the relative between W_k - value of all rock samples and their locations along the profile of Lansang Waterfall can be presented. The rock sample LS- 12 and LS- 13 fall in same

ranged of W_k with the highest angle θ - values, $W_k = 1.00$ and $\theta = 40^\circ$ while LS- 4, LS- 11 and LS- 14 fall nearby. Lower than them are LS- 5 and LS- 17 which W_k ranged between 0.95 with the angle θ - values 33 and 34, respectively. LS- 1, LS- 18 and LS- 23 fall nearby together as same as LS- 10 and LS- 15 which LS- 10 gave the lowest W_k and angle θ - values.

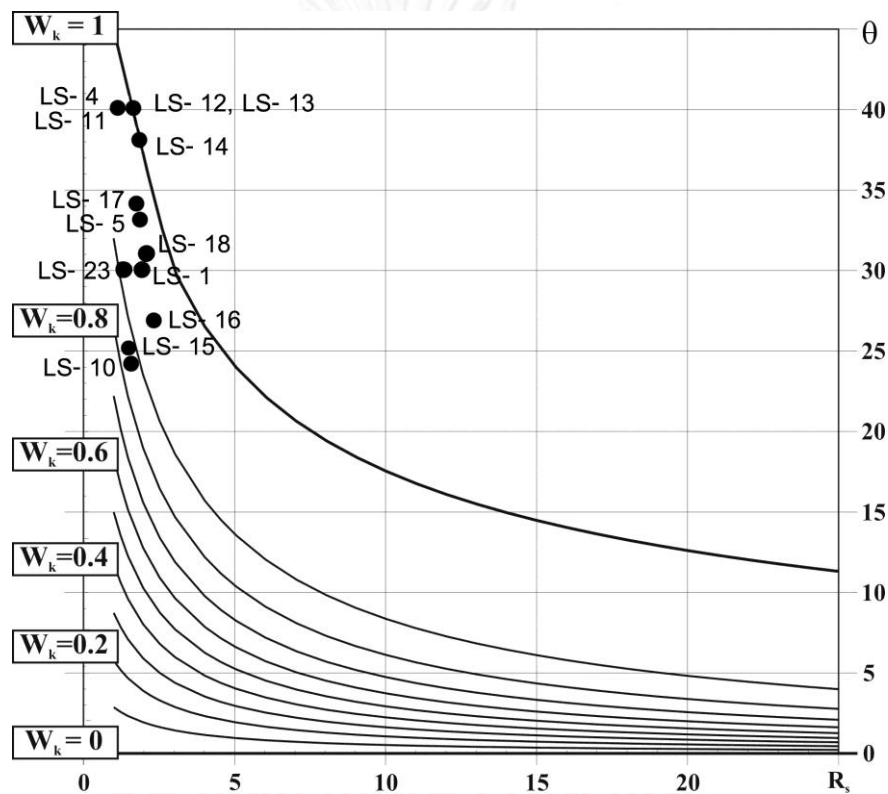


Figure 4. 27 Diagram plots of the averaged kinematic vorticity number ($W_{k, avg.}$) and the angle between the longest axes of strain ellipse and the deformation boundary (θ) showing the strain ratios of the finite strain ellipsoid (R_s).

Besides, the averaged finite strain value and shape of strain ellipsoid of all samples can be mapped together with the location map, including with the trend of plane which defined by rose diagram for describe the characteristic of ellipsoid from each location as shown by Figure 4.28.

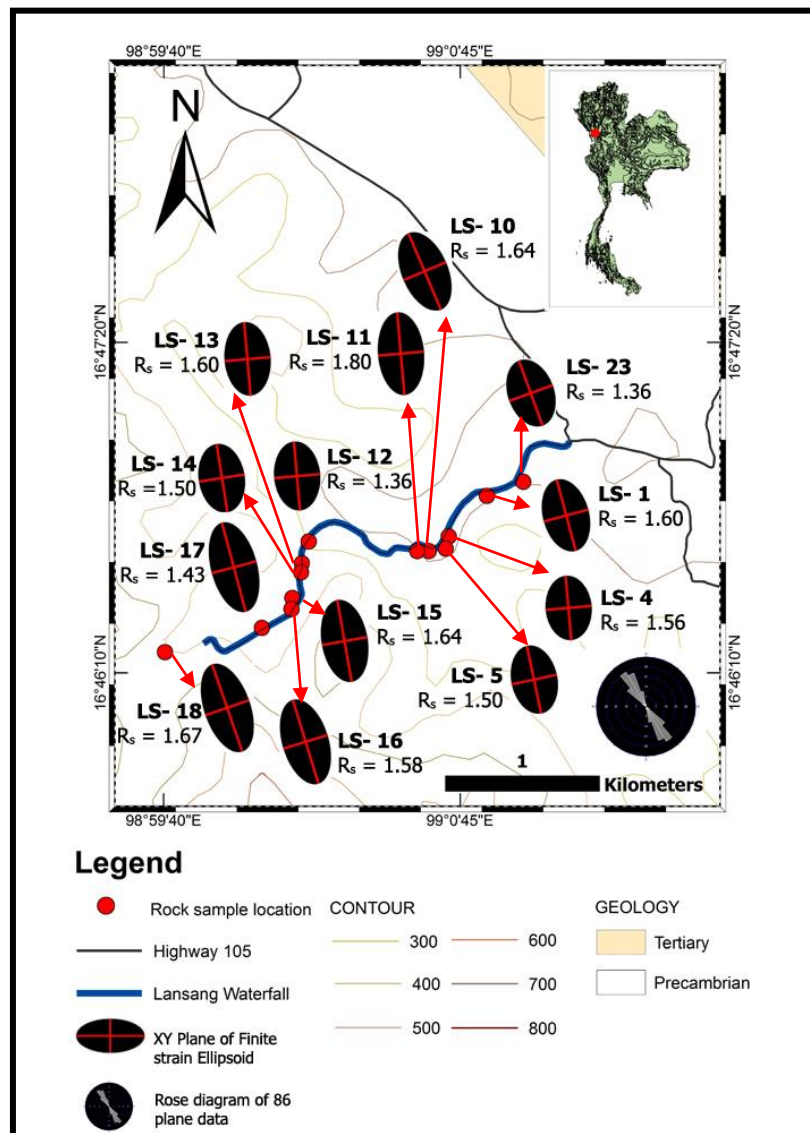


Figure 4. 28 Geological map of Lansang Waterfall, Tak, northwestern Thailand and adjacent area, including with rock sample locations and XY plane of finite strain ellipsoid of all 13 locations along the profile of Lansang Waterfall.

CHAPTER V

DISCUSSIONS

The Mae Ping shear zone and Ailao- Shan- Red River shear zone are considered as a result of last India's penetration by the dominant feature of left-lateral strike-slip motion on those high strain zones. After the past India- Asia collision, there were an effect over Tibet and adjacent region which facing with the Indian's indenter and left the geological and geophysical evidence of this past indentation on rocks within those areas. By the successive of India penetration, the strike-slip N- S trending of metamorphic rocks and granitic intrusions extended across northwestern Thailand and bended into large scale shear zone (R. Lacassin, Leloup, & Tapponnier, 1993). As a step of those, the structural of rock on northwestern Thailand were deformed and clearly intense the shear sense which are the criteria to define the major deformation phases and the timing of this past penetration.

This research have strong motivated to study in sense of quantitative analysis for determine the direction and sense of the movement on this shear zone by applied the application of Fry method (Fry, 1979) on deformed rocks from Lansang Waterfall within Lansang National Park, Tak, northwestern Thailand. Based on the field investigation followed by the traverse line method along the profile of Lansang Waterfall, it was found that the rock samples consisting of orthogneiss and paragneiss which later were progressed by microscope laboratory and the recrystallized quartz grains were selected as strain marker for quantify finite strain of rock followed the Fry's method. The results of this research presented in previous chapter and lead three main parts are discussing in this chapter.

5.1 Quantifying the deformation

The product of two- dimension strain quantitative analysis followed by Fry's method, the strain ratios of deformed minerals; the recrystallized quartz grains which occurred in case of homogeneous deformation and the angle θ - value related to each other and led the kinematic vorticity numbers were measured. Based on the deformation theory (Fossen, 2010), the deformation type and their relative between the pure shear and simple shear in case of steady- state deformation can be defined or described by a quantity of kinematic vorticity number, W_k where $W_k = 0$ for pure shear component, vice versa $W_k = 1$ for simple shear component. Moreover, in natural the plane strain deformation always occurred in the combination of a vertical simple shearing and pure shearing which is described in terms of transpressional- transtensional deformation. The transpressional deformation can be consisted into pure shear- dominated and simple shear- dominated by the W_k - value which W_k fall from 0 to 0.81 imply the characteristic of pure shear- dominated transpression. Beside, in case of simple shear- dominated transpression, W_k ranged between 0.81to 1 (Fossen & Tikoff, 1993). Therefore, the deformation types that occurred and involved with the deformation process of rocks on the high strain zone can be defined by W_k - value.

As the theory that were mentioned earlier and the result of two- dimension strain quantitative analysis of rocks in Lansang Waterfall in chapter IV that a quantity of W_k and angle θ of all samples ranged between 0.79to 1.00 and 22° to 41° , respectively clearly described the characteristic of simple shear- dominated transpression (Fig. 5.1). By this type of deformation, it assured that an area of Lansang Waterfall, Tak, northwestern Thailand was effected by the strike- slip motion of Mae Ping fault which finally generate the large scale of high strain zone; the Mae Ping shear zone.

Moreover, (R. Lacassin, Leloup, & Tapponnier, 1993) studied in one-dimension strain quantitative analysis; the boudinaged restoration on both Ailao-Shan- Red River shear zone and Mae Ping shear zone, the result found that on the Mae Ping shear zone has some reliable results from the boudin trail that were too short. Nevertheless, the reliable extension values gained from leucocratic veins at Mae Ping shear zone around Lansang site which ranged between 265 to 786% and gave the mean quadratic extension value of 430%. Outside the shear zone present undeformed leucocratic veins which are the low grade metamorphism, thus the veins that were measured are pre-tectonic. However, the study of (R. Lacassin, Leloup, & Tapponnier, 1993) addressed the problem in define the initial orientation of the markers from the outcrop observation and used the observation data proposed the fundamental assumption that the deformation process on the Mae Ping shear zone was close to simple shear. Then, to better describe the kinematics of either high strain zones, the strain quantitative analysis was applied.

By this method the elongation was measured followed (Ramsay & Huber, 1983) and gave the quadratic extension of a line and making the initial orientation or initial angles of the marker (α) with the shear plane. To quantify the function of shear strain (γ), the quadratic extension and the initial angles are involved. Based on the theory and initial angles- value which depend on strain markers; amphibolite boudins and leucocratic veins, for this study the initial angles- value consisting of three values; 15° , 45° and 90° . Thus, (R. Lacassin, Leloup, & Tapponnier, 1993) can proposed the first order estimate of minimum Tertiary left- lateral displacement followed by that assumption which for the Mae Ping shear zone is 35 ± 20 km and the shear strain ($\gamma = 7$) with an initial angle (α) 45° . As the result of one- dimension strain quantitative analysis and the characteristic of markers on the observation corroborated together and assured their fundamental assumption of left- lateral simple shear on the Mae Ping shear zone.

Based on the result of this research, the value of kinematic vorticity number, W_k ranged between 0.79 to 1.00 intense that the process of simple shear was applied on Mae Ping shear zone under the transpression condition. Besides, the value of initial angle, α and one- dimension shear strain, γ of Mae Ping shear zone are 45° and $\gamma = 7$, respectively also described the simple shear process. Therefore, the result of both studies on Mae Ping shear zone corroborated together and assured that left-lateral simple shear processed on this shear zone.

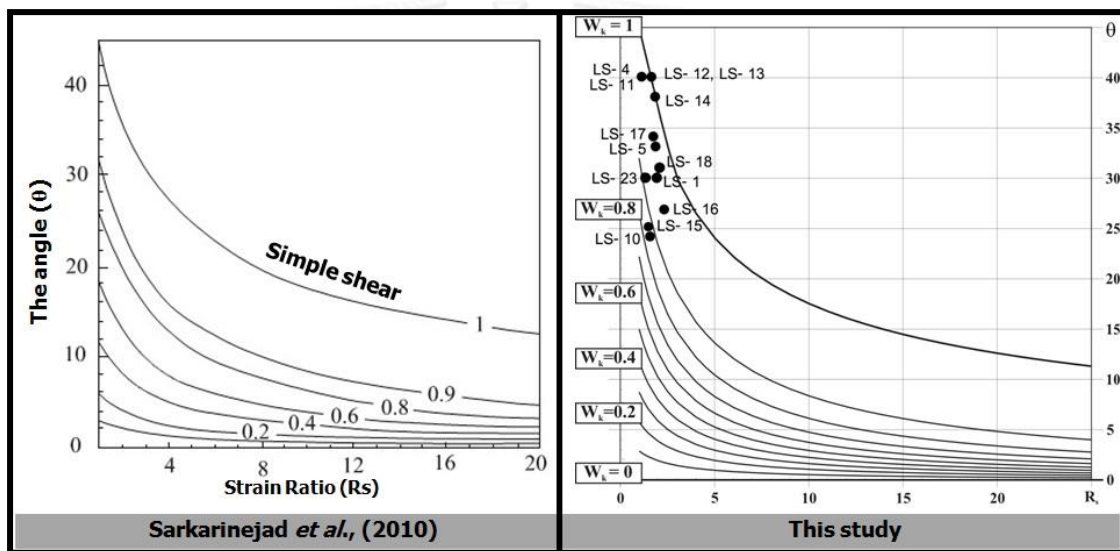


Figure 5. 1 Diagram presents W_k ranged of this research; ranged between 0.79 to 1.00 which corroborated with theory and clearly described the characteristic of simple shear- dominated in area of Lansang Waterfall, Tak, northwestern Thailand.

5.2 The sinistral shear

Based on the Fry's theory (Fry, 1979), to be quantify and define the deformation history of rocks on this large shear zone; the Mae Ping shear zone, the strain markers take an important role on this part. In case of homogeneous deformation the characteristic of deformed minerals under the microscope; the recrystallized quartz grains in gneisses intense clear sense of shearing and the

mineralogy of quartz which strongly to the deformation temperature on shear zone and no cleavage appropriate them to be the strain markers for indicate sense of movement of this shear.

The result of two- dimension strain quantitative analysis of rocks from Lansang Waterfall within Lansang National Park followed by Fry's method, the finite strain ellipsoid can be quantified and consisting of finite strain ratios, R_s and the angle between the longest axes of the ellipse and the deformation boundary, the angle θ (Fig. 5.2). To define sense of the movement of shearing, shape of the strain ellipsoid of rocks and also the shape of selected markers under the microscope from all locations (13 rock sample locations) were considered. The characteristic of strain ellipsoid of rocks and marker under microscope from all location imprint the dominant feature of sinistral shear or left- lateral shear during the shear process as same as the results from strain markers of previous study (Fig. 5.3). According to (R. Lacassin, Maluski, H., Leloup, P. H., Tapponnier, P., Hinthong, C., Siribhakdi, K., Chauaviroj, S. and Charoenravat, A, 1997), a part of this study involved and proposed about evidence that intense characteristic of left- lateral shear which were observed along Huai Lansang, Northwestern Thailand. Under the microscope study left- lateral shear sense imprint on various type of markers.

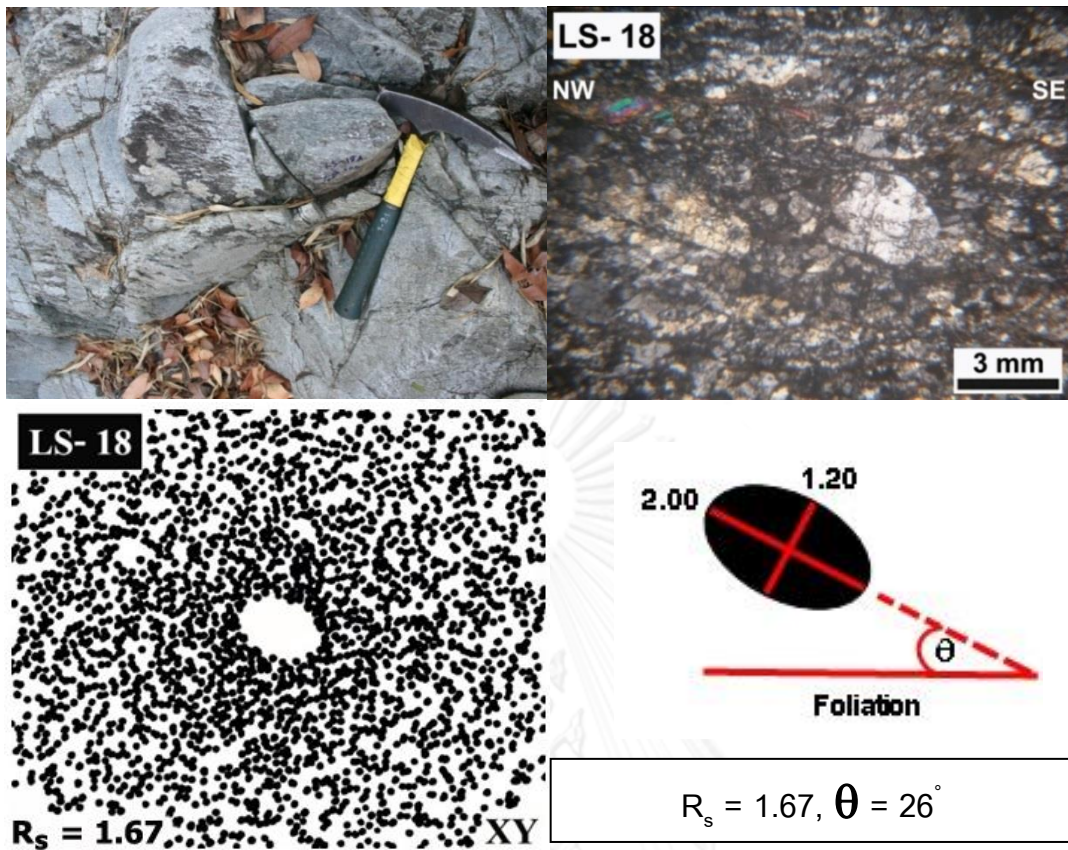


Figure 5. 2 Diagram presents the macro and micro scale of strain quantitative study, including with rock sampling (upper left), selection strain marker (upper right) and the Fry's product (lower left and right) which represented by strain ellipsoid of rocks.

The different in shape of strain ellipsoid of rock from each location were affected by the amount of strain that rock on each area accumulated inside. Based on the deformation theory, an ellipsoid represents that there is deformation in rock and referred the level of deformation by their shape.

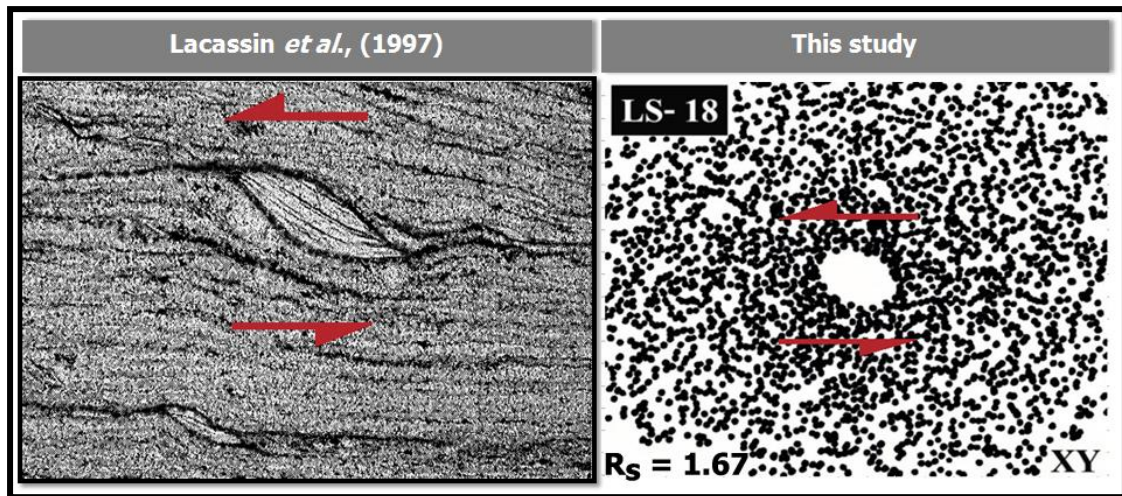


Figure 5. 3 Diagram presents the strain ellipsoid of rocks in area of Lansang Waterfall followed by Fry's method which clearly intense the characteristic of sinistral shear and corroborated with sense of movement of kinematic indicator; σ - clast of (R. Lacassin, Maluski, H., Leloup, P. H., Tapponnier, P., Hinthong, C., Siribhakdi, K., Chauaviroj, S. and Charoenravat, A, 1997).

5.3 Tectonic implication

To better understand in the tectonic evolution and the plate- scale kinematic reconstructions of this past India's penetration, both geochronological analysis and quantitative analysis require on affected area or the large scale of shear zone; Ailao-Shan- Red River and Mae Ping shear zones. Based on the result of (R. Lacassin, Leloup, & Tapponnier, 1993) and also result of this research, the direction and sense of the movement on both large scale shear zone can be concluded that left- lateral simple shear was applied on. Thus, (R. Lacassin, Leloup, & Tapponnier, 1993) modeled the mechanism of Tertiary left- lateral movement on Mae Ping shear zone from the age of the greenschist metamorphism that this shear occurred after the indentation of India into Asia continent, later rotated and pushed large slices of Indochina southeastward leading the formation of the South China Sea.

According to (R. Lacassin, Maluski, H., Leloup, P. H., Tapponnier, P., Hinthong, C., Siribhakdi, K., Chauaviroj, S. and Charoenravat, A, 1997) used $^{40}\text{Ar}/^{39}\text{Ar}$ dating the age of Lansang gneisses along the Mae Ping shear zone and Ailao- Shan- Red River shear zone. The results concluded that the deformation started around 30.5 Ma and the lower Mesozoic metamorphic and magmatic belt of northern Thailand had rapid cooling in the period of Tertiary or about 23 Ma. Based on the results, the extrusion of a part of Indochina occurred during the upper Eocene- lower Oligocene and the age of Lansang gneisses suggested to be an evidence of ductile left- lateral shear zone. Besides, the result used for model tectonic evolution of major strike- slip faults of eastern and southeastern Asia relative with the northward motion of Indian East corner as shown by Figure 5.4.

Besides, (Palin et al., 2013) applied geochronological analysis of monazite on sheared biotite- K- feldspar orthogneiss and the result implied two events of recrystallization. For the core regions, Th- Pb ages between c. 123 to c. 114 and for the rim regions ages younger between c. 45 to c. 37 Ma. Based on these result, the ductile shearing along the Mae Ping fault occurred during or after the metamorphic events which the last event of metamorphism occurred during the Eocene. Besides, the monazite analyzed from undeformed garnet- two- mica granite dyke, which intruding the metamorphic rock at Bhumibol Lake, a Th- Pb ages between 66.2 ± 1.6 Ma. From this age implied that the Mae Ping fault cut earlier formed magmatic and high- grade metamorphic rocks. Therefore, based on (R. Lacassin, Leloup, & Tapponnier, 1993; R. Lacassin, Maluski, H., Leloup, P. H., Tapponnier, P., Hinthong, C., Siribhakdi, K., Chauaviroj, S. and Charoenravat, A, 1997; Palin et al., 2013) could be implied that the ductile left- lateral shear was applied on Mae Ping shear zone during the Eocene (40 Ma to 35 Ma) and then during the lower Oligocene (30 Ma) is the latest shear process along the Mae Ping shear zone and adjacent area.

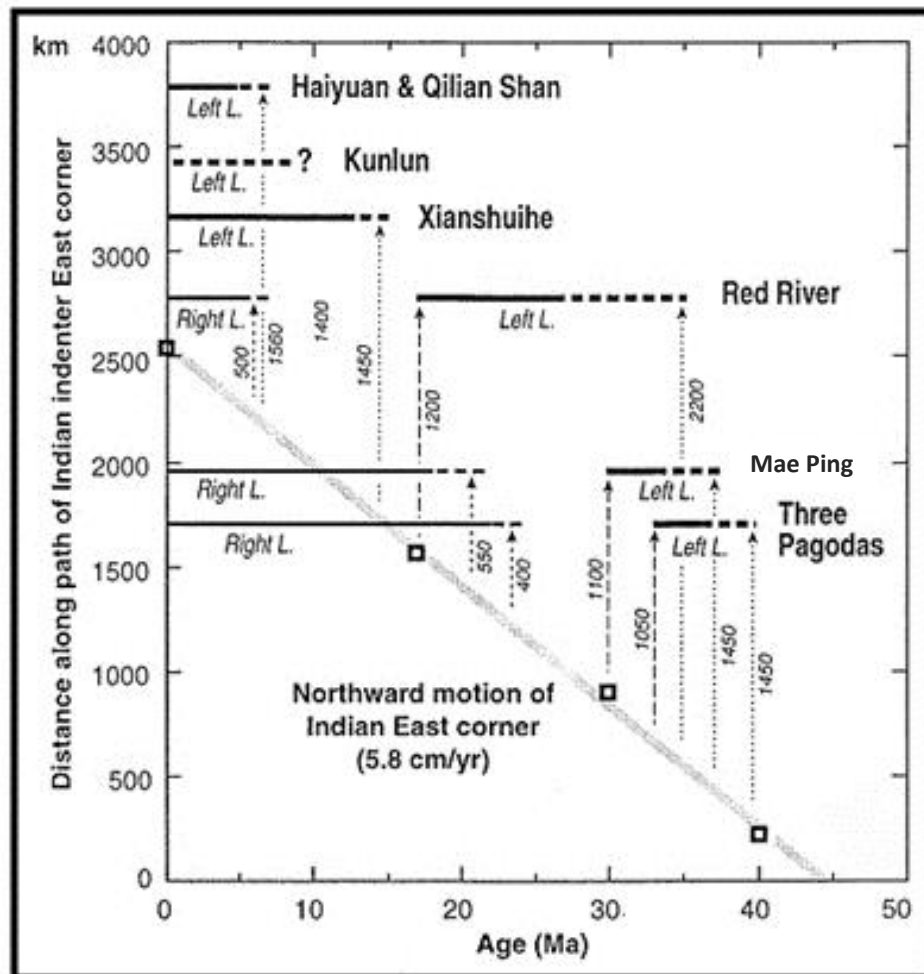


Figure 5. 4 Diagram describes the model of tectonic evolution of (R. Lacassin, Maluski, H., Leloup, P. H., Tapponnier, P., Hinthong, C., Siribhakdi, K., Chauviroj, S. and Charoenravat, A, 1997) by the plotted of age of the motion of the major strike-slip faults of eastern and southeastern Asia. An open squares and bold gray line define motion of India relative with Asia at 5.8 cm/yr. Arrowed lines show approximate distances between India and fault traces of left- lateral motion (dotted) and end of the motion (long dashes) while the short dashes show the right- lateral motion (Modified from R. Lacassin, Maluski, H., Leloup, P. H., Tapponnier, P., Hinthong, C., Siribhakdi, K., Chauviroj, S. and Charoenravat, A, 1997).

CHAPTER VI

CONCLUSION

The result of study in sense of two- dimension strain quantitative analysis for determine the direction and sense of the movement on Mae Ping shear zone by applied the application of Fry method (Fry, 1979) on strain markers; recrystallized quartz grains of orthogneiss and paragneiss from Lansang Waterfall within Lansang National Park, Tak, northwestern Thailand found that the averaged finite strain ratio ($R_{s, avg.}$) and the angle (θ) ranged between 1.35 to 1.69 and 22° to 41° , respectively. Based on relative between two values, the kinematic vorticity number (W_k) ranged between 0.79 to 1.00 and clearly described the characteristic of simple shear-dominated transpression. As same as the result of (R. Lacassin, Leloup, & Tapponnier, 1993) in one- dimension strain quantitative analysis on the Mae Ping shear zone mentioned that this zone was applied by the simple shear- dominated transpression with the left- lateral shear movement. Thus, it assured that an area of Lansang Waterfall, Tak, northwestern Thailand was effected by the strike- slip motion of Mae Ping fault which an effect of this motion generate the large scale of high strain zone; the Mae Ping shear zone.

The shear sense movement of this study was defined by the strain markers which are shear criteria and based on Fry's theory, the characteristic of deformed minerals under the microscope; the recrystallized quartz grains in orthogneiss and paragneiss intense clear sense of shearing. Besides, the mineralogy of quartz which strongly to the deformation temperature on shear zone and no cleavage appropriate them to be the strain markers for indicate shear sense movement. Followed by the Fry's theory for selection strain marker and Fry's methodology, the finite strain ellipsoid of rocks were created and shape of the strain ellipsoid and shape of selected markers under the microscope from all location imprinted the dominant feature of sinistral shear or left- lateral shear during the shear process as same as the results from strain markers of (R. Lacassin, Maluski, H., Leloup, P. H., Tapponnier, P., Hinthong, C., Siribhakdi, K., Chauaviroj, S. and Charoenravat, A, 1997). Under the

microscope study left- lateral shear sense imprint on various type of markers; leucocratic veins or quartz veins, boudinaged structure, rolling structure, deformed mica fishes and oblique shape fabric of quartz.

The tectonic evolution and the plate- scale kinematic reconstructions of this past India's penetration were studied in sense of geochronological analysis and quantitative analysis. (R. Lacassin, Leloup, & Tapponnier, 1993) modeled that the mechanism of Tertiary left- lateral movement on the Mae Ping shear zone occurred after the indentation of India into Asia continent and age of Lansang gneisses is an evidence which (R. Lacassin, Maluski, H., Leloup, P. H., Tapponnier, P., Hinthong, C., Siribhakdi, K., Chauaviroj, S. and Charoenravat, A, 1997) concluded that the deformation process started around 30.5 Ma. The lower Mesozoic metamorphic and magmatic belt of northern Thailand had rapid cooling in the period of Tertiary or about 23 Ma and the extrusion of a part of Indochina occurred during the upper Eocene- lower Oligocene. Beside, (Palin et al., 2013) implied that the ductile shearing along the Mae Ping fault occurred during or after the metamorphic events which the last event of metamorphism also occurred during the Eocene and the Mae Ping fault cut earlier the formed magmatic and high- grade metamorphic rocks. Thus, it implied that the ductile left- lateral shear was applied on Mae Ping shear zone during the Eocene.

REFERENCES

- Ahrendt, H., Chonglakmani, C., Hansen, B. T. and Helmcke, D. (1993). Geochronological cross section through northern Thailand. *Journal of SE Asia Earth Sciences*, 8, 207- 217.
- Ailleres, L., & Champenois, M. (1994). Refinements to the Fry method (1979) using image processing. *Journal of Structural Geology*, 16, 1327-1330.
- Bailey, C. M., & Eyster, E. L. (2003). General shear deformation in the Pinaleno Mountains metamorphic core complex, Arizona. *Journal of Structural Geology*, 25, 1883- 1892.
- Campbell, K. V. (1976). Metamorphic and deformational events recorded in the Lansang gneiss. Chiang Mai.
- Crespi, J. M. (1986). Some guidelines for the practical application of Fry's method of strain analysis. *Journal of Structural Geology*, 8, 799- 808.
- Dheeradilok, P., & Lumjuan, A. (1983). *On the Metamorphic and Precambrian Rocks of Thailand*. Paper presented at the Proceeding of the Conference on Geology and Mineral Resources of Thailand, Bangkok.
- Dunnet, D., & Siddans, A. W. B. (1971). Non-random sedimentary fabrics and their modification by strain. *Tectonophysics*, 12(4), 307-325. doi: [http://dx.doi.org/10.1016/0040-1951\(71\)90019-9](http://dx.doi.org/10.1016/0040-1951(71)90019-9)
- Erslev, E. A. (1988). Normalized center- to- center strain analysis of packed aggregates. *Journal of Structural Geology*, 10, 201- 209.
- Fossen, H. *Structural Geology*: Cambridge University Press.
- Fossen, H., & Tikoff, B. (1993). The deformation matrix for simultaneous simple shearing, pure shearing and volume change, and its application to transpression- transtension tectonics. *Journal of Structural Geology*, 15, 413- 422.
- Fry, N. (1979). Random point distributions and strain measurement in rocks. *Tectonophysics*, 60, 89- 105.
- Genier, F., & Epard, J. L. (2007). The Fry method applied to an augen orthogneiss: Problems and results. *Journal of Structural Geology*, 29, 209- 224.
- Ghaleb, A. R., & Fry, N. (1995). CSTRAIN: A fortran 77 program to study Fry's plots in two- dimensional simulated models. *Computers and Geosciences*, 21, 825- 831. .

- Hanna, S. S., & Fry, N. (1979). A Comparison of methods of strain determination in rocks from southwest Dyfed (Pembrokeshire) and adjacent areas. *Journal of Structural Geology*, 1, 155- 162.
- Lacassin, R., Leloup, P. H., & Tapponnier, P. (1993). Bounds on strain in large Tertiary shear zones of SE Asia from boudinage restoration. *Journal of Structural Geology*, 15, 677- 692.
- Lacassin, R., Maluski, H., Leloup, P. H., Tapponnier, P., Hinthong, C., Siribhakdi, K., Chauaviroj, S. and Charoenravat, A. (1997). Tertiary diachronic extrusion and deformation of western Indochina: structural and $^{40}\text{Ar}/^{39}\text{Ar}$ evidence from NW Thailand. *Journal of Geophysical Research*, 102, 13- 37.
- Lacassin, R., & Van Den Driessche, J. (1983). Finite strain determination of gneiss: application of Fry's method to porphyroid in the southern Massif Central (France). *Journal of Structural Geology*, 5, 245- 253.
- Means, W. D. (1994). Rotational quantities in homogeneous flow and the development of small- scale structure. *Journal of Structural Geology*, 16, 437- 445.
- Means, W. D., Hobbs, B. E., Lister, G. S., & Williams, P. F. (1980). Vorticity and non-coaxiality in progressive deformations. *Journal of Structural Geology*, 2, 371- 378.
- Morley, C. K. (2002). A tectonic model for the Tertiary evolution of strike- slip faults and rift basins in SE Asia. *Tectonophysics*, 347, 189- 215.
- Morley, C. K., Smith, M., Carter, A., Charusiri, P. and Chantraprasert, S. (2007). Evolution of deformation styles at a major restraining bend, constraints from cooling histories, Mae Ping fault zone, western Thailand. *Journal of Geological society London Special Publication*, 290, 325- 349.
- Palin, R. M., Searle, M. P., Morley, C. K., Charusiri, P., Horstwood, M. S. A., & Roberts, N. M. W. (2013). Timing of metamorphism of the Lansang gneiss and implication for left-lateral motion along the Mae Ping (Wang Chao) strike-slip fault, Thailand. *Journal of Asian Earth Sciences*, 76, 120-136.
- Ramsay, J. G., & Huber, M. I. (1983). *The Techniques of Modern Structural Geology: Strain analysis*: Academic Press.
- Resources, D. o. M. (1999). *Geological map of Thailand, Scale 1: 2,500,000*. Bangkok.
- Sarkarinejad, K. (2007). Quantitative finite strain and kinematic flow analyses along the Zagros transpression zone, Iran. *Tectonophysics*, 442, 49- 65.
- Sarkarinejad, K., Samani, B., Faghih, A., Grasemann, B., & Moradipoor, M. (2010). Implications of strain and vorticity of flow analyses to interpret the

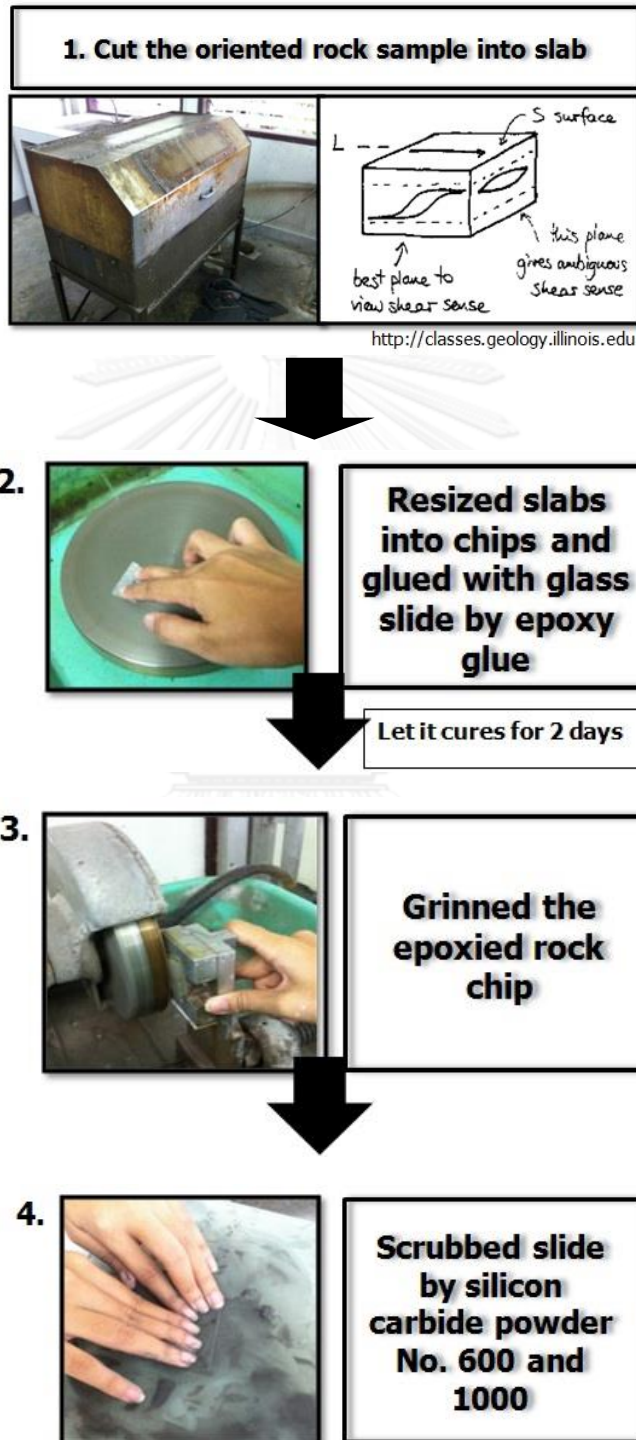
- kinematics of an oblique convergence event (Zagros Mountains, Iran). *Journal of Asian Earth Sciences*, 38, 34- 43.
- Tapponnier, P., Peltzer, G. and Armijo, R. (1986). On the mechanism of collision between India and Asia (G. S. o. London, Trans.). In M. P. C. a. A. C. Ries (Ed.), *Collision Tectonics* (Vol. 19, pp. 115-157).
- Tapponnier, P., Peltzer, G., Le Dain, A. Y. and Armijo, R. (1982). Propagating extrusion tectonics in Asia: new insights from simple experiments with plasticine. *Geology*, 10, 611-616.
- Tikoff, B., & Fossen, H. (1995). The limitations of three- dimensional kinematic vorticity analysis. *Journal of Structural Geology*, 17, 1771- 1784.
- Tikoff, B., & Fossen, H. (1999). Three-dimensional reference deformations and strain facies. *Journal of Structural Geology*, 21(11), 1497-1512. doi: [http://dx.doi.org/10.1016/S0191-8141\(99\)00085-1](http://dx.doi.org/10.1016/S0191-8141(99)00085-1)
- Wallis, S. R. (1992). Vorticity analysis in a metachert from the Sanbagawa Belt, SW Japan. *Journal of Structural Geology*, 14, 271- 280.



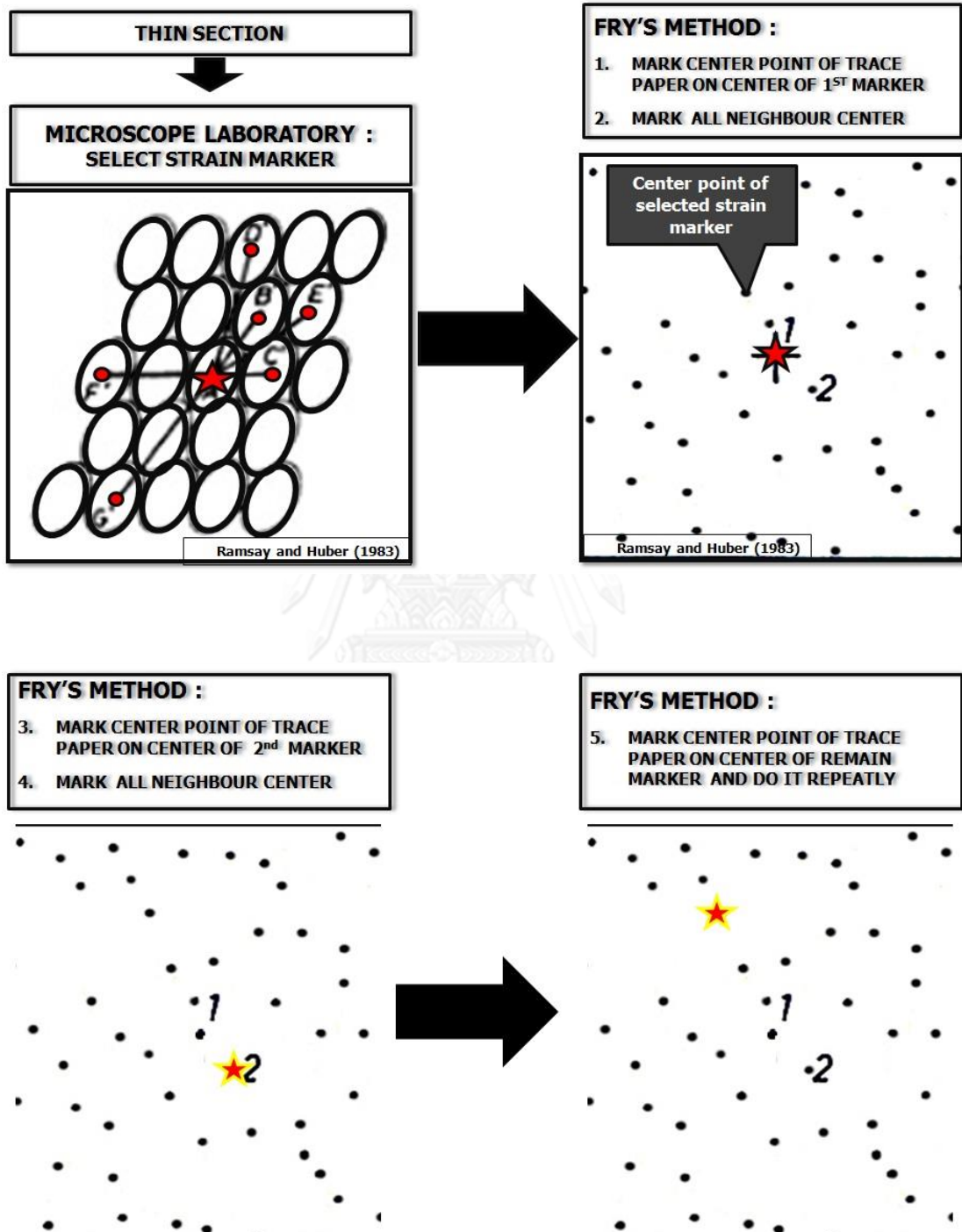
APPENDIX

จุฬาลงกรณ์มหาวิทยาลัย
CHULALONGKORN UNIVERSITY

APPENDIX 1: Preparing rock samples into thin section

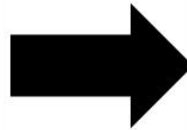
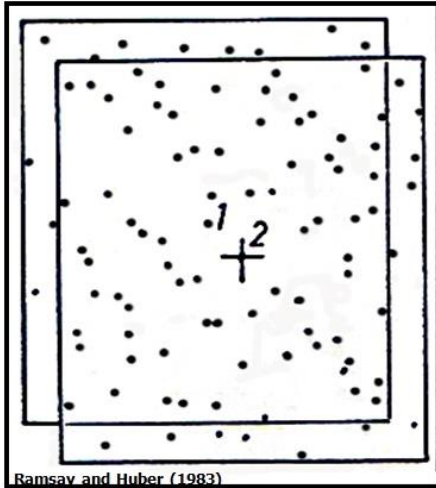


APPENDIX 2: The process of strain quantitative analysis followed by Fry's method

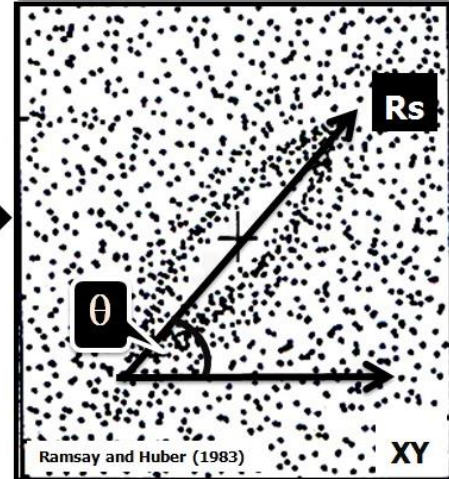


FRY'S METHOD :

6. ALL CENTER POINT OF EACH MARKER WILL BE MARKED TOGETHER AS SHOWN IN FIGURE.

**FRY'S METHOD :**

7. THE VACANCY FIELD OF FRY'S DIAGRAM REPRESENT THE STRAIN ELLIPSOID OF ROCK.
8. STRAIN ELLIPSOID CONSISTING OF R_s AND ANGLE θ



Strain quantitative analysis, Fry (1979)

Position	Ellipsoid Axis			Strain ratio		Angles			Kinematic vorticity number									
	longest axis	shortest axis		Rs	Rs max.	Rs min.	θ (°)	$\alpha(\theta)$ radian	$\sin(\alpha\theta)$	$\cos(2\theta)$	Rs+1	Rs-1	$\frac{(Rs+1)}{(Rs-1)}$	$\frac{\sin(\alpha\theta)}{\{[(Rs+1)/(Rs-1)] - \cos(2\theta)\}} = V$	$\arctan V$	$\frac{\sin(\arctan V)}{V} = \frac{\sin(\arctan \{[(Rs+1)/(Rs-1)] - \cos(2\theta)\}}{\{[(Rs+1)/(Rs-1)] - \cos(2\theta)\}}$		
Longitudinal	1.60	1.10	1.45				30	60	0.866	0.800	2.45	0.45	5.40	4.90	0.18	0.17	0.94	
	1.40	0.90	1.56				40	80	0.985	0.174	2.56	0.56	4.60	4.43	0.22	0.22	1.00	
	1.60	1.00	1.60	1.60	1.45		30	60	0.866	0.800	2.60	0.60	4.33	3.83	0.23	0.22	0.95	
99° 00' 50''	1.80	1.30	1.38				33	66	0.914	0.407	2.38	0.38	6.20	5.79	0.16	0.16	0.97	
	1.60	1.00	1.60				33	66	0.914	0.407	2.60	0.60	4.33	3.93	0.23	0.23	0.98	
	1.40	0.90	1.56				40	80	0.985	0.174	2.56	0.56	4.60	4.43	0.22	0.22	1.00	
	1.80	1.00	1.80	1.80	1.38		40	80	0.985	0.174	2.80	0.80	3.50	3.33	0.30	0.29	0.99	
99° 00' 42''	1.60	1.10	1.45				32	64	0.899	0.438	2.45	0.45	5.40	4.96	0.18	0.18	0.96	
	1.60	1.10	1.45				33	66	0.914	0.407	2.45	0.45	5.40	4.99	0.18	0.18	0.97	
	1.40	0.90	1.56				32	64	0.899	0.438	2.56	0.56	4.60	4.16	0.22	0.21	0.97	
	1.50	1.00	1.50	1.56	1.45		33	66	0.914	0.407	2.50	0.50	5.00	4.59	0.20	0.20	0.98	
99° 00' 38''	1.80	1.10	1.64				22	44	0.695	0.719	2.64	0.64	4.14	3.42	0.20	0.20	0.82	
	1.80	1.30	1.38			1.38	40	80	0.985	0.174	2.38	0.38	6.20	6.03	0.16	0.16	1.00	
	1.60	1.00	1.60	1.64			40	80	0.985	0.174	2.60	0.60	4.33	4.16	0.24	0.23	1.00	
	1.60	1.00	1.60				24	48	0.84	0.743	0.669	2.60	0.60	4.33	3.66	0.20	0.20	0.86
99° 00' 35''	1.80	1.00	1.80	1.80	1.45		40	80	0.985	0.174	2.80	0.80	3.50	3.33	0.30	0.29	0.99	
	1.60	1.10	1.45				40	80	0.985	0.174	2.45	0.45	5.40	5.23	0.19	0.19	1.00	
	1.80	1.00	1.80	1.80	1.45		30	60	0.866	0.500	2.80	0.80	3.50	3.00	0.29	0.28	0.97	
	1.40	1.00	1.40				30	60	0.866	0.500	2.40	0.40	6.00	5.50	0.16	0.16	0.93	
99° 00' 11''	1.50	1.10	1.36				40	80	0.985	0.174	2.36	0.36	6.50	6.33	0.16	0.15	1.00	
	1.60	1.20	1.33	1.40	1.33		40	80	0.985	0.174	2.33	0.33	7.00	6.83	0.14	0.14	1.00	
	1.60	1.00	1.60				40	80	0.985	0.174	2.60	0.60	4.33	4.16	0.24	0.23	1.00	
	1.80	1.30	1.38				29	58	1.01	0.848	2.38	0.38	6.20	5.67	0.15	0.15	0.92	
99° 00' 10''	1.80	1.20	1.50	1.60	1.38		40	80	0.985	0.174	2.50	0.50	5.00	4.83	0.20	0.20	1.00	
	1.70	1.00	1.70				38	76	1.33	0.970	0.242	2.70	0.70	3.86	3.62	0.27	0.26	1.00
	1.50	1.00	1.50	1.50	1.46		39	78	1.36	0.978	0.208	2.50	0.50	5.00	4.79	0.20	0.20	1.00
	1.50	1.00	1.50	1.70	1.50		36	72	1.26	0.951	0.309	2.50	0.50	5.00	4.69	0.20	0.199	0.99
99° 00' 08''	1.80	1.10	1.64				35	70	1.22	0.940	0.342	2.64	0.64	4.14	3.80	0.25	0.24	0.99
	1.90	1.30	1.46				22	44	0.77	0.695	0.719	2.46	0.46	5.33	4.61	0.15	0.15	0.79
	1.80	1.20	1.50	1.64	1.46		25	50	0.87	0.766	0.643	2.50	0.50	5.00	4.36	0.18	0.17	0.87
	2.00	1.00	2.00				27	54	0.94	0.809	0.588	3.00	1.00	3.00	2.41	0.34	0.32	0.95
99° 00' 07''	1.80	1.20	1.50	2.00	1.50	40	80	1.40	0.985	0.174	2.50	0.50	5.00	4.83	0.20	0.20	1.00	

VITA

Peekamon Ponmanee was born in Bangkok, Thailand, on November 16th, 1988. She received Bachelor of Science (Marine Science) in 2010 from Department of Marine Science, Faculty of Science, Chulalongkorn University. She started as a Master's student in Earth Science program, Department of Geology, Faculty of Science, Chulalongkorn University in 2011 and completed the program in May 2014.

Publication list

Journal

- Ponmanee, P. and Kanjanapayont, P. Strain analysis of rocks in Lansang Waterfall, Tak province, northwestern Thailand. Bulletin of Earth Sciences of Thailand (BEST) International Journal of Earth Sciences. 6(1) (2014).